UDK 621.3:(53+54+621+66)(05)(497.1)=00 ISSN 0352-9045

INFORMACIJE MIDEM 3 ∘ 1993

Strokovno društvo za mikroelektroniko elektronske sestavne dele in materiale

Časopis za mikroelektroniko, elektronske sestavne dele in materiale
Časopis za mikroelektroniku, elektronske sastavne dijelove i materijale
Journal of Microelectronics, Electronic Components and Materials

INFORMACIJE MIDEM, LETNIK 23, ŠT. 3(67), LJUBLJANA, SEPTEMBER 1993

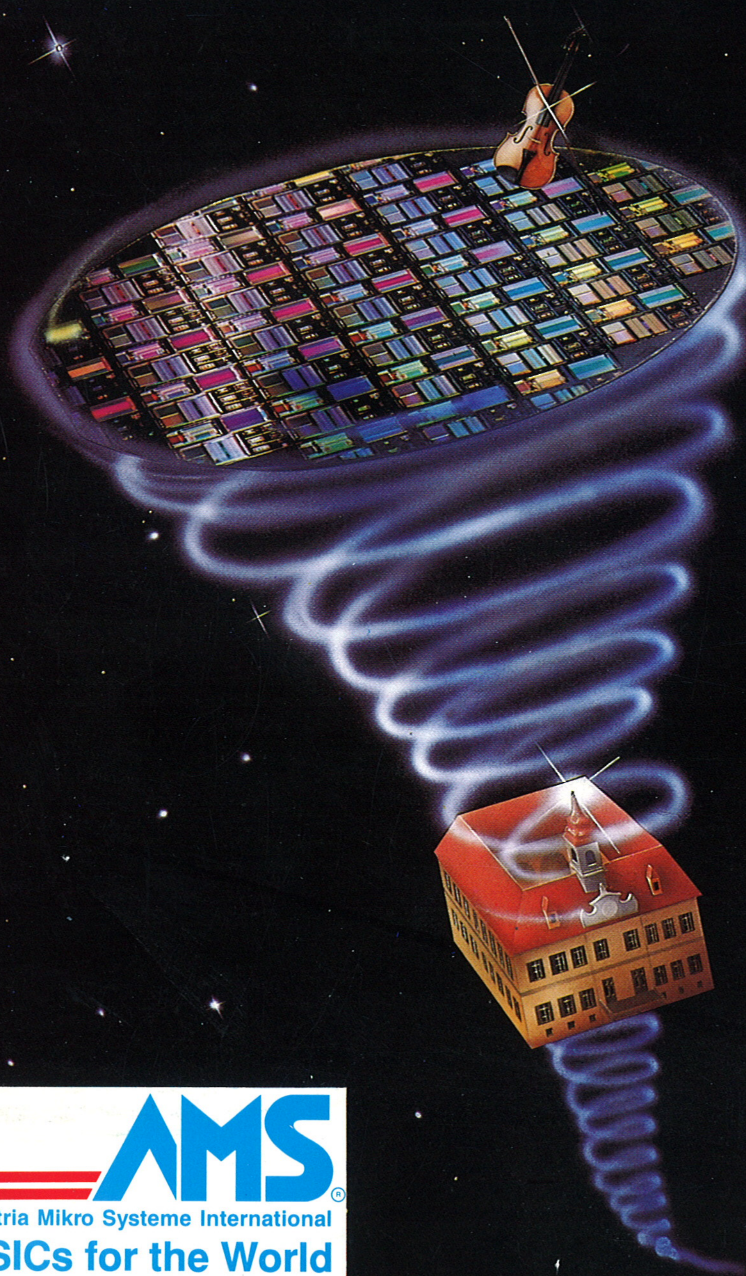

INFORMACIJE MIDEM 3 ° 1993

INFORMACIJE MIDEM	LETNIK 23, ŠT. 3(67), LJUBLJANA,	SEPTEMBER 1993
INFORMACIJE MIDEM	GODINA 23, BR. 3(67), LJUBLJANA,	SEPTEMBAR 1993
INFORMACIJE MIDEM	VOLUME 23, NO. 3(67), LJUBLJANA,	SEPTEMBER 1993

Izdaja trimesečno (marec, junij, september, december) Strokovno društvo za mikroelektroniko, elektronske sestavne dele in materiale.
Izdaja tromjesečno (mart, jun, septembar, decembar) Stručno društvo za mikroelektroniku, elektronske sastavne dijelove i materiale.
Published quarterly (march, june, september, december) by Society for Microelectronics, Electronic Components and Materials - MIDEM.

Glavni in odgovorni urednik
Glavni i odgovorni urednik
Editor in Chief

Iztok Šorli, dipl.ing.,
MIKROIKS d.o.o., Ljubljana

Tehnični urednik
Tehnički urednik
Executive Editor

Janko Colnar,
MIDEM, Ljubljana

Uredniški odbor
Redakcioni odbor
Publishing Council

Dr.Rudi Babič, dipl.ing., Tehniška fakulteta Maribor
Dr.Rudi Ročak, dipl.ing., MIKROIKS d.o.o., Ljubljana
mag.Milan Slokan, dipl.ing., MIDEM, Ljubljana
Zlatko Bele, dipl.ing., MIKROIKS d.o.o., Ljubljana
Miroslav Turina, dipl.ing., Zagreb
mag.Meta Limpel, dipl.ing., MIDEM, Ljubljana
Miloš Kogovšek, dipl.ing., Iskra INDOK d.o.o., Ljubljana

Časopisni svet
Izdavački savet
Publishing Council

Dr.Slavko Amon, dipl.ing., Fakulteta za elektrotehniko in računalništvo, Ljubljana, PREDSEDNIK
Dr.Marko Hrovat, dipl.ing., Inštitut Jožef Stefan, Ljubljana
Prof.Dr.Zvonko Fazarinc, dipl.ing., CIS, Stanford University, Stanford, USA
Dr.Marija Kosec, dipl.ing., Inštitut Jožef Stefan, Ljubljana
Prof.dr.Drago Kolar, dipl.ing., Inštitut Jožef Stefan, Ljubljana
RNDr. DrSc. Radomir Kužel, Charles University, Prague
Prof.dr.Stane Pejovnik, dipl.ing., Kemijski inštitut Boris Kidrič, Ljubljana
Prof.dr.Janez Trontelj, dipl.ing., Fakulteta za elektrotehniko in računalništvo, Ljubljana
Dr.Anton Zalar, dipl.ing., IEVT, Ljubljana
Dr. Peter Weissglas, Swedish Institute of Microelectronics, Stockholm

Naslov uredništva
Adresa redakcije
Headquarters

Uredništvo Informacije MIDEM
Elektrotehniška zveza Slovenije
Dunajska 10, 61000 Ljubljana, Slovenija
(0)61 - 316 886

Letna naročnina znaša 7000,00 SIT, cena posamezne številke je 1750,00 SIT. Člani in sponzorji MIDEM prejemajo Informacije MIDEM brezplačno.
Godišnja pretplata iznosi 7000,00 SIT, cijena pojedinog broja je 1750,00 SIT. Članovi i sponzori MIDEM primaju Informacije MIDEM besplatno.
Annual subscription rate is DEM 100, separate issue is DEM 25. MIDEM members and Society sponsors receive Informacije MIDEM for free.

Znanstveni svet za tehnične vede I je podal pozitivno mnenje o časopisu kot znanstveno strokovni reviji za mikroelektroniko, elektronske sestavne dele in materiale. Izdajo revije sofinanci rajo Ministrstvo za znanost in tehnologijo in sponzorji društva.
Scientific Council for Technical Sciences of Slovene Ministry of Science and Technology has recognized Informacije MIDEM as scientific Journal for microelectronics, electronic components and materials.
Publishing of the Journal is financed by Slovene Ministry of Science and Technology and by Society sponsors.

Znanstveno strokovne prispevke objavljene v Informacijah MIDEM zajemamo v:
* domačo bazo podatkov ISKRA SAIDC-el, kakor tudi
* v tujo bazo podatkov INSPEC
Scientific and professional papers published in Informacije MIDEM are assessed into:
* domestic data base ISKRA SAIDC-el and
* foreign data base INSPEC

Po mnenju Ministrstva za informiranje št.23/300-92 šteje glasilo Informacije MIDEM med proizvode informativnega značaja, za katere se plačuje davek od prometa proizvodov po stopnji 5 %.

Grafična priprava in tisk
Grafička priprema i štampa
Printed by

BIRO M, Ljubljana

Naklada
Tiraž
Circulation

1000 izvodov
1000 primjeraka
1000 issues

UDK 621.3:(53+54+621+66),ISSN0352-9045 Informacije MIDEM 23(1993)3,Ljubljana

VSEBINA		CONTENT
R.Ročak : Kriza na Vzhodu, ozdravljenje na Zahodu	172	R.Ročak : Crises in the East, Recovery in the West
ZNANSTVENO STROKOVNI PRISPEVKI		PROFESSIONAL SCIENTIFIC PAPERS
Z.Fazarinc: Algoritmi za večdimenzionalno računalniško analizo polprevodnikov iz osnovnih fizikalnih principov	173	Z.Fazarinc: Algorithms for Multi-dimensional Analysis of Semiconductors Derived from First Principles
R.Osredkar : Termična obdelava poliimidnih umetnih smol za uporabo v mikroelektronskih tehnologijah	183	R.Osredkar : Polyimide Resin Curing in Microelectronic Applications
A.Žnidaršič : Nova generacija Mn-Zn feritov za močnostne aplikacije	186	A.Žnidaršič : A New Generation Mn-Zn Ferrites for Power Applications
M.Jenko : Raziskave segregacije antimona na površini neorientirane elektro pločevine z metodo AES	190	M.Jenko : AES Investigation of Surface Segregation of Antimony in Non Oriented Electrical Sheets
D.Đonlagić, J.Koprivnikar, V.Matko : Princip senzorjev na osnovi oscilatorske diferencialne strukture	196	D.Đonlagić, J.Koprivnikar, V.Matko : Differential Ocsillator Sensors
J.Skvarč : Avtomatski sistem za analizo slike TRACOS	201	J.Skvarč : Automatic Image Analysis System TRACOS
D.Gradišnik, D.Đonlagić : Laserski merilnik debeline s statistično obdelavo rezultatov	206	D.Gradišnik, D.Đonlagić : Laser Thickness Measurer with Statistical Processing of Measurement
UPORABA POLPREVODNIŠKIH IN MIKROELEKTRONSKIH KOMPONENT		APPLICATION OF SEMICONDUCTOR AND MICROELECTRONIC COMPONENTS
C.Heberling : ASICs - kako izbrati optimalno rešitev	212	C.Heberling : ASICs - Selecting the Optimum Solution
J.Varl, J.Žmavc : Elektronsko vezje za mini časovni števec	214	J.Varl, J.Žmavc : ASIC for Mini Timer
Supresorske diode iz programa Iskre SEMICON	215	Suppressor and Limiter Diodes from Iskra SEMICON
KONFERENCE, POSVETOVANJA, SEMINARJI, POROČILA		CONFERENCES, COLLOQUYUMS, SEMINARS, REPORTS
A.Pregelj : Tečaj osnove vakuumske tehnike	220	A.Pregelj : Seminar on Basic Vacuum Technology
A.Pregelj : Prvo srečanje vakuumistov Slovenije in Hrvaške	220	A.Pregelj : First Meeting of Slovene and Croat Vacuum Societies
PREDSTAVLJAMO PODJETJE Z NASLOVNICE		REPRESENT OF COMPANY FROM FRONT PAGE
Austria Mikrosysteme International	220	Austria Mikrosysteme International
VESTI	222	NEWS
TERMINOLOŠKI STANDARDI	229	TERMINOLOGICAL STANDARDS
MIDEM prijavnica	235	MIDEM Registration Form

Slika na naslovnici : "Integrirana vezja po naročilu za ves svet". Austria Mikro Systeme International GmbH, AMS, je firma, ki se je specializirala za razvoj in proizvodnjo integriranih vezij po naročilu (ASIC) in standardnih integriranih vezij za specifično uporabo (ASSP). Firma zaseda posebej močan položaj na trgu vezij za telekomunikacije, avtoelektronike in industrijske elektronike.

Front page : "ASICs for the World". Austria Mikro Systeme International GmbH, AMS, specializes in the development and production of application specific integrated circuits (ASICs) and application specific standard products (ASSPs). The company is in a strong position within the market segments telecommunications, automotive and industrial electronics.

VSEBINA CONTENT

CRISES IN THE EAST, RECOVERY IN THE WEST

After the fall of eastern political wall the whole eastern Europe economy collapsed. This was extremely pronounced in the high tech area, especially in the electronics. Opening the door to the western electronic goods all the domestic, technologically poor and in the productivity weak industry could not compete with the well known western and Asiatic electronic industry. As a result of such situation the whole eastern semiconductor and microelectronics industry failed. In the former Yugoslav countries only the Trbovlje factory Iskra Semicon is still producing diodes. The Hungarian, Bulgarian, Czech and Slovakian, former DDR microelectronics practically does not exist or is surviving extremely hard times.

Also some western microelectronic companies had very hard time last year. The most known was the dismantling of a part of IBM microelectronics. The world equipment market for semiconductors dropped by about 9.4% in 1992 also because of the deep recession in Japan.

The first forecasting made by SEMI and SEAJ shows that manufacturers are expecting a recovery in the equipment industry this year with a rise of 11.2% on a value of US$ 9000 Millions.

INTEL is spending US$ 1000 Millions to add 13.000 sq. m of class 1 clean room in its largest wafer fab at Rio Rancho in New Mexico. This fab makes 80486 microprocessors and other VLSI logic circuits. The technology will be of 0.4 μm on 200 mm wafers. The new plant should start production in 1995.

On MIEL92 conference at Portorose Dr. Ianuzzi, an invited speaker from ST Microelectronics, presented the necessity for such billion dollar fabs. Let us hope that also MIEL93 at the door will give some contribution to this marvellous world of microelectronics.

MIDEM PRESIDENT
Dr. Rudolf Ročak

UDK 621.3:(53+54+621+66), ISSN0352-9045 Informacije MIDEM 23(1993)3, Ljubljana

ALGORITHMS FOR MULTI-DIMENSIONAL ANALYSIS OF SEMICONDUCTORS DERIVED FROM FIRST PRINCIPLES

Zvonko Fazarinc

KEYWORDS: semiconductors, semiconductor structure, computer analysis, algorithms, C-language, charge carriers, transport equation, electron distribution, hole distribution, electric field, basic principles, multi-dimensional

ABSTRACT: Expressions for multi-dimensional analysis of semiconductor structures in the discrete domain are derived from first principles. A simple structure is analyzed and the algorithms are cast in C-language.

Algoritmi za večdimenzionalno računalniško analizo polprevodnikov iz osnovnih fizikalnih principov

KLJUČNE BESEDE: polprevodniki, strukture polprevodniške, računalniška analiza, algoritmi, C jezik, nosilci nabojev, enačba transportna, porazdelitev elektronov, porazdelitev vrzeli, polje električno, principi osnovni, večdimenzionalnost

POVZETEK: Izrazi za večdimenzionalno računalniško analizo polprevodniških struktur so izvedeni iz osnovnih fizikalnih zakonov. Uporaba je ilustrirana na enostavnem primeru in algoritmi so prikazani v C-jeziku.

1. Introduction

Multi-dimensional analysis of semiconductor structures is commonly deferred to pre-canned computer programs [1] which often drape a veil of mystery over the inner workings of such design tools. The Poisson's equation is usually taken as the basis for evaluation of Fermi levels which then control the distribution of charged carriers. When the transport equation is used instead, the carrier distributions are computed from its discrete counterpart. This is prone to producing wrong answeres and makes the imposition of boundary conditions quite difficult.

The purpose of this paper is to derive the relevant equations for multi-dimensional analysis of semiconductors in discrete form directly from first physical principles. Such approach effectively avoids the hazards of discretization of partial differential equations [2], makes the imposition of boundary conditions. intuitive and, most importantly, it provides the practicing engineer and the novice with an insight which enables them to independently access the analytical powers of computers. The limitations of a paper prevent us from developing anything resembling a complete source code. Nevertheless, we will address the crucial ideas and make them understandable so that they can be embellished with refinements when needed.

We will be making use of the classical physics principles which are applicable to semiconductor structures larger than a few tenths of microns. For smaller structures quantum mechanics must be invoked and the reader should take note of this.

2. The Method of Approach

Before we address the general case we introduce the methodology with a simple example. Fig. 1 illustrates three points in space separated by Δx. With each location we associate a particle count $C(x,t)$ at time t.

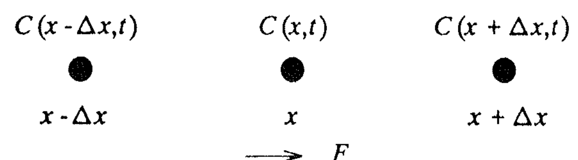

Fig. 1: Illustration of three points in one-dimensional space.

Particles are assumed to be in random thermal agitation which implies that they are equally likely to move to the left or to the right. We denote the likelyhood of their motion in one and the other direction by l. This means

that l-times the number of particles in a given position will move to the left and the same number will move to the right. We make a simplifying assumption that particles which do move make one single space step Δx in one time increment Δt. Armed with this information we can entertain the following question: "What will the concentration be in position x at time $t+\Delta t$ given the status at time t?" The answer proceeds along the following line of reasoning. If the likelyhood of motion is l then l-times the number of particles in position $x - \Delta x$ will move into position x during one time interval Δt. During the same time l-times the number of particles will move into position x form $x + \Delta x$. $2l$-times the number of particles initially residing at x will have moved out of this position. What we have then left at x is

$$C(x,t+\Delta t) = C(x,t) + l\,C(x-\Delta x,t) + l\,C(x+\Delta x,t) - 2l\,C(x,t) \quad (1)$$

The mathematical manipulation below is intended to show that (1) is the discrete form of the diffusion equation with diffusivity D given by

$$D = l\,\Delta x^2/\Delta t \quad (2)$$

First we subtract $C(x,t)$ on both sides of equation (1) and divide by Δt. Then we multiply and divide the RHS of the resulting equation by Δx^2 and obtain

$$\frac{C(x,t+\Delta t) - C(x,t)}{\Delta t} = \frac{l\,\Delta x^2}{\Delta t}\,\frac{C(x-\Delta x,t)+C(x+\Delta x,t) - 2C(x,t)}{\Delta x^2}$$

We recognize the numerator of the LHS of the above equation as the temporal difference of $C(x,t)$ and the numerator of the RHS as the second spatial difference of $C(x,t)$. Upon taking the limit as Δx and Δt go to zero we end up with the familiar basic diffusion equation for which the relationship (2) applies.

$$\frac{\partial C(x,t)}{\partial t} = D\frac{\partial^2 C(x,t)}{\partial x^2}$$

A temporal sequence of plots produced by (1) when the initial distribution is a δ-function in the center and a unit step at the left is shown in Fig.2.

An implementation of our example in C-language is shown below

```
// Initialization:
for (x = 0; x<200; x+ +) C[x] = 0;
for (x=0; x<20; x+ +) C[x] = 1.0;
C[100] = 10.0;

//Time loop of N passes:
for (t = 0; t< N; t+ +)
 { // Space loop:
   L = 1.0;
```

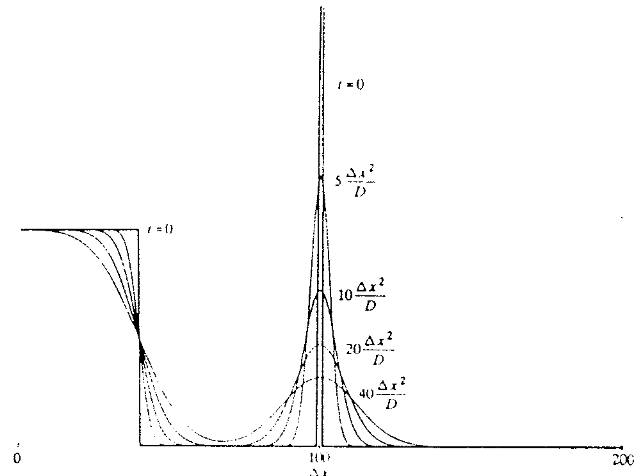

Fig. 2: Solution of discrete diffusion equation in one dimension

```
    for (x = 0; x< 200; x+ +)
{ temp = 0.25*C[x-1] + 0.25*C[x+1] + 0.5*C[x];
C[x-1] = L; L = temp;
      // Plot temp vs x
      }
  }
```

The timing required by (1) has been implemented in the above algorithm by reliance on memory management of computers. The values on the RHS of an equation are always taken to be the old values and those on the LHS of equation as the new ones. But we update C[x] by the new value only after we have computed C[x+1] which requires the old value of C[x]. This is accomplished by swapping the temp variable with L every time we pass through the space loop. It is obvious that the l value has been taken to be 0.25 in the example. One may wonder if such simple algorithm truly represents the solution of the diffusion equation. A quantitative comparison of (1) with the continuous diffusion equation is given in reference [2].

Next we allow a force F, indicated in Fig.1, to act uniformly on all particles. It is not difficult to conclude that a positive force - one that pushes to the right - will increase the likelyhood of particles moving to the right. At the same time it will decrease their chances of moving to the left. We can modify equation (1) for this case by introducing a skew factor f which is related to the force F and which biases the likelyhood l in the direction of force F.

$$C(x,t+\Delta t) = C(x,t) + (l+f)\,C(x-\Delta x,t) + (l-f)\,C(x+\Delta x,t) - 2l\,C(x,t) \quad (3)$$

The effect of force on $C(x,t)$ cancels out in this simple example as the reader may verify. Expression (3) is the transport equation in one dimension with constant diffu-

sivity and force. To prove this we subtract $C(x,t)$ on both sides, divide by Δt and separate the l and f contributions

$$\frac{C(x,t+\Delta t)-C(x,t)}{\Delta t}=\frac{l}{\Delta t}[C(x-\Delta x,t)+C(x+\Delta x,t)$$

$$-2C(x,t)]+\frac{f}{\Delta t}[C(x-\Delta x,t)-C(x+\Delta x,t)]$$

Now we need a relationship between the factor f and the force F. This is best done by comparing the energies involved during the move. The thermal energy kT is related to l in the same manner as the energy derived from the force field is related to f. A formal expression to that effect is

$$l:f=kT:\frac{F\Delta x}{2}$$

It yields the following for the force factor

$$f=l\,\frac{F\Delta x}{2kT} \tag{4}$$

We substitute (4) into our last equation, multiply and divide the first term on the right by Δx^2, and the second term by $2\Delta x$ and end up with the following difference equation

$$\frac{C(x,t+\Delta t)-C(x,t)}{\Delta t}=$$

$$\frac{l\,\Delta x^2}{\Delta t}\,\frac{C(x-\Delta x,t)+C(x+\Delta x,t)-2C(x,t)}{\Delta x^2}$$

$$-\frac{2l\,\Delta x^2}{\Delta t}\,\frac{F}{2kT}\,\frac{C(x+\Delta x,t)-C(x-\Delta x,t)}{2\Delta x}$$

The second term on the right is readily recognized as the first central difference in x of $C(x,t)$. It becomes the first derivative with respect to x when the limit is taken. The above equation then assumes the form

$$\frac{\partial C(x,t)}{\partial t}=D\frac{\partial^2 C(x,t)}{\partial x^2}-D\frac{F}{kT}\frac{\partial C(x,t)}{\partial x}$$

In the above we have substituted (2) for $l\Delta x^2/\Delta t$. Fig.3 shows a plot of expression (3) as function of x for a uniform force F with time being a parameter. Initial conditions are identical to those in Fig.2.

The numeric values for the plot of Fig.3 were generated by a source code identical to that shown earlier. The only difference is that the skew factor is introduced. We have chosen its value to be $f = 0.4\ l = 0.1$. Consequently the only modification of the algorithm is in the space loop which now reads: *temp* = 0.35*C[x-1] + .15*C[x+1] + .5*C[x]; Everything else remains the same. The reader, familiar with problems arising in computer solutions of transport equation may find (3) to be of considerable interest. Its simplicity and the physical basis from which

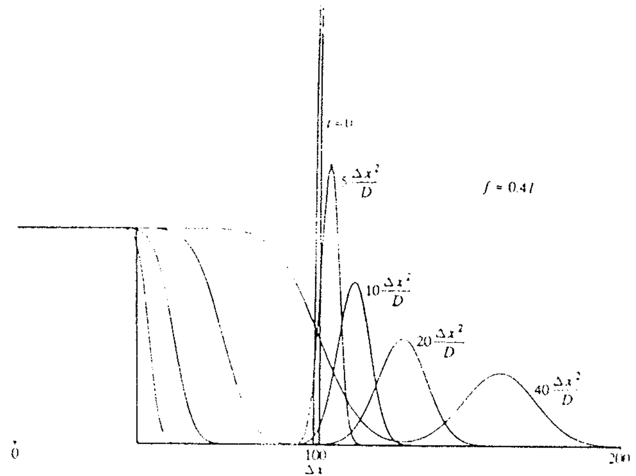

Fig. 3: *Solution of transport equation for one-dimensional case.*

(3) has been derived make the introduction of boundary conditions particularly easy.

We will now exploit the method just introduced for answering some of the more profound questions. One of them involves the diffusivity gradient. If D is a function of space, does it appear under the first or the second derivative sign? What if the diffusivity and force have different gradients along the spatial directions? How do we handle multidimensional analysis of semiconductors in general? These and some other questions will be addressed as we proceed.

3. Transport of Particles in Two Dimensions

The motion of charge carriers in semiconductors is governed by thermal energy, by electrical forces* and by properties of material through which they are moving. Their number depends on influx and outflow and on generation and recombination of oppositely charged pairs. We will derive the relevant equations taking into consideration the spatial variability of these effects and will allow, in addition, the temporal variation of electric fields and of carrier concentrations. In order to shield the derivation from excessive notational complexity we will limit it to the two-dimensional case. The extension to three dimensions will become self evident as we proceed.

We start with the illustration in Fig.4 which shows two points in x-space separated by Δx and a third point displaced in y-space by Δy. We assign the likelyhood of thermal motion in x-direction by l_x and that in y-direction

* Gravitational forces are negligible in comparison

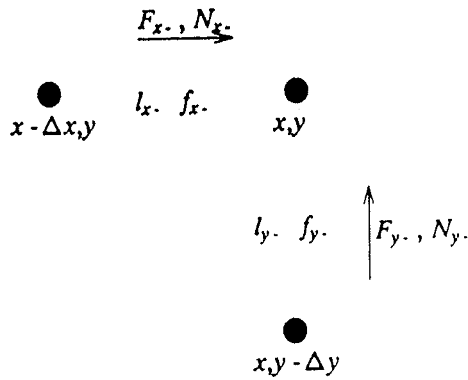

Fig. 4: Illustration of three points in two-dimensional space.

by l_y. We also allow a force F_x to act in the x-direction and a force F_y in the y-direction. These forces are responsible for the respective skew factors f_x and f_y through the relationship (4).

The motion likelyhood l and its skew f are assigned to the space between discrete spatial locations rather than to the locations themselves. The reason for this can be understood physically if we consider the case where the point $(x - \Delta x,y)$ belongs to the conducting region and the point (x,y) to an insulating layer characterized by $l = 0$. The particles can move into the insulator but they could never escape if the property of space $l = 0$ were assigned to (x,y) itself. On the other hand, if $l = 0$ is assigned to the space between the two points, no particle exchange can take place across the boundary. Force factor f, being a bias to l must share the same space. The rule is implemented in Fig.4 by making the subscript "x_-" to mean "half Δx to the left of x" and "y_-" to mean "half Δy below y". Using this notation we can state that during one time interval Δt there will be $[l_x(x_-,y) + f_x(x_-,y)]C(x-\Delta x,y,t)$ particles flowing from left to right and $[l_x(x_-,y)-f_x(x_-,y)]C(x,y,t)$ particles flowing from right to left. The net number of particles $N_x(x_-,y)$ flowing from $(x - \Delta x,y)$ to (x,y) is the difference of these two terms

$$N_x(x_-,y) = [l_x(x_-,y)+f_x(x_-,y)]C(x-\Delta x,y,t) - [l_x(x_-,y) - f_x(x_-,y)]C(x,y,t) \tag{6}$$

Similarly we get for the vertical or y-direction the following expression for the net number of particles $N_y(x,y_-)$ flowing from $(x,y - \Delta y)$ towards (x,y)

$$N_y(x,y_-) = [l_y(x,y_-)+f_y(x,y_-)]C(x,y-\Delta y,t) - [l_y(x,y_-) - f_y(x,y_-)]C(x,y,t) \tag{7}$$

Equations (6) and (7) contain the particle flux information which we intend to address later. At this time we remain focussed on our goal to obtain the complete transport equation of the form (3) in two dimensions and for

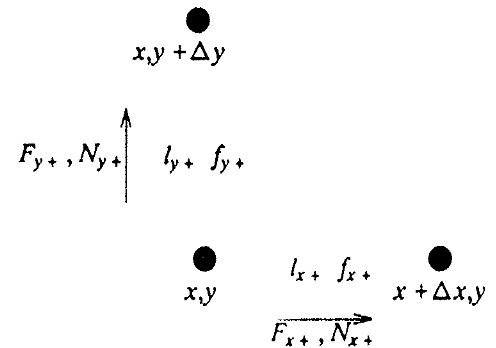

Fig. 5: The other points in two-dimensional space

variable diffusivities and forces. This requires that we know all the influxes and outflows from (x,y). Fig.4 guided us to obtain two of them, expressed in (6) and (7). With the aid of Fig.5 we obtain the other two which flow to the right and upward of (x,y) respectively.

We denote the net number of particles flowing out of (x,y) towards $(x + \Delta x,y)$ by $N_x(x_+,y)$. Their count is

$$N_x(x_+,y) = [l_x(x_+,y)+f_x(x_+,y)]C(x,y,t) - [l_x(x_+,y) - f_x(x_+,y)]C(x+\Delta x,y,t) \tag{8}$$

The net number of particles $N_y(x,y_+)$, flowing from (x,y) upward towards $(x,y+ \Delta y)$ is

$$N_y(x,y_+) = [l_y(x,y_+)+f_y(x,y_+)]C(x,y,t) - [l_y(x,y_+) - f_y(x,y_+)]C(x,y+\Delta y,t) \tag{9}$$

We can write an expression for the particle count at time $t + \Delta t$ at the point (x,y) by adding all inflowing particles to $C(x,y,t)$ and subtracting all outflowing particles from it. We will allow for the possibility that in addition to particle exchange some of them are being generated at the rate $G(x,y)$ while some are being lost at the rate $R(x,y)$. This produces a net particle increase of $[G(x,y) - R(x,y)]\ \Delta t$ during the time interval Δt. The total particle count at (x,y) at $t + \Delta t$. The total particle count at (x,y) at $t + \Delta t$ is then

$$C(x,y,t+\Delta t) = C(x,y,t) + N_x(x_-,y)+N_y(x,y_-)-N_x(x_+,y)-N_y(x,y_+) + [G(x,y)-R(x,y)]\Delta t \tag{10}$$

Equation (10) in association with (6) through (9) is the discrete form of the two dimensional transport equation and we will make use of it shortly. But first we will perform a limiting process on it to obtain the equivalent differential equation. Rather than blindly substituting expressions (6) through (9) into (10) by noting that the difference $N_x(x_+,y,t) - N_x(x_-,y,t)$ refers to the midpoint between (x_-,y) and (x_+,y). But this is excatly (x,y) by our definition of x_- and x_+. Consequently we can write the difference $N_x(x_+,y,t) - N_x(x_-,y,t)$ as $\Delta_x N_x(x,y,t)$ where Δ_x signifies that the difference is with respect to x. When we do the same with the *y*-difference we get for (10)

$$C(x,y,t+\Delta t) = C(x,y,t) - \Delta_x N_x(x,y,t) - \Delta_y N_y(x,y,t) + [G(x,y) - R(x,y)]\Delta t \tag{11}$$

The value for $N_x(x,y,t)$ can be formally derived from (6) or (8) by respectively incrementing or decrementing all x-arguments by x/2. The result is

$$N_x(x,y,t) = [l_x(x,y) + f_x(x,y)]C(x_-,y,t) - [l_x(x,y) - f_x(x,y)]C(x_+,y,t) \tag{12}$$

In the above we have used the established notation for half-Δx values as, for example, $C(x - \Delta x/2,y,t) = C(x_-,y,t)$.

Similarly we get by either incrementing (7) or decrementing (9) by $\Delta y/2$ the expression for $N_y(x,y)$

$$N_y(x,y,t) = [l_y(x,y) + f_y(x,y)]C(x,y_-,t) - [l_y(x,y) - f_y(x,y)]C(x,y_+,t) \tag{13}$$

Substitution of (12) and (13) into (11) yields

$$C(x,y,t+\Delta t) = C(x,y,t) - \Delta_x\left[l_x(x,y)[C(x_-,y,t) - C(x_+,y,t)]\right] - \Delta_x\left[f_x(x,y)[C(x_-,y,t) + C(x_+,y,t)]\right] - \Delta_y\left[l_y(x,y)[C(x,y_-,t) - C(x,y_+,t)]\right] - \Delta_y\left[f_y(x,y)[C(x,y_-,t) + C(x,y_+,t)]\right] + [G(x,y) - R(x,y)]\Delta t$$

This time we recognize the term $C(x_-,y,t) - C(x_+,y,t)$ to be the negative difference centered on (x,y). Consequently we can denote it by $-\Delta_x C(x,y,t)$. Similarly for the *y*-direction. Furthermore the sum of $C(x_-,y,t) + C(x_+,y,t) \approx 2C(x,y,t)$ and becomes exact when the increments go to zero which we are just about to do. We have now

$$C(x,y,t+\Delta t) = C(x,y,t) + \Delta_x[l_x(x,y)\Delta_x C(x,y,t)] - \Delta_x[f_x(x,y)2C(x,y,t)] + \Delta_y[l_y(x,y)\Delta_y C(x,y,t)] - \Delta_y[f_y(x,y)2C(x,y,t)] + [G(x,y) - R(x,y)]\Delta t$$

By means of (4) we convert *f*-factors to *l* and then employ (2) to convert *l*-factors to diffusivity *D*. We also subtract $C(x,y,t)$ on both sides of equation and divide them by Δt. A straightforward algebraic manipulation leads to

$$\frac{C(x,y,t+\Delta t) - C(x,y,t)}{\Delta t} = \frac{\Delta_x}{\Delta x}\left[D_x(x,y)\frac{\Delta_x C(x,y,t)}{\Delta x}\right] - \frac{\Delta_x}{\Delta x}\left[D_x(x,y)\frac{F_x(x,y,t)}{kT}C(x,y,t)\right] + \frac{\Delta_y}{\Delta y}\left[D_y(x,y)\frac{\Delta_y C(x,y,t)}{\Delta y}\right] - \frac{\Delta_y}{\Delta y}\left[D_y(x,y)\frac{F_y(x,y,t)}{kT}C(x,y,t)\right] + [G(x,y) - R(x,y)]$$

In the limit when all increments go to zero the above becomes a differential equation

$$\frac{\partial C(x,y,t)}{\partial t} = \frac{\partial}{\partial x}D_x(x,y)\left[\frac{\partial C(x,y,t)}{\partial x} - \frac{F_x(x,y)C(x,y,t)}{kT}\right] + \frac{\partial}{\partial y}D_y(x,y)\left[\frac{\partial C(x,y,t)}{\partial y} - \frac{F_y(x,y)C(x,y,t)}{kT}\right] + G(x,y) - R(x,y)$$

While this equation may be the correct starting point for a computerized solution of the transport equation when diffusivities, forces and concentrations vary in both dimensions it certainly does not guarantee the correctness of the solution. There are countless possible ways to discretize a differential equation but very few of them yield correct answers. Therefore it is strongly advisable to start from equation (10) which is derived from fundamental physical principles and circumvents the discretization problem altogether.

4. Flux of Particles in Two Dimensions.

Equations (12) and (13) provide us with the number of particles moving in the *x* and y direction, respectively, across the point (x,y). The corresponding flux is that number multiplied by the particle velocity. Our initial supposition was that particles move one space interval in one time interval Δt. Consequently their velocity is $\Delta x/\Delta t$ in the x-direction and $\Delta y/\Delta t$ in the *y*-direction. The two respective fluxes are then

$$\Phi_x(x,y,t) = -l_x(x,y)\frac{\Delta x^2}{\Delta t}\frac{C(x_+,y,t) - C(x_-,y,t)}{\Delta x}$$
$$+ f_x(x,y)[C(x_-,y,t) + C(x_+,y,t)]$$

$$\Phi_y(x,y,t) = -l_y(x,y)\frac{\Delta y^2}{\Delta t}\frac{C(x,y_+,t) - C(x,y_-,t)}{\Delta y}$$
$$+ f_y(x,y)[C(x,y_-,t) + C(x,y_+,t)]$$

The same kind of reasoning which led to the last differential equation in the previous Section guided us from here to the particle flux equations in differential form

$$\Phi_x(x,y,t) = -D_x(x,y)\left[\frac{\partial C(x,y,t)}{\partial x} - \frac{F_x(x,y)}{kT}C(x,y,t)\right]$$

$$\Phi_y(x,y,t) = -D_y(x,y)\left[\frac{\partial C(x,y,t)}{\partial y} - \frac{F_y(x,y)}{kT}C(x,y,t)\right]$$

If we multiply the flux by electric charge q we get the electric current density. The forces in this case are qE_x and qE_y, respectively for positive charges, i.e., holes and $-qE_x$ and $-qE_y$ for electrons where E_x and E_y are the electric fields. The concentrations $C(x,y,t)$ are $n(x,y,t)$ for electrons and $p(x,y,t)$ for holes. The corresponding four current density equations are

$$j_{nx}(x,y,t) = qD_{nx}(x,y)\left[\frac{\partial n(x,y,t)}{\partial x} + \frac{q}{kT}E_x(x,y,t)n(x,y,t)\right]$$

$$j_{ny}(x,y,t) = qD_{ny}(x,y)\left[\frac{\partial n(x,y,t)}{\partial y} + \frac{q}{kT}E_y(x,y,t)n(x,y,t)\right]$$

$$j_{px}(x,y,t) = -qD_{px}(x,y)\left[\frac{\partial p(x,y,t)}{\partial x} - \frac{q}{kT}E_x(x,y,t)p(x,y,t)\right]$$

$$j_{py}(x,y,t) = -qD_{py}(x,y)\left[\frac{\partial p(x,y,t)}{\partial y} - \frac{q}{kT}E_y(x,y,t)p(x,y,t)\right]$$

The reader may note that the so called Einstein relationship between carrier diffusivity D and their mobility μ is contained in the above equations

$$\mu = D\frac{q}{kT}$$

Before we leave this section let us examine equations (12) and (13) for physical consistency. Assume that the force factor f which depends on the electric field becomes larger than l in (12) or (13). This implies that the particle flow represented by the second term of either equation reverses its direction. This could quickly deplete the particles at the adjacent point and would even make their concentration go negative. Such physical impossibilities usually present themselves as numeric instabilities. We can therefore derive a stability condition from requiring that f never exceedes the value of l. Using (4) this condition can be writen as $F\Delta x/kT < 1$. For the electric case this translates into $E\Delta x < kT/q$. Because $E\Delta x$ represents the potential difference over one grid point our stability condition requires that this potential difference never exceeds 25 mV at room temperature.

5. Forces on Particles in Two Dimensions.

The last unresolved quantity that appears in equations (6) through (9) is the force factor f. According to (4) this is directly related to the electric field for the two respective directions. The electric field, on the other hand, emanates from electric charges as suggested by the Coulomb's law. Before we apply it to our case a discussion is in order.

In real, three-dimensional space the electric field surrounding a charge possesses spherical symmetry and is as such decaying as the square of the distance from the charge. If we were dealing with a three-dimensional case we would compute the field at a given position (x,y) by adding vectorially the contributions from all surrounding charges using an inverse square law. Then we would resolve that field into its Cartesian or other components as needed by the analysis. Instead of spherical symmetry we have a cylindrical symmetry for our two-dimensional case and consequently we can allow the electric field to decay only linearly with distance away from the source charge. This may appear unconventional but is no more so than is a two-dimensional space. In a one-dimensional space the field does not decay at all and we therefore compute the field as the sum of net charges without prorating their effects for distance. One must be quite cautious when applying natural laws to unnaturals spaces. With this in mind we continue now with the evaluation of force factors to be applied to equations (6) through (9).

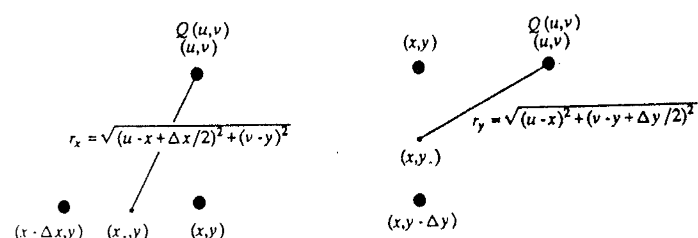

Fig. 6: *Aid to calculation of the electric field components*

We remember that the force factors have been defined halfway between discrete points. With the aid of Fig.6 we compute the x-component of the electric field at the point (x,y) as produced by the charge $Q(u,v)$ a distance

r_x away. A linear decay of the field with distance is employed as appropriate for our two-dimensional case.

$$E_x(x_-,y) = E(x_-,y)\frac{u-x_-}{r_x} = \frac{Q(u,v)}{2\pi r_x}\frac{u-x_-}{r_x} =$$

$$\frac{Q(u,v)}{2\pi}\frac{u-x_-}{(u-x_-)^2+(v-y)^2}$$

Similarly we get for the y-component at (x,y-) according to Fig.6

$$E_y(x,y_-) = E(x,y_-)\frac{v-y_-}{r_y} = \frac{Q(u,v)}{2\pi r_y}\frac{v-y_-}{r_y} =$$

$$\frac{Q(u,v)}{2\pi}\frac{v-y_-}{(v-y_-)^2+(u-x)^2}$$

The total field is the summation of components due to all charges Q(u,v)

$$E_x(x_-,y) = \sum_x\sum_y\sum_u\sum_v\frac{\frac{Q(u,v)}{2\pi}(u-x+\frac{\Delta x}{2})}{(u-x+\frac{\Delta x}{2})^2+(v-y)^2} \quad (16)$$

and

$$E_y(x,y_-) = \sum_x\sum_y\sum_u\sum_v\frac{\frac{Q(u,v)}{2\pi}(v-y+\frac{\Delta y}{2})}{(u-x)^2+(v-y+\frac{\Delta y}{2})^2} \quad (17)$$

We will now illustrate how (10) can be applied to impurity redistribution and to subsequent charge migration and how (16) and (17) can be used to compute the resulting forces opposing such migration. This is done in the hopes that the reader will be encouraged to experiment with multidimensional electric transport problems on his own.

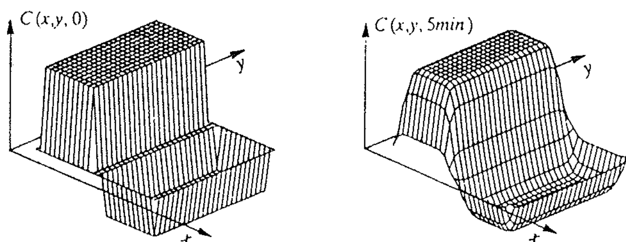

Fig. 7: Impurity profile before and after annealing.

6. An Example of a Two-Dimensional Semiconductor Structure

We start with the doping profile $C(x,y)$ shown on the LHS of Fig.7. It represents a PIN junction with a very narrow intrinsic region, with a donor density of $N_D=4*10^{16}$ and an acceptor density of $N_A=2*10^{16}$. The profile shows the difference $C(x,y) = N_D(x,y) - N_A(x,y)$.

The widths of the two regions are approximately 2.5μ each. Next we anneal the sample by subjecting it to 1100°C for about 5 minutes. The diffusivity was chosen to be $5*10^{-13}$ at this temperature which is representative of commonly used dopants. The redistributed impurities are shown on the RHS of Fig.7.

This result was achieved by using (6) through (10) with the following parameters:

$l_x = l_y = .125$ independently of x and y, and $f_x = f_y = 0$ and $G - R = 0$ everywhere.

Equation (10) simplifies then into

$$C(x,y,t+\Delta t) = 0.5\,C(x,y,t)+0.125[C(x-\Delta x,t)+C(x+\Delta x,t)+C(x,y-\Delta y,t)+C(x,y+\Delta y,t)] \quad (18)$$

Denote the number of Δx steps by X and the number of Δy steps by Y and assign a two-dimensional array $C(x,y)$ to the impurity concentration. We can then write the algorithm which represents the above equation in C-language as

```
for (y = 0; y<Y; y++)
  L[y] = 0.0; for (x = 1; x < X; x++)
  { for (y = 0; y < Y; y++)
    {temp = .5*C[x,y] + .125*(C[x - 1,y] + C[x + 1,y]
    + C[x,y - 1] + C[x,y + 1]);
    C[x - 1,y] = L[y]; L[y] = temp;
    }
} for (y=0; y < Y; y++)
{C[X -1,y] = L[y]; L[y] = 0.00;}
```

A few explanations are in order. First, the choice of l seems fairly open since it represents the diffusivity in conjuction with space and time steps according to (2). But if you consider the case where all the matter is initially concentrated in position (x,y) then we can have no more than 1/8 of the central matter moving out in each direction while preserving an equal amount of matter in the center. If we allow higher depletion, instabilities may occur. The rule of thumb is then to choose l_{max}=0.125 for highest diffusivity and proportionately less for all other values of D. In a three-dimensional case the maximum value of l should be chosen to be 1/12 and for the one- dimensional analysis l_{max}=.25.

For our example we have chosen 25 segments along the entire width and 25 along the entire lenght of the

sample corresponding to a space step of 0.2μ. According to (2) the time step Δt for our chosen diffusivity amounts to 100 seconds, meaning that every time we traverse the algorithm the time advances by this amount. Consequently, the annealed profile in Fig.7 is achieved by executing the algorithm only three times (five minutes).

In the C-algorithm above we have taken care of timing implied by (18) which demands that all RHS variables be taken at time *t*. As the execution moves from lower to higher values of x and y we must postpone the update of concentrations until we have moved to the next x-column. Therefore we save one whole x-column in L[y] and load it into C[x - 1,y] column after the old values are no longer needed. The first "for-loop" initializes the L-array to whatever boundary value we wish to assign to the *x* = 0 column. As the x-loop starts with the index 1, the column *x* = 0 receives the initial values contained in L[y]. The very last "for-loop" updates the last x-column at X-1 and resets the L-array to the initial value which will subsequently restore the boundary value at the *x* = 0 column again. Whatever we load into the X column which lies outside the reach of the x-loop becomes the upper boundary value for x. This column never gets updated so it supplies the boundary conditions which it contains to the X-1 column. In a similar fashion we can impose the boundary values to the y-column or to any point in the x-y domain, for that matter. This we do by loading such conditions into the appropriate location everytime the loops are traversed and the initial value there has been changed by the algorithm.

This lenghty discussion of the boundary value problem is intended to encourage those who have experienced difficulties with similar problems in the continuous domain. The discrete nature of computerized analysis makes the imposition of boundary conditions almost intuitive.

Next we must compute the concentrations of holes and electrons produced by the annealed profile. This is quite straightforward when we invoke the neutrality condition $N_D - N_A + p - n = 0$ and the mass- action law $n\,p = n_i^2$ [3,4].

The following algorithm has been used to obtain Fig.8

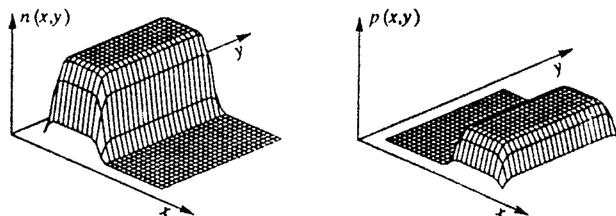

Fig. 8: *Electron and hole distribution.*

```
for (x = 0; x < X; x++)
 { for (y = 0; y < Y; y++)
 {if (C[x,y] > 0.0)
  {n[x,y] = C[x,y]/2.0 + sqrt(C[x,y]*C[x,y]/4.0 +
    2.0e20);
  p[x,y] = 2.0e20/n[x,y];
   }
 if (C[x,y] < 0.0)
  {p[x,y] = - C[x,y]/2.0 + sqrt(C[x,y]*C[x,y]/4.0 +
    2.0e20);
   n[x,y] = 2.0e20/p(x,y);
   }
 if (C[x,y]= = 0.0) (n[x,y] = 0.0; p[x,y] = 0.0;}
  }
}
```

where 2.0e20 stands for squared intrinsic concentration of Silicon.

Gradients of holes and electrons seen in Fig.8 give rise to their migration into the adjacent regions of low density which destroys the initially imposed neutrality. This gives rise to electric fields which tend to oppose the migration and which we will compute later. First we use (10) again to compute the movement of charges but this time we want to distinguish the migration rates of holes and

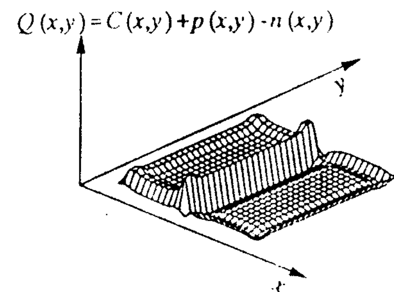

Fig. 9: *Net charge distribution after 10 picoseconds*

electrons. We assign a diffusivity D_n = 28 to the latter and D_p = 9 to the former. These numbers are in fair agreement with the respective impurity concentrations. We assign the value I_n = .125 to the highest diffusivity. The corresponding value of I_p must then be .125x9/28 ≈ .04. With these values and with the force factors initially set to zero we have obtained the net charge density distribution *Q(x,y)* shown in Fig.9 after approximately 10 picoseconds.

It is apparent from Fig.9 that the departure of electrons along the four boundaries of the *N*-region produces a net positive charge. Similarly the departure of holes from the *P*-region produces a net negative charge all around the boundary. A charge reversal is observed at the junction. Implemention in C-language of equations (8) through (10) which have produced Fig.9 is shown below.

```
for (i = 0; i < 5; i++)
  {for (x= 0; x < X; x++)
   { for (y= 0; y < Y; y++)
    {Fxy = .125*(fx[x,y] - fx[x+1,y] + fy[x,y]
      - fy[x,y+ 1]);
   tempN = (.5-Fxy)*n[x,y] + .125*(1.0-fx[x,y])*n[x-1,y]
+ .125*(1.0 + fx[x+1,y])*n[x+1,y]+.125*(1.0-
fy[x,y])*n[x,y-1] + .125*(1.0 + fy[x,y+1])*n[x,y+1];
   n[x-1,y] = L[y]; L[y] = tempN;
   tempP= (.84 + Fxy)*p[x,y] + .04*(1.0 + fx[x,y] *p[x-
1,y] + .04*(1.0 - fx[x+1,y]*p[x+1,y] + .04*(1.0 +
fy[x,y])*p[x,y-1] + .04*(1.0 - fy[x,y+1])*p[x,y+1];
      p[x-1,y] = L[y]; L[y] = tempP;
    }
} } for (x= 0; x < X; x++)
  for (y= 0; y < Y; y++)
    Q[x,y] = C[x,y] + p[x,y] - n[x,y];
```

In the above we have made the following substitutions

$$\text{fx}[x,y] = E_x(x_-,y)\Delta x\frac{q}{kT} \qquad \text{fx}[x+1,y] = E_x(x_+,y)\Delta x\frac{q}{kT}$$

$$\text{fy}[x,y] = E_y(x,y_-)\Delta y\frac{q}{kT} \qquad \text{fy}[x,y+1] = E_y(x,y_+)\Delta y\frac{q}{kT}$$

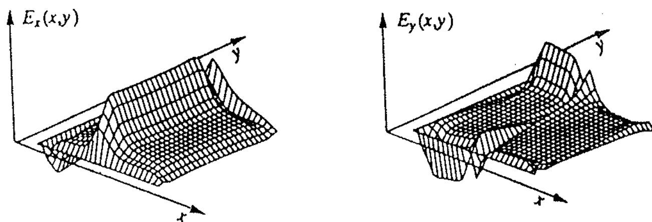

Fig. 10: Components of the electric field.

We have allowed five passes through the algorithm. Because the time interval is $\Delta t = l\,(\Delta x)^2/D$ each pass is somewhat shorter than 2 picoseconds. The net charge density $Q(x,y)$ is obtained from the resulting distributions of $p(x,y)$ and $n(x,y)$ as the last step in the algorithm. When we substitute this into (16) and (17) we obtain the two components of the electric field. These are shown in Fig.10 and a C-version of the algorithm which generated the numeric values is reproduced below the figure.

```
for (y = 0; y < Y; y++)
  for (x = 0; x < X; x++)
   {EX = EY = 0.0;
    for (u = 0; u < X; u++)
      for (v = 0; v < Y; v++)
    {delY = v-y;
   if(delY! = 0)
    {delX = u - x + .5;
    EX = EX + Q [u,v] *delX/(delY*delY + delX*delX);
    }
      delX = u - x;
      if (delX! = 0)
       {delY = v - y + .5;
      EY = EY + Q[u,v] *delY/ (*delY*delY + delX*delX),
       }
     }
   fx[x,y] = EX*1.0e-10;
   fy[x,y] = EY*1.0e-10;
   }
```

The factor 10^{-10} in the above takes account of the permittivity of Silicon, of the integration intervals of the factor q/kT and of the conversion between surface and volume density of charges involved. An interpretation of the major features of Fig. 10 tells us that the force on electrons and holes is directed inward both along the x-axis. The y field shows more intensity in the N-region than in the P which has its origin in the higher donor concentration and electron diffusivity. One major but expected feature of the electric field E_x is its high intensity along the junction region. This field eventually blocks the further migration of electrons and holes into the adjacent regions. An actual simulation of a semiconductor structure would alternate between the last two algorithms, computing the net charges from the first one and finding the resulting force factors from the latter one. These would then be substituted back into the first one. An equilibrium would eventually be established at which point te migration would cease completely.

Before we conclude let us recognize that the electronic fields could be computed in an alternate way. It is known [5], [6], [7] that the expression we have derived for the electric field from Coulomb's law is in fact the formal solution of the Poisson's differential equation

$$\frac{\partial E_x}{\partial x} + \frac{\partial E_y}{\partial y} = \frac{Q(x,y)}{\epsilon}$$

Where Q is the charge density. Unfortunately this one equation with two unknowns and as such not very useful. But it is also known from the field vector theory [8] that field components E_x and E_y are the gradients of a function $V(x,y)$ which satisfies the Poisson equation in the following way

$$\frac{\partial^2 V(x,y)}{\partial x^2} + \frac{\partial^2 V(x,y)}{\partial y^2} = -\frac{Q(x,y)}{\epsilon}$$

When this equation is solved for the scalar quantity $V(x,y)$ the field components can be obtained as the respective partial derivatives

$$E_x(x,y) = -\frac{\partial V(x,y)}{\partial x} \quad \text{and} \quad E_y(x,y) = -\frac{\partial V(x,y)}{\partial y}$$

It turns out that the effort in solving the Poisson equation for the potential is comparable to what we have done and our approach is more in keeping with the promise of staying close to first principles. Nevertheless it ought

to be pointed out that the Poisson equation in terms of potential $V(x,y)$ can be solved by the same algorithm we have developed for the particle transport by diffusion. The diffusion equation in two dimensions with constant diffusivity has the differential form

$$\frac{\partial V(x,y,t)}{\partial t} = \frac{\partial^2 V(x,y,t)}{\partial x^2} + \frac{\partial^2 V(x,y,t)}{\partial y^2}$$

When add a source function $\frac{Q(x,y)}{\varepsilon}$ to the RHS of the above and solve the equation for steady state condition, i.e. $\partial V(x,y,t)/\partial t$ the equation goes over into the form

$$\frac{\partial^2 V(x,y)}{\partial x^2} + \frac{\partial^2 V(x,y)}{\partial y^2} = -\frac{Q(x,y)}{\varepsilon}$$

Consequently we can solve the Poisson equation with the aid of equation (15) as implemented in the respective C-algorithm when we add the source function $Q(x,y)/\varepsilon$ to the RHS of the temp expression. When there are no more changes between two successive evaluations of temp the resulting distribution C[x,y] is the solution of the Poisson equation. The results obtained for our test case are identical with one or the other method and the time consumed is about the same.

7. Conclusions

The transport equation and the equivalent of the Poisson equation were derived from first principles without invocation of unsubstantiated abstraction. The two-dimensional case has been tested on a simple semiconductor structure and the corresponding algorithms have been presented in the C-language. The intent was to show that the availability of computers warrants a fresh look at the traditionally accepted mathematical models and that more intuitive approaches are made possible by taking advantage of present-day computer performance.

Ackknowledgement

The highly efficient and versatile algorithm which was used to plot the two-dimensional distributions was developed and given to me by Ing. Dragan Fidler of Zemun.

References

[1] SUPREME by Stanord, PISCES and DEPICT by Tehnology Modeling Associates, SIMPEL by Berkeley, MASTER by Silvacor.

[2] Z.Fazarinc, Discretization of Partial Differential Equations for Computer Evaluation, Computer Applications in Engineering Education, Vol.1, No.1, pp.73-85, John Wiley, 1992-93.

[3] C.Kittel and H.Kroemer, Thermal Physics 2-nd Ed., Freeman & Co., San Francisco 1980, p270 Derived from Thermodynamics, p268 from reaction rates, p361-3 from density of states.

[4] A.S.Grove, Physics and Technology of Semiconductor Devices, John Wiley 1967, p100-1.

[5] James C. Maxwell, A Treatise on Electricity & Magnetism, Clarendon Press, 1891, Chapter II.

[6] Oliver Heaviside, Electrician, Phil. Mag. XXVII, 1889, p.324

[7] Simeon D.Poisson, Bull.de la Soc. Philomathique iii, 1813, p.388

[8] I.Sokolnikoff and R.Redheffer, Mathematics of Physics and Modern Engineering, McGraw Hill, 1958, p386-7

prof. Zvonko Fazarinc, Ph.D
Stanford University, ret.
Hewlett-Packard Laboratories, ret.
880 La Mesa Drive
Menlo Park, CA 94025

Prispelo: 27.08.93 ***Sprejeto:17.09.93***

POLYIMIDE RESIN CURING IN MICROELECTRONIC APPLICATIONS

Radko Osredkar

KEYWORDS: microelectronics, resins, polymide resins, polymerizartion temperature, film quality, thin films, film degradation, film curing

ABSTRACT: Curing cycles of polyimide resins may be tailored to a specific microelectronics application, and polymerization times shortened without compromising the quality of the resulting film. However, curing these resins below 300°C may prevent full imidization and degrade the film.

Termična obdelava poliimidnih umetnih smol za uporabo v mikroelektronskih tehnologijah

KLJUČNE BESEDE: mikroelektronika, smole umetne, smole poliimidne, temperatura polimerizacije, kakovost plasti, plasti tanke, degradacija plasti, vulkanizacija plasti

POVZETEK: Termično obdelavo poliimidnih umetnih smol, ki jih uporabljajo v mikroelektronskih tehnologijah, je moč prilagoditi neki specifični uporabi. Vendar pa polimerizacija ne sme potekati pri temperaturah pod 300°C, ker sicer reakcija ne steče do kraja in kvaliteta takih polimernih tankih plasti je slaba.

1. Introduction

The polyimide group of cross linkable polymers has been investigated extensively in recent years, and successfully applied as planarization layers, intermetal dielectrics, passivation films, alpha particle barriers, adhesives, etc. in integrated as well as hybrid circuit technologies /1,2/.

Photosensitive polyimide resins have considerably increased the number of different applications of these materials /3/. The use of polyimide resins is primarily justified by its superior chemical and physical properties when cured, by its compatibility with many of the materials used in hybrid and integrated circuit technologies, and ease of their application which is similar to photoresist processing, including the required deposition and curing equipment.

Some of the drawbacks of the polyimide resins, their relatively short shelf life and gelled in time which influences their viscosity stability, can be bypassed by good housekeeping and are usually of little concern in a production environment.

Polyimide processing is relatively simple, convenient and adaptable. However, with respect to times and temperatures used in a curing cycle, there are restrictions which have to be observed when designing a curing schedule for a specific application. IR spectroscopy is a convenient tool for studying the state of polymerization of these resins /8, 9/, and a study of polyimide polymerization by this method is presented. (Results of this study have been previously published /8/.)

2. Materials and methods

The polyimide resin used in this work was Hitachi Chemical Co. PIQ (polyimide isoindoloquinazolinedione). The viscosity of the uncured resin is 1130 cps at 23°C. To facilitate spin coating the resin has been diluted with DMSO (4 parts resin to 1 part solvent). No adhesion promoter was used, even though in IC applications its use seems to be necessary /11/. Silicon wafers were coated with 2 successive coats of polyimide resin, resulting in a 2.0 μm thick film. The first coat was applied at 3000 RPM (30 sec) and dried at a 85°C for 30 min. to remove the solvents. The second coat was then applied and the resulting polyimide film cured. The two step coating cycle has been used in order to obtain a uniform film thick enough to yield IR spectra with an adequate signal to noise ratio (100 : 1 in fully cured films). The IR spectrometer used is a Perkin Elmer Model 783, operated in the transmission mode.

The curing cycle recommended by the vendor of the resin is comprised of consecutive bakings at 100°C, 220°C, and 350°C for 1 hour each, in air ambient /4/. This is similar to the curing schemes for other polyimide products /1/.

The intensity of the imide bond absorption line at 1377 cm^{-1} /5/ was measured after the curing of the resin. No increase of the line intensity could be observed by increasing the duration and temperature of the recommended curing cycle, and therefore a sample cured as described above was considered to be fully cured.

The degree of polymerization of a partially cured resin was obtained by measuring the intensity of the imide absorption line, relative to the intensity of the line in a fully cured resin.

3. Results and discussion

Time dependence of the degree of imidization during curing at 200°C and 300°C is shown on Fig. 1. It can be observed that at 300°C the resin is fully cured already after 20 min. of curing time, without any previous baking at a lower temperature. Obviously the recommended curing cycle is set quite conservatively and can be shortened without compromising the degree of polymerization of the polyimide film.

Curing the polyimide film even for extended periods at 200°C will not cause it to polymerize fully. Subsequent curing of the resin at 300°C, after it has been exposed to 200°C for 20 hours, does not increase its degree of imidization. This indicates that prolonged exposure of uncured polyimide films to temperatures below 300°C will inhibit complete curing of the films, thereby degrading their properties. This incomplete curing may be a solvent effect, as described in literature /10/. In particular, the otherwise excellent scratch resistance of the polyimide passivation films seems to be much reduced by incomplete curing.

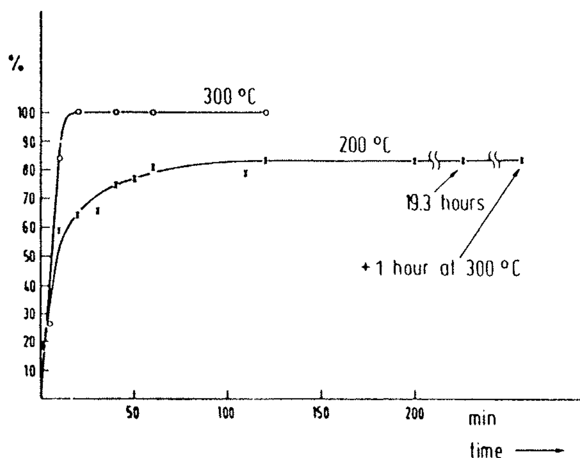

Fig. 1: Dependendence of the degree of imidization (in %) on curing time at 200 deg. C and 300 deg.C. After 19.3 hours at 200 deg. C the sample was baked at 300 deg. C for one hour.

The activation energy of polymerization of the polyimide resin is 70 kJ/mole, as calculated from the data in Fig. 1. This value is on the high side of the range of the activation energies of similar polymers /6,7/.

Temperature dependence of the degree of imidization is shown on Fig. 2. Uncured films of polyimide resin were baked for 1 hour at a certain temperature, and the degree of imidization relative to the fully cured film measured. As above, the degree of imidization at 200°C remains limited, even after 20 hours baking time, and the film will not cure fully under subsequent exposure to 300°C. However, in films cured at 100°C subsequent high temperature curing will somewhat increase the degree of imidization.

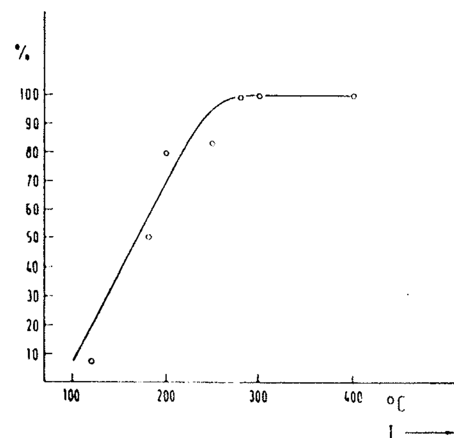

Fig. 2: Temperature dependence of the degree of imidization (in %) after 1 hour of curing time.

4. Conclusion

The standard curing schedule of the polyimide resin offers some latitude with respect to the reduced baking times. This is not true for the curing temperatures - extended exposures of the uncured resin films to temperature below 300°C will prevent full imidization of the material, thereby considerably reducing the properties of the polyimide films. This has to be taken into the account when designing a curing schedule for a specific application.

The author gratefully acknowledges the discussions and assistance with the IR measurements of Dr. F. Černec of the Institut za celulozo in papir, Ljubljana.

5. References

/1/ J. Rhodes, Semiconductor Internat., 65, (March 1981)

/2/ Schlitz et al., J. Electrochem. Soc.: Solid-State Sc. and Tech., 133, No 1, 178, (Jan. 1986)

/3/ C. Miller, Circuits Manuf., (April 1977)

/4/ Hitachi Chemical Co. Publication No. Y,2077

/5/ Hummel Scholl, Atlas der Kunststoff Analyse, Karel Hanser Verlag, (1968)

/6/ W. Lenz, Organic Chemistry of Synthetic High Polymers, Interscience Publishers, John Wiley, New York, (1967)

/7/ H. Solomon (Editor), Step Growth Polymerizations, D. C. Jones and T. R. White, 62, Marcel Deker, New York, (1972)

/8/ Osredkar, Microelectron. Reliab., Vol 28, No. 4, pp 599603, (1988)

/9/ N. Krasovskii et al, Polym. Sci. USSR, Vol 21, 1038 (1980)

/10/ T.-C. J. Hsu and Z.-L. Liu, J. Appl. Polymer Sc., Vol 46, 1821-1833 (1922)

/11/ G. Narechania et al, 1984 Int. Electron. Devices Meeting, pp 214-217, IEEE-IRPS (1984)

dr. Radko Osredkar, dipl.ing
University of Ljubljana,
Faculty of Electrical Engineering and Computer Science, Tržaka 25, 61 000, Ljubljana, Slovenia

Prispelo: 12.07.93 ***Sprejeto: 03.09.93***

NOVA GENERACIJA Mn - Zn FERITOV ZA MOČNOSTNE APLIKACIJE

Andrej Žnidaršič

KLJUČNE BESEDE: materiali magnetni, feriti močnostni, MnZn feriti, lastnosti magnetne, pretvorniki napetostni, napajalnik močnostni, raziskava materiala, področje frekvenčno, permeabilnost začetna, predmagnetizacija, izgube magnetne

POVZETEK: Študirali smo feritne materiale uporabne v različnih napetostnih pretvornikih. Izboljšali smo njihove magnetne lastnosti, zvišali začetno permeabilnost μ_i in nasičenjsko magnetizacijo B_s ter zmanjšali magnetne izgube P/V. Novi feritni materiali so posebno primerni za aplikacijo s predmagnetizacijo v frekvenčnem področju od 300 kHz do 1 MHz.

A new generation Mn - Zn ferrites for power applications

KEY WORDS: magnetic materials, power ferrites, MnZn ferrites, magnetic properties, voltage converters, power supplies, materials research, frequency domain, initial permeability, premagnetization, magnetic losses

ABSTRACT: Ferrite materials for different switch power supplies were studied. The magnetic properties were improved. Initial permeability - μ_i and saturation magnetisation - B_s were increased, while the magnetic losses P/V were decreased.
The popular frequency range for switching power supplies is from 10 to 300kHz at present, but it is more likely to be 500 kHz to some MHz in the near future.
It is well-known that predominant losses in Mn-Zn ferrite are hysteresis and eddy current losses. The main motivation for using ferrite in transformers cores are low eddy current losses. Eddy current loss can be reduced by increasing the resistivity of the ferrite which depends on the grain boundary resistivity and the grain resistivity.
Three type of additions can be distinguished with respect to the kind of incorporation in the basic ferrite. The first type of addition acts indirectly via liquid phase formation and influence the microstructural development during sintering.
Additions of the second type modify the grain boundary chemistry and increase the grain boundary resistivity, as for example Ca, Si.
The third type of cation is soluble in the spinel lattice, as for example Ta, Sn etc. They effect the intrinsic properties such as magnetization, anistropy, resistivity and after effects.
The desired chemical composition must lead to a high saturation magnetization and to a total anistropy optimized according to the operating frequency, the operating temperature and the ceramic microstructure.
Raw material quality determines ferrite quality. The microstructure of high frequency power ferrite must be controlled very carefully. So for synthetising a power ferrite with high performances, the raw materials impurities content and powder reactivity before firing have to be controlled precisely.
Firing is a very important step in the process, because it is during this step that the ferrite is definitively synthesized and that the microstructure is performed. So atmosphere control in firing profile have to be carefully chosen.
Our main goal was to obtain a fine and uniform microstructure and this has been possible by controlling sintering temperature, heating rate and high temperature soak time. Moreover, during the firing, the oxygen partial pressure pO_2 determines the Fe^{2+} / Fe^{3+} ratio and then increase the resistivity by decreasing the hopping mechanism.
A new power ferrite designated as 35G, 45G and 65G for switching power supplies in frequency range from 300 kHz to 1 MHz has been successfully developed and put in the market already.

UVOD

Feriti so in ostajajo tehnično zelo pomembni oksidni materiali. Obseg in uporaba feritnih jeder se na različnih področjih elektronike zelo spreminja. Zavisi od razvoja in aplikativnih sposobnosti samih feritov, kot tudi drugih pasivnih in aktivnih komponent. S prehodom od analogne na digitalno telekomunikacijsko tehniko se večajo potrebe po širokopasovnih prenosnikih, s prodorom elektronike na različna področja tehnike pa naraščajo potrebe po necentraliziranih tokovnih izvorih, impulznih napetostnih pretvornikih itd., v katerih so vgrajeni visokofrekvenčni maloizgubni močnostni Mn - Zn feriti. Potrebe po prenosu večjih moči ob istočasnih zahtevah po miniaturizaciji pa narekujejo raziskave v smeri razvoja novih feritnih materialov z nizkimi magnetnimi izgubami v širokem frekvenčnem področju.

Z razvojem nove generacije močnostnih Mn - Zn feritnih materialov in izpopolnjenih geometrijskih oblik jeder, ki omogočajo prenose večjih moči pa prodira uporaba feritnih jeder tudi na področje širokopotrošne in profesionalne elektronike (napajalniki, linijski transformatorji, impulzni transformatorji, vrstični transformatorji, impulzni napetostni pretvorniki, razne dušilke, varilne elektrode), torej na področje tako imenovane energetske elektronike. Z razvojem tranzistorja, močnostnega MOSFET in hitrega bipolarnega tranzistorja smo v zadnjih tridesetih letih doživeli takoimenovano drugo elektronsko revolucijo. Uporaba in razvoj MOSFET in

hitrih bipolarnih tranzistorjev omogoča delovanje in uporabo različnih napetostnih pretvornikov pri frekvencah tudi nad 500 kHz. Delovanju pri tako visokih frekvencah pa morajo biti prilagojene tudi lastnosti močnostnih feritnih materialov in jeder. Feritni materiali uporabni v navedenih aplikacijah in širokem frekvenčnem področju od 300 kHz do 1 MHz se odlikujejo po visoki nasičenjski gostoti B_s, Curievi temperaturi T_c, notranji upornosti (ρ) in začetni permeabilnosti μ_i, prilagojeni delovni (uporabni) frekvenci ter po nizkih temperaturno in frekvenčno odvisnih magnetnih izgubah (P/V), ki dosegajo minimalno vrednost pri delovni temperaturi magnetnega sklopa. Pri delovnih frekvencah Mn - Zn feritnega jedra $f \geq 500$ kHz je zelo pomembna temperaturna odvisnost magnetnih izgub. Magnetne izgube v splošnem naraščajo z rastočo frekvenco, kar povzroča segrevanje feritnega jedra in celotnega magnetnega sklopa. Zato je zelo pomembno, da imajo močnostni Mn - Zn feritni materiali visoko Curievo temperaturo $T_c \geq 200^{\circ}C$, kar dosežemo s primerno kemijsko sestavo bogato s Fe_2O_3in Mn_3O_4, ter visoko nasičenjsko gostoto pri delovni temperaturi T_{del} = 90 do 105°C. Magnetne izgube ustreznega Mn - Zn ferita morajo imeti negativni temperaturni koeficient in doseči minimalno vrednost na področju delovne temperature magnetnega sklopa. Na magnetne izgube feritnega materiala vplivajo različni faktorji, kot so: kemijska sestava, valenca ionov, nečistoče, dodatki (Sn, Ti, Ca, Ta), pore in njihova porazdelitev ter pojavi na mejah med zrni. Zato je potrebno za zmanjšanje magnetnih izgub preprečiti vse navedene vplive, dobro obvladovati tehnološki proces izdelave feritnih jeder, posebno pripravo feritnega prahu in sintranje. Feriti z nizkimi magnetnimi izgubami so zaželeni skoraj v vseh aplikacijah, izjema je le absorbcija elektromagnetnih valov v področju resonančnih frekvenc. Pri feritih z visoko nasičenjsko gostoto in nizko magnetokristalno anizotropijo, dosegamo sicer visoke permeabilnosti, vendar pa nizke specifične upornosti zaradi prisotnosti Fe^{2+}in takoimenovanega Hooping efekta $Fe^{2+} \leftrightarrows Fe^{3+} + 1^{e-}$, ki zvišujejo magnetne izgube zaradi vrtinčastih tokov. Hooping efekt začne postopno naraščati, ko prekoračimo delovno frekvenco $f \geq 100$ kHz. Dušenje omenjenega efekta je možno z zvišanjem specifične upornosti, kar dosežemo z dopiranjem različnih malih dodatkov (npr. Ti^{4+}). Ti zasedejo v kristalni rešetki B mesta v bližini Fe^{2+} iona in tako preprečijo gibanje elektronov med Fe^{2+} in Fe^{3+}. Druga možnost dušenja omenjenega efekta ter s tem zmanjševanja magnetnih izgub, kot posledica vrtinčastih tokov, je tvorba izolacijskega filma na mejah med zrni, kar dosežemo z dopiranjem različnih malih dodatkov (npr. Ca^{2+}, Si^{2+}). Kemijska sestava samih zrn se pri tem ne spreminja, dopanti se koncentrirajo na mejah med zrni, kar omogoča ohranjanje nizkih magnetnih izgub feritnega materiala. Tretja možnost zvišanja specifične upornosti in s tem zmanjšanja magnetnih izgub, je pravilen razvoj mikrostrukture končnega feritnega materiala, na katero vplivamo predvsem s fazo sintranja. Če je mikrostruktura nehomogena in se kemijska sestava v posameznih zrnih spreminja je distribucija magnetnega pretoka in permeabilnosti v zrnih neenakomerna. Ker razmerje med gostoto magnetnega pretoka B in močnostnimi izgubami ni linearno, povzroči nehomogenost magnetnega pretoka, zvišanje magnetnih izgub v samem feritu. Zato pri pripravi močnostnih feritnih materialov uporabnih pri višjih frekvencah uporabljamo zelo čiste vhodne surovine, rast zrn pri sintranju pa zaviramo z uvajanjem raznih dodatkov (npr. Ta^{5+}, Sn^{4+}).

TIPIČNE MAGNETNE LASTNOSTI

Močnostni Mn - Zn feriti so poleg trajnih keramičnih magnetnih materialov, komercialno najuspešnejše področje, s trendom rasti cca. 10 - 15 % na leto. Potrebe po prenosu večjih moči ob istočasnih zahtevah po miniaturizaciji pa usmerjajo raziskave v smeri razvoja novih materialov, novih geometrijsko prilagojenih oblik, kakor tudi v smeri izboljšave že obstoječih feritnih materialov.

Tudi v Feritih, edinem proizvajalcu feritnih materialov na področju Slovenije, se zavedamo, da brez sledenja in prilagajanja hitrim tehnološkim dosežkom, ki jih vsak dan doživljamo na področju širokopotrošne in profesionalne elektronike ni mogoče dolgo ostati na zahtevnih trgih razvitega sveta, kamor smo zaradi majhnosti našega tržišča prisiljeni izvažati cca. 80 % celotnega proizvodnega programa. Zaprtost in skope informacije na področju tržno zanimivih elementov za elektroniko nas sili, da veliko pozornost posvečamo lastni razvojni dejavnosti, v tesnem sodelovanju z IJS - K 5. Plod skupnega razvojnega dela mešanega tima R.O. - Feriti in IJS - K 5 je tudi razvoj in vpeljava redne proizvodnje nove generacije močnostnih Mn - Zn feritov, s katerimi smo se izenačili z materiali, ki jih proizvajata renomirana proizvajalca Siemens in Philips.

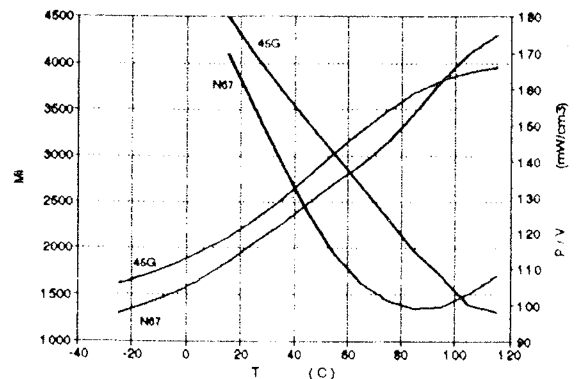

Diagram 1: Začetna permeabilnost in W izgube v odvisnosti od temperature (45G, N67)

Tabela 1.- Močnostni Mn - Zn ferit uporaben v frekvenčnem področju do 300 kHz

Material	μ i	P/V (mW/cm³) 25°C	f = 100 kHz, 100°C	B = 0.1 T 25°C	B (mT) 100°C
45G - Iskra	2300	≤ 170	≤ 110	≥ 500	≥ 320
N67 - Siemens	2300	≤ 160	≤ 100	≥ 510	≥ 320
3C85 - Philips	2000	≤ 230	≤ 165	≥ 500	≥ 330

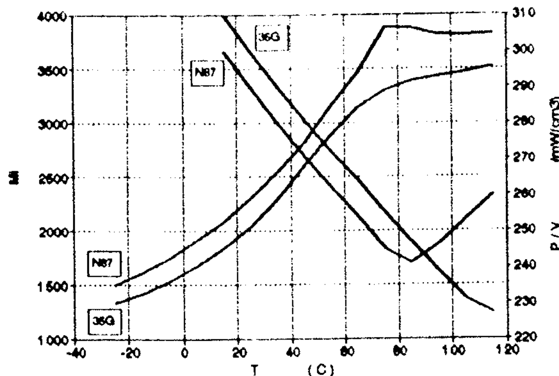

Diagram 2: Začetna permeabilnost in W izgube v odvisnosti od temperature (35G, N87)

Tabela 2.- Močnostni Mn - Zn ferit uporaben v frekvenčnem področju do 500 kHz

Material	μ i	P/V (mW/cm³) 25°C	f = 500 kHz, 100°C	B = 0.1 T 25°C	B (mT) 100°C
35G - Iskra	2000	≤ 300	≤ 230	≥ 500	≥ 320
N87 - Siemens	2300	≤ 290	≤ 240	≥ 510	≥ 320
3F3 - Philips	2000	≤ 225	≤ 230	≥ 500	≥ 330

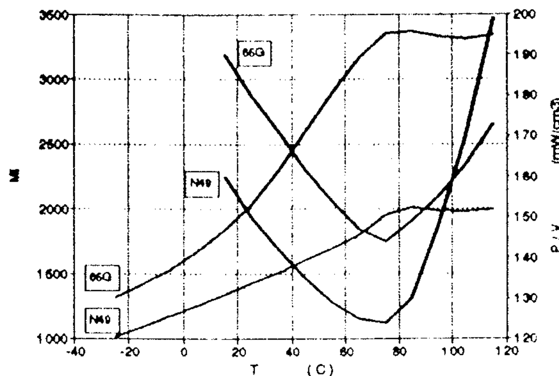

Diagram 3: Začetna permeabilnost in W izgube v odvisnosti od temperature (65G, N49)

Tabela 3.- Močnostni Mn - Zn ferit uporaben v frekvenčnem področju do 1 MHz

Material	μ i	P/V (mW/cm³) 25°C	f = 500 kHz, 100°C	B = 0.1 T 25°C	B (mT) 100°C
65G - Iskra	2000	≤ 180	≤ 190	≥490	≥ 320
N49 - Siemens	1400	≤ 150	≤ 170	≥ 510	≥ 320
3F4 - Philips	2000	≤ 175	≤ 180	≥ 500	≥ 330

ZAKLJUČEK

Recesija, ki je zajela svetovni trg elektronske industrije v letih 1991, 1992 in se v določeni meri prenesla tudi v leto 1993, je močno vplivala na strukturo povpraševanja po feritnih materialih. Tako imenovan klasičen program feritnih materialov, ki je v preteklem obdobju obvladoval predvsem področje zabavne elektronike in različne telekomunikacijske sisteme, zaradi zasičenosti, velike ponudbe na svetovnem trgu in spremembe tehnologije izdelave, izgublja svoj prvotni namen. Glede na trende, ki se pojavljajo na področju elektronske industrije v smeri video teleinformatike, prenosne telefonije, satelitskih telekomunikacij, zabavne elektronike (HDTV) in napajalnikov različnih oblik in dimenzij, se spreminja tudi struktura tržno zanimivih Mn-Zn feritnih materialov. Najvišjo stopnjo rasti predstavljajo visokofrekvenčni močnostni Mn-Zn feriti, ki pokrivajo frekvenčno področje od 300 kHz do 1MHz, vgrajeni v različnih napetostnih pretvornikih in napajalnikih, med katerimi so prav gotovo najpomembnejši SMPS (Switch Mode Power Supplies), ki pomenijo pravo revolucijo v omenjenem razvoju. Razvoj omenjenih napajalnikov sovpada z razvojem hitrih bipolarnih tranzistorjev, ki usmerjene signale na vhodu spremenijo v pulze visokih frekvenc, ter jih nato s feritnimi transformatorji transformiramo na zahtevano izhodno napetost.

Z razvojem nove generacije močnostnih Mn - Zn feritov, smo razširili svoj program tržno zanimivih visokokvalitetnih Mn - Zn feritnih materialov ter se po lastnostih izenačili s Siemensom in Philipsom, ki sta trenutno edina evropska proizvajalca omenjenih kvalitet.

Zaradi hitrih sprememb, ki jih vsak dan doživljamo na področju elektronike, usmerjamo svoje nadaljne razvojne akcije skladno s trendi svetovnih proizvajalcev, v razvoj višje frekvenčnih Mn-Zn feritov, ki bodo vgrajeni v različnih visokonapetostnih transformatorjih v frekvenčnem področju do 1.5 MHz ter novo kvaliteto visokopermeabilnih Mn-Zn feritov (μ_i = 15000), ki bodo vgrajeni v različnih transformatorjih, induktorjih ter visokoselektivnih filtrih na področju profesionalne, prenosne in zabavne elektronike ter telefonije, zaradi prodora miniaturizacije in prehoda iz analognih na digitalne telefonske sisteme.

ZAHVALA

Na koncu bi se želel zahvaliti mag. Marjeti Limpel in prof. dr. Mihu Drofeniku za strokovno pomoč ter Ministrstvu za znanost in tehnologijo, ki je z velikim razumevanjem finančno podprlo razvoj omenjenih materialov.

REFERENCE:

/1/ A. ŽNIDARŠIČ: Vpliv Sn^{4+}na Mn-Zn ferite za močnostne aplikacije - SD 91, Portorož

/2/ A. ŽNIDARŠIČ, M. LIMPEL, G. DRAŽIČ, M. DROFENIK Investigation of power ferrites - ECERS second conference - Augsburg 1991 - ZRN

/3/ A. ŽNIDARŠIČ, M. LIMPEL, G. DRAŽIČ, M. DROFENIK Influence of Ta_2O_5on microstructure in low loss power ferrites - MIEL SD 92, Portorož

/4/ A. ŽNIDARŠIČ, M. LIMPEL, M. DROFENIK: Microstructure control in low loss power ferrites - ICF 6 1992 - Tokyo, Japonska

/5/ A. ŽNIDARŠIČ: Mn-Zn feriti za močnostne aplikacije Prvo slovensko posvetovanje - ELEKTRIČNE NAPRAVE - SPEN 92, Maribor

/6/ A. ŽNIDARŠIČ, M. LIMPEL, M. DROFENIK: Patentna prijava 9300259 - Urad Republike Slovenije za varstvo indust. lastnine - Kemijska sestava, tehnološki in proizvodni postopek priprave močnostnih Mn-Zn feritov, uporabnih v frekvenčnem področju od 16 kHz do 1 MHz

Andrej ŽNIDARŠIČ dipl.ing.
ISKRA FERITI d.o.o., Stegne 29,
61000 LJUBLJANA

Prispelo: 19.07.93 ***Sprejeto: 03.09.93***

RAZISKAVE SEGREGACIJE ANTIMONA NA POVRŠINI NEORIENTIRANE ELEKTRO PLOČEVINE Z METODO AES

M. Jenko, F. Vodopivec, B. Praček, M. Godec, D. Steiner

KLJUČNE BESEDE: pločevina elektro, pločevina silicijeva, jekla silicijeva, pločevina elektro neorientirana, lastnosti magnetne, izgube v jedru, termodinamika segregacije, antimon, difuzija antimona, rekristalizacija, orientacija zrn kristalografska

POVZETEK: Segregacijo antimona na površini neorientirane elektro pločevine smo raziskali z eksperimentalno metodo osnovano na spektroskopiji Augerjevih elektronov, ki smo jo razvili v ta namen. V temperaturnem področju od 500 do 850°C smo določili kinetiko rasti segregirane plasti antimona. Ocenili smo difuzijski koeficient antimona v siliciranem feritu in izračunali aktivacijsko energijo difuzije.

AES Investigation of Surface Segregation of Antimony in Non Oriented Electrical Sheets

KEY WORDS: electro sheet, silicon sheet, silicon steels, nonoriented electric sheet, magnetic properties, core losses, segregation thermodinamics, antimony, antimony diffusion, recrystallization, crystalographic grain orientation

EXTENDED ABSTRACT: The segregation of antimony on the surface and interfaces of iron-base alloys is interesting from different point of view and has been discussed in several papers. It is well known that several elements act as severely embrittling impurities in steel, among them antimony, and that they strongly segregate to grain boundaries of body centered cubic iron-base alloys. A beneficial effect of a small amount of antimony 0.03 - 0.1 wt% Sb in silicon electrical steels on the recrystalization behaviour and on energy losses was also found (1-10). It has been recognized that the small addition of Sb results in substantial texture improvement in non oriented and oriented silicon steels. The possible explanation of this effect is that antimony being a surface active element, segregates on the surface and grain boundaries and affects the recrystalization behaviour producing an increase of the number of ferrite grains with soft magnetic lattice space orientation in the sheet plane. It is suggested that the nucleation of grains with (111) orientation occurs in the vicinity of the original hot band grain boundary (13) and antimony might be responsible for retarding the nucleation rate of the (111) orientation.

The aim of this work was to determine the kinetics of surface antimony segregation in Fe-Si alloy dopped with antimony using an AES surface analytical method (20). Such alloy of Fe-Si with approximatly 2 %Si is widely used as nonoriented silicon electrical sheet, where grain orientation improves magnetic properties (1-6).

Kinetics of surface segregation of antimony in Fe-Si alloy in the temperature range from 500 to 850°C was measured using a new developed experimental method based on Auger Electron Spectroscopy.

The amount of segregated antimony on the surface of transformer steel increased in temperature range from 600 to 700°C. The saturated layer thickness of 0.3 nm was estimated with AES depth profile analysis, which correspond to the calculated value of one Sb monolayer. At the temperatures $T \geq 750°C$ a diminution of the amount of segregated antimony was measured, probably provoked by surface evaporation process or connected with the phenomenon of maximum of reversible segregation (11-15).

In the temperature range from 650 to 750°C only Sb segregation was measured. From the surface segregation kinetics and its temperature dependence in the temperature range from 650 to 750°C, the diffusion coefficient and activation energy of Sb diffusion in bulk of 260 kJ mol^{-1} were determined in good agreement with data of Nishida (25).

On the basis of obtained results we assume that Sb segregation could decrease the surface energy of grains emerging to the surface and through it could affect also the kinetics of grains growth.

The investigation of recrystallized grain growth in silicon electrical sheet shows that antimony grain boundary segregation hinders the formation of recrystallized nuclea in the temperature range from 500 to 700°C (16,17,26) and it is supposed that the surface segregation affects the recrystallization by decrease of surface energy of soft magnetic grains, and their growth to the final texture and through it decreases the core loss.

1. UVOD

Elektro pločevina je ključni material za generiranje in transformacijo električne energije. Mehko magnetni materiali se v obliki lamel uporabljajo za jedra električnih, vrtečih se strojev, transformatorjev in naprav. V teh se spreminja smer magnetnega polja v odvisnosti od frekvence izmeničnega toka. Za spremembo smeri magnetenja je potrebna energija, ki se izraža v obliki vatnih izgub na kilogram teže pločevine (W/kg) pri določeni magnetilnosti (1). Vatne izgube so torej energija, ki je potrebna za preusmerjanje elementarnih magnetnih domen z zasukom mej med njimi (Blochove stene) in za pokrivanje izgubnih tokov. Na vatne izgube vplivajo naslednji faktorji: kemijska sestava, nečistoče, napetosti, velikost zrn, orientacija zrn, debelina lamel in stanje površine (1,2).

Med ekonomsko pomembne mehko magnetne materiale sodijo silicijeva jekla, ki jih uporabljamo v proizvodnji neorientiranih in orientiranih elektro pločevin (1-6).

Neorientirana, oz. neteksturirana elektro pločevina, dinamo pločevina, mora biti izotropna, da so vatne izgube neodvisne od smeri pod katero se glede na smer valjanja iz nje izrežejo lamele za magnetna jedra. Orientirane elektro pločevine pa morajo imeti tako teksturo, da so v ravnini valjanja le kristalna zrna z lego (110) ali (100), kristalna smer /001/ pa se ujema s smerjo valjanja. Te vrste pločevine, imenovane tudi trafo pločevine, imajo nižje vatne izgube in iz njih izdelujejo posebno oblikovana magnetna jedra za transformatorje (1-6).

Naraščajoči energijski stroški so privedli do zahteve po energijsko zmogljivejših motorjih in transformatorjih ter do vedno novih raziskav in razvoja jekel za elektro pločevine. Elektromagnetne lastnosti, ki jih zahtevamo od elektro pločevin so: visoka magnetilnost, visoka permeabilnost in nizke vatne izgube ob čim nižjih proizvodnih stroških (1-6).

Znano je, da majhni dodatki antimona (0.03% - 0.1% Sb) v silicijeva jekla ugodno vplivajo na nastanek teksture, v neorientiranih elektro pločevinah in zmanjšajo vatne izgube (8- 16).

Antimon je površinsko aktiven element, ki segregira po mejah zrn in po prostih površinah. Segregacija je v metalurgiji uveljavljen izraz za adsorbcijo. Na rekristalizacijo vpliva s tem, da pospešuje rast rekristaliziranih zrn z magnetno mehko lego blizu ploskve (100), oz. zavira rast rekristaliziranih zrn z magnetno trdo lego blizu ploskve (111) v ravnini pločevine, slika 1.

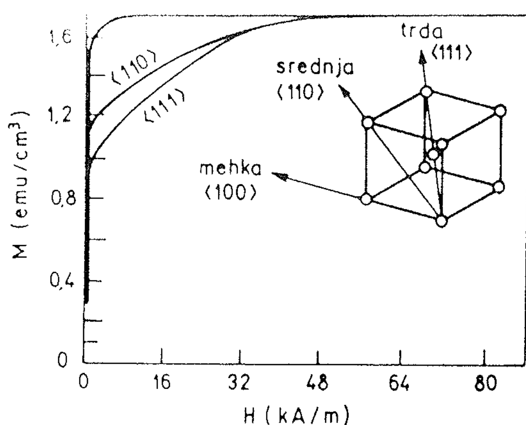

Slika 1: Magnetilne krivulje za monokristal prostorsko centriranega železa v odvisnosti od kristalografske smeri (1).

Kinetika segregacije je odvisna od koncentracije segregirajočega elementa v masivnem materialu in od difuzije. Grabkejeva skupina je raziskala binarne sisteme Fe-C, Fe-Si, Fe-Al, Fe-P, Fe-S, Fe- Sn, Fe-Sb z namenom, da bi določili ravnotežno segregacijo in njihovo medsebojno delovanje z različnimi elementi (23).

Komercialna jekla so kompleksni sistemi in za ocenitev segregacije v njih je potrebno raziskati vsako jeklo posebej (14).

Segregacijo antimona na površini neorientirane elektro pločevine smo študirali v ultra visokem vakuumu v temperaturnem področju od 500 do 850°C. Kinetiko rasti segregirane plasti na površini neorientirane elektro pločevine smo zasledovali z metodo AES, z direktnimi meritvami; to je z zasledovanjem časovnega poteka spremembe razmerja intenzitet vrhov Augerjevih elektronov antimona in železa I_{Sb}/I_{Fe}.

Kinetiko segregacij smo zasledovali na površini, ki je bila predhodno očiščena z ionskim jedkanjem. Koncentracijo antimona, ki je segregiral na površino smo določili v odvisnosti od temperature in od koncentracije v masivnem materialu. Iz kinetike segregacije Sb na površini smo ocenili difuzijski koeficient in aktivacijsko energijo difuzije antimona v siliciranem feritu.

2. IZHODIŠČE RAZISKAVE

Študij segregacije elementov po mejah zrn, po faznih mejah in po prostih površinah je bil omogočen šele z razvojem modernih, občutljivih metod za karakterizacijo trdnih površin. Legirni elementi in elementi nečistoč segregirajo v posameznih fazah proizvodnega procesa in povzročajo različne transformacije v trdnem. Nekateri elementi selektivno vplivajo na procese, ki se začenjajo na površini kot so adsorbcija, oksidacija, rekristalizacija itd.; krhkost materiala, sintranje, lezenje itd., pa so v direktni povezavi s sestavo na mejnih površinah (2,20,21).

V zadnjem desetletju je bila s tega področja objavljena cela vrsta del, v katerih avtorji študirajo segregacije elementov, ki se v zelo nizkih koncentracijah nahajajo v jeklih in njih vpliv na kvaliteto končnega izdelka (2,11-17).

O koristnem vplivu Sb v silicijevih jeklih za neorientirano elektro pločevino na razvoj teksture je poročalo več avtorjev (3-17).

Študij segregacij na površini elektro pločevine je v slovenskem prostoru pogojeval razvoj nove eksperimentalne metode, ki temelji na metodi AES (11-14). Omogoča raziskave v vakuumski posodi spektrometra Augerjevih elektronov v UVV pri temperaturah do 850°C.

Cilj naših raziskav je razumevanje segregacije antimona na površini neorientirane elektro pločevine in njenega vpliva na razvoj teksture, ki je v neposredni povezavi z vatnimi izgubami, ki so osnovno merilo za kakovost elektro pločevine.

3. EKSPERIMENTALNO DELO

Jeklo za neorientirano elektro pločevino je bilo izdelano s taljenjem v laboratorijski vakuumski indukcijski peč na Inštitutu za kovinske materiale in tehnologije. Ulito je bilo v ingote, ki so bili vroče izvaljani v trak debeline 2,5 mm. Ta je bil nato hladno izvaljan do debeline 1,2mm in po vmesnem žarjenju za razogljičenje in rekristalizacijo, izvaljan do končne debeline 0.5mm.

Študij segregacije antimona na površini neorientirane elektro pločevine, je potekal v dodatno opremljenem spektrometru Augerjevih elektronov PHI, Model SAM 545 A.

Vzorce iz jekla, s kemijsko sestavo: 1,89 % silicija, 0,5 % aluminija, 0,15 % mangana 0,003 % ogljika, 0,011 % žvepla, 0,016 % fosforja in 0,052 % antimona, dimenzij 30 x 1,5 x 0,1 mm, smo elektro uporovno segrevali. Debelejših vzorcev ne moremo uporabiti zaradi omejitev, ki nastopijo pri elektro uporovnem segrevanju vzorca v ultra visokem vakuumu. Temperaturo smo kontrolirali s termočlenom Fe-CuNi, premera 0,1mm, ki smo ga točkovno privarili na zadnjo stran vzorca v neposredno bližino analiznega mesta.

Površino vzorca smo pred segrevanjem v vakuumski posodi spektrometra očistili z ionskim jedkanjem med cikličnim segrevanjem. Na ta način smo lahko, na površini, odstranili vse nečistoče razen ogljika. V temperaturnem področju od 300 do 500°C segregira na površini ogljik, ki se pri višjih temperaturah raztaplja v feritu.

S profilno AES analizo smo ocenili debelino segregirane plasti antimona na površini vzorca (19,21). Hitrost jedkanja antimona smo ocenili s primerjavo hitrosti jedkanja tanke Sb plasti znane debeline (21).

Po končanem eksperimentu smo površino vzorca očistili z Ar^+ ioni in s ponovnim segrevanjem znova zasledovali nastanek segregacije na površini. Tako smo lahko brez poseganja v vakuumsko posodo spektrometra en vzorec uporabili za več poskusov.

AES analize so bile izvedene s statičnim elektronskim curkom 3keV / 1μA, premera 45 μm pri vpadnem kotu 30°.Ionsko jedkanje je potekalo z Ar^+ ioni, energije 1 keV in 3 keV , pri gostoti ionskega toka $0{,}138 Am^{-2}$, merjeni pri vpadnem kotu 47°.

Občutljivost AES metode je 0,1 at.%, relativna natančnost pa 0,5%.

4. REZULTATI

Kinetiko segregacije antimona na površini vzorca smo določili z direktnimi meritvami, to je z zasledovanjem časovnega poteka spremembe razmerja intenzitet prehodov Augerjevih elektronov $Sb(M_{4,5}N_{4,5}N_{4,5})$ in $Fe(LM_{2,3}V)$ pri kinetičnih energijah 454 eV za Sb in 651 eV za Fe. Kinetika segregacije antimona na površini neorientirane elektro pločevine pri konstantnih temperaturah 550, 650, 700, 750, 800 in 850°C je prikazana na sliki 2.

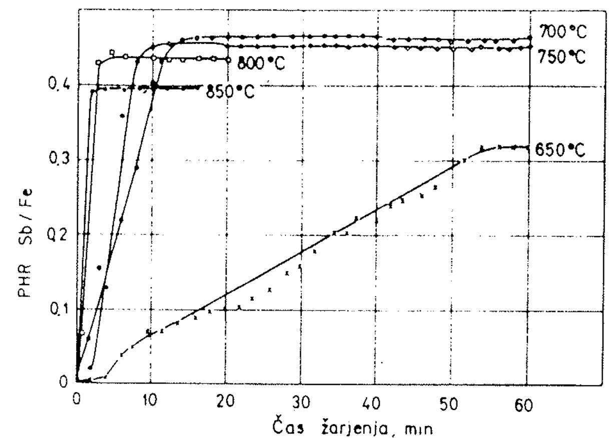

Slika 2: Kinetika segregacije antimona na površini neorientirane elektro pločevine pri temperaturah 650, 700, 750, 800 in 850°C.

Vsebnost antimona v neorientirani elektro pločevini, to je v masivnem materialu je 0,02 at.%, kar je pod mejo občutljivosti AES metode. Rast segregirane plasti antimona smo z metodo AES lahko zasledovali šele pri procesu segrevanja, pri temperaturah T≥600°C. Antimon prične na površini neorientirane elektro pločevine segregirati z zaznavno hitrostjo šele pri 600°C in doseže maksimalno vrednost pri 700°C, s koncentracijo okrog 15 at.% Sb. Pri višjih temperaturah (T≥750°C) je debelina segregirane plasti antimona nekoliko nižja, kar si lahko razlagamo s pojavom maksimuma reverzibilne segregacije, oz. z odparevanjem antimona, ki ima visok parni tlak; slika 3.

Kinetika segregacije je odvisna od koncentracije segregirajočega elementa v masivnem materialu in od stopnje difuzije.

S profilno AES analizo smo ocenili debelino segregirane plasti antimona na površini pločevine, ki je nastala po 30 minutah žarjenja na 700°C. Ocenjena vrednost debeline segregirane plasti Sb je 0.3 nm, kar je enako izračunani vrednosti debeline za 1 monoplast antimona. Debelino ene monoplasti antimona smo izračunali s pomočjo atomske mase in gostote $d=(M/N_A)^{1/3}$, pri čemer je: d-poprečna debelina monoplasti, M- molska ali atomska masa - gostota snovi in N_A - Avogadrovo število (18). Hitrost jedkanja antimona smo ocenili z jedkanjem tanke naparjene Sb plasti znane debeline (11).

Iz kinetike segregirane plasti antimona na površini neorientirane elektro pločevine in njene temperaturne odvisnosti smo v temperaturnem intervalu 650-750°C z uporabo Cranckove enačbe (22) $C_s= 2c_b(\frac{Dt}{\Pi})^{1/2}$, kjer

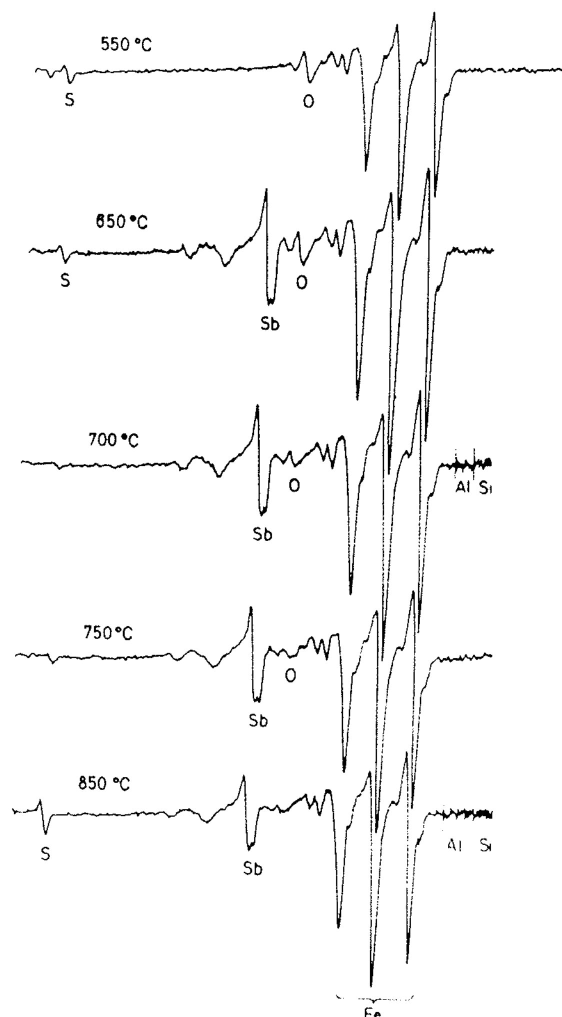

Slika 3: AES spektri površine neorientirane elektro pločevine z Augerjevimi vrhovi Fe (598eV, 651 eV in 703 eV), Sb (454 eV), C(272 eV), O(510 eV), P(120 eV), S(152 eV), Al(1396 eV) in Si(1616 eV) v segregirani plasti na površini pločevine po 20 minutah žarjenja pri temperaturi 550°C, po 60 minutah žarjenja pri 650, 700, 750 in 800°C ter po 10 minutah pri temperaturi 850°C.

pomeni c_s, c_b- koncentraciji antimona na površini, oz. v masivnem materialu, D-difuzijski koeficient antimona v masivnem materialu in t- čas; ocenili difuzijski koeficient in aktivacijsko energijo difuzije.

Aktivacijska energija difuzije antimona v siliciranem feritu je enaka 260 kJ/mol, frekvencijski faktor D_o smo izračunali iz enačbe, ki jo podaja Nishida (25): $\ln D_o = 9.3 \times 10^{-5} Q - 25.9$

Antimon segregira na površini neorientirane elektro pločevine v temperaturnem področju v katerem poteka tudi proces rekristalizacije, ki je ključen pri izdelavi le-te. Torej lahko vpliva na tvorbo teksture in s tem posredno na zmanjšanje izgub. Raziskali smo vpliv antimona na rast rekristaliziranih zrn tako, da smo raziskali dve jekli iz enakih osnovnih surovin od tega je bilo eno mikrolegirano z antimonom. V temperaturnem področju od 700

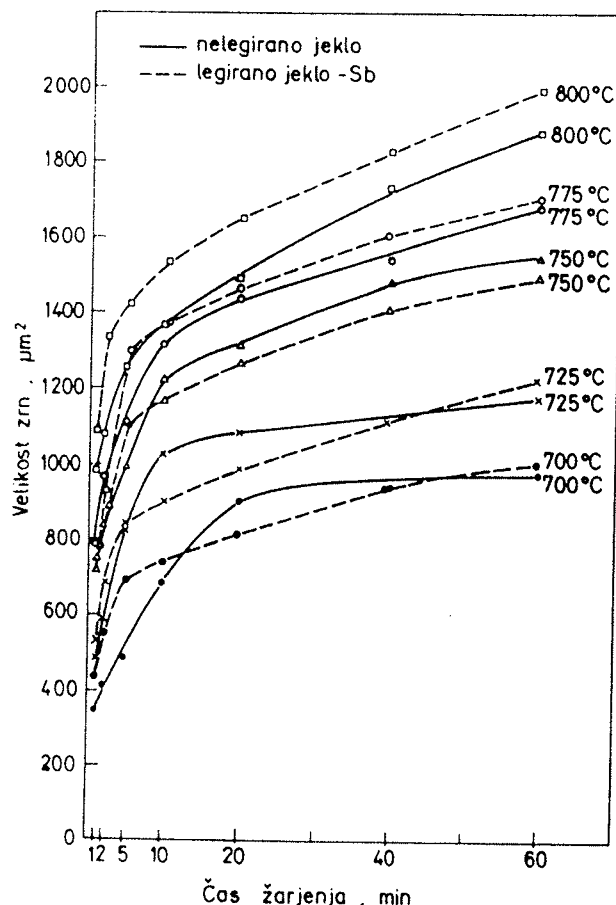

Slika 4: Odvisnost med trajanjem žarjenja in velikostjo zrn za jekla z in brez antimona

do 800°C smo določili velikost rekristaliziranih zrn v obeh preiskovanih jeklih, slika 4.

Iz rezultatov te raziskave je mogoče sklepati, da je v jeklu z antimonom nastanek rekristalizacijskih kali počasnejši kot v jeklu brez antimona. Zato so zrna po končani rekristalizaciji večja v jeklu z kot v jeklu brez antimona, kar si razlagamo z dejstvom, da je v prvem primeru mogoča dalj časa rast kali v deformiranem matriksu (16, 17, 26).

Z uporabo jedkala in postopka opisanega v referenci 27 smo dobili jedkalne figure, katerim smo s SEM posnetki v vrstičnem mikroskopu določili približno kristalografsko orientacijo zrn glede na smer valjanja v vzorcih jekel z in brez antimona, po žarjenju za rekristalizacijo, slika 5.

Iz slike 5 je razvidno, da je gostota zrn z magnetno mehko lego blizu ploskve (100) veliko večja v jeklu mikrolegiranim z antimonom (b), kot v nelegiranem jeklu (a), kar potrjuje hipotezo ugodnega vpliva mikrolegiranja jekel za neorientirano elektro pločevino z antimonom.

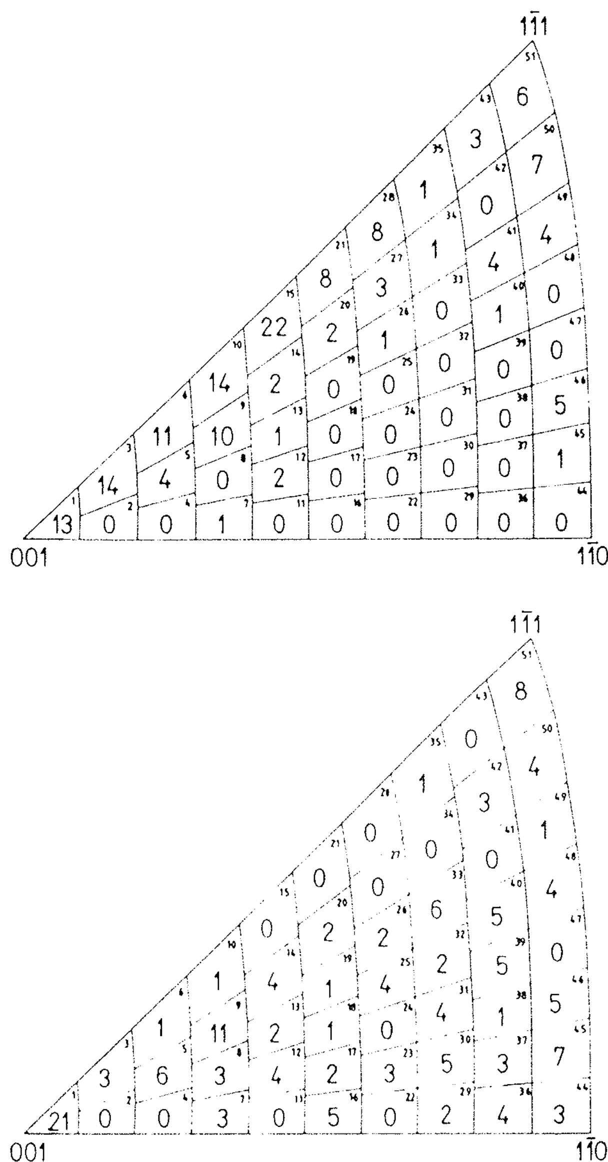

Slika 5: Pozicije jedkalnih figur kristalnih zrn glede na pravokotno projekcijo v standardnem trikotniku
a) za nelegirano jeklo
b) za jeklo legirano z antimonom

5. ZAKLJUČEK

Določili smo kinetiko segregacije antimona na površini neorientirane elektro pločevine pri temperaturah 650, 700, 750 in 800°C.

Antimon prične segregirati na površini neorientirane pločevine pri temperaturi 600°C z zaznavno hitrostjo.

Debelina segregirane plasti z naraščajočo temperaturo narašča in doseže maksimalno vrednost, približno 1 monoplast, pri 700°C.

Z naraščajočo temperaturo (T ≥ 750°C) debelina segregirane plasti upada.

Rezultati raziskave rasti rekristaliziranih zrn v silicijevih elektro pločevinah kažejo, da segregacija antimona po mejah zrn vpliva na nastanek rekristalizacijskih kali in predpostavljamo, da površinska segregacija vpliva na rekristalizacijo s tem, da zniža površinsko energijo zrn z nizkim indeksom prostorske orientacije in povzroča njihovo rast in formiranje teksture, kar ima za posledico znižanje vatnih izgub.

6. LITERATURA

1. G.Lyudkovski, P.K.Rastogi, M. Bala, Journal of Metals, 1 (1986) 18-26.

2. F.E.Luborsky, J.D.Livingstone, G.V.Chin: Magnetic properties of Metals and Alloys, Chpt. 26, str.1698, v knjigi R.W.Cahn, P.Hassen Edts., Physical Metallurgy, North-Holand Physic, Amsterdam 1983.

3. E. D. Hondros, M. P. Seah, Interfacial and Surface Microchemistry, Chpt. 13, str. 856, v knjigi R.W. Cahn, P.Haasen, Edts., Physical Metallurgy, North Holand Physics, Amsterdam 1983.

4. F.Vodopivec, F.Marinšek, M.Torkar, F.Grešovnik,B.Praček: Poročilo Metalurškega inštituta 88-034/I, Ljubljana 1988.

5. G. Lyudkovski, P.K.Rastogi, Metall. Trans. A, 15A (1984) 257.

6. F .Vodopivec, F.Marinšek: Poročilo Metalurškega inštituta 89-039/I, Ljubljana 1989.

7. H. Shimanaka, Y.Ito, K Matsumura, B.Fukuda, J.Mag.Mag.Mat. 26,57 (1982).

8. P.Marko, A.Solyom, V.Frič, J.Mag.Mag.Mat. 41,74 (1984).

9. R.Bol Edt., Soft Magnetic Materials, Siemens, Heyden & Son LTD, London 1978.

10. F.Vodopivec,F. Marinšek, D.Gnidovec, B.Praček, M.Jenko, J.Mag.Mag.Mat. 97, 281 (1991).

11. M.Jenko, F.Vodopivec, B.Praček, Žel. zbor.25, 3(1991).

12. M.Jenko, F.Vodopivec, B.Praček, Kovine,zlitine, tehnologije, 26, 1-2(1992) 201-204

13. M.Jenko, F.Vodopivec, B.Praček, Vacuum 43 (1992) 449.

14. M.Jenko, F.Vodopivec, B.Praček, App. Surf. Sci. 70/71 (1993) 118-122

15. F.Vodopivec, M.Jenko, F.Marinšek, F.Grešovnik, Vacuum 43 (1992) 497.

16. F.Vodopivec, M.Jenko, A.Rodič, B.Breskvar, Poročila Inštituta za kovinske materiale in tehnologije, 92-14 in 92-54/I, Ljubljana 1992

17. F.Vodopivec, M.Jenko, A.Rodič, B.Breskvar, Kinetics of Recrystallized Grain Growth in Fe-Si Steel, J.Magn.Magn.Mater (in print).

18. M.Wutz, A.Adam, W.Walcher, Theorie und Praxis der Vakuumtechnik, Friedr. Vieweg & Sohn, Wiesbaden 1982.

19. L.E.Davis, N.C. Mac Donald, P.W.Palmbereg, G.E.Riach, R.E.Weber, Handbook of Auger Electron Spectroscopy, Eden Prairie 1976.

20. S.Hofmann, Vacuum 40, 1/2, 9 (1990).

21. M.P.Seah, W.A. Dench, Surf.Interface Anal. 1,2 (1979).

22. J.Cranck, The Mathematics of diffusion, Claredon, Oxford 1967.

23. H.J.Grabke, ISIJ Intern. 129, 7,529 (1989).

24. G.Bruggeman, J.Roberts, J.Met. 20, 8, 54 (1968).

25. K.Nishida H.Murohashi, T.Yamamoto, Trans.Jpn.Inst.Met 20 (1979) 269.

26. D.Steiner, M.Jenko, F.Vodopivec, L.Kosec, M.Godec, Kovine, zlitine tehnologije 27, 1-2 (1993) v tisku.

27. M.Godec, M.Jenko, M.Lovrečič, F.Vodopivec, L.Kosec, Kovine, zlitine, tehnologije 27, 1-2 (1993) v tisku.

Doc.dr. Monika Jenko
Prof.dr.Franc Vodopivec
Mag.Matjaž Godec
Darja Steiner
Inštitut za kovinske materiale in tehnologije, Lepi pot 11, 61001 Ljubljana

Borut Praček, dipl.ing.
Inštitut za elektroniko in vakuumsko tehniko, Teslova 30, 61000 Ljubljana

Prispelo: 27.08.93 ***Sprejeto: 14.09.93***

Informacije MIDEM 23(1993)3, Ljubljana UDK 621.3:(53+54+621+66), ISSN0352-9045

PRINCIP SENZORJEV NA OSNOVI OSCILATORSKE DIFERENCIALNE STRUKTURE

D.Đonlagić, J.Koprivnikar, V.Matko

KLJUČNE BESEDE: merjenje veličin, veličine neelektrične, senzorji oscilatorski, senzorji diferencialni, kristali kapacitivno odvisni, kristali kvarčni, DDM metode, metode direktne, metode digitalne, metode merilne, korekcija križna, modulacija impulzno širinska

POVZETEK: V delu je analizirana diferencialna quartz-oscilatorska metoda, ki bazira na malem frekvenčnem premiku dveh oscilatorjev. Frekvenčni premik je dosežen s spremembo kapacitivnosti sonde v območju pod 1 pF, kjer je tudi uporabno območje metode. Metoda vsebuje kompenzacijo drifta zaradi napetostnih in temperaturnih vplivov. S pomočjo Direktne digitalne metode (DDM), ki zmanjša vpliv motenj, je izboljšana negotovost merilnih rezultatov. DDM metoda je linearna v območju delovanja in zagotavlja negotovost merilnih rezultatov pod 0.01%. Experimentalno je bilo raziskanih več primerov uporabe. Negotovost merjenja je za določeno merilno veličino odvisna od negotovosti ostalih vplivnih parametrov, ki so vključeni v izhodno senzorsko enačbo.

Differential Oscillator Sensors

KEY WORDS: measurement of quantities, non-electric quantities, oscilator sensors, diferential sensors, capacitive dependent crystaly, quartz crystals, direct digital methods, direct methods, digital methods, measuring methods, cross-correlation, pulse width modulation

ABSTRACT: In the paper the use of a differential oscillator sensor structure in a capacitance sensor is presented. Investigation was focused on the operation analysis of the oscillator differential structure in which the oscillation frequencies of the oscillators are very close, and on the application analysis of capacitive dependent crystals. In addition, the excitation of the entire sensor with stochastic test signals has been analysed by the correlation deconvolution method which is also called the Direct Digital Method (DDM).

When designing the capacitance sensor the problems regarding the source of stable oscillation, compensation of temperature, the influence of supply voltage, noise, and A/D and D/A conversion occur in the operation range under 1pF. The pulse width module, which forms pulse width modulated high frequency current pulses, is the proposed solution. With these pulses the capacitor in the integration element is charged or discharged. In this way we benefit from the fact that the capacitor's voltage increases linearly if it is charging by a constant current. As the charging is affected only by the current pulses which require an adequate current the disturbing noise signals do not affect the capacitor charging. Likewise, the pulse width module compensates the effects of temperature and voltage by means of modulation. The correlation determination of the measuring value is primarily important for the determination of end values. Two computer aided modes of operation are suggested: dynamic measurement control and the correlation determination of differences.

1. Uvod

Prikazani senzorski izsledki nakazujejo široko uporabo pri merjenju fizikalnih, kemijskih in biotehniških veličin. Predstavljene so raziskave na področju novih senzorskih pristopov merjenja s poudarkom na uporabi kapacitivno odvisnih quartz kristalov in modificiran pristop v merilni tehniki v območju, kjer ni uporabna običajna instrumentacija. Prav tako je nakazana splošna rešitev merjenja majhnih sprememb neelektričnih veličin z veliko preciznostjo in ceneno izvedbo.

Dobro znana metoda v metrologiji je kapacitivna mostična metoda. Slabost kapacitivne mostične metode je, da morata biti dostopni obe plošči kondenzatorja, drugače je metoda neuporabna. Prav tako je potrebno uravnovešanje mostiča, razmerje signal/šum pa mora biti veliko. Zaradi parazitnih kapacitivnosti metoda ni uporabna v femtofaradnem območju. Druga znana metoda je Millerjeva metoda, ki uporablja sorazmerno enostaven princip določanja malih kapacitivnih sprememb pri 5pF - 20pF kondenzatorju prek fazne spremembe v serijskem resonančnem vezju /1/. Kondenzator je vgrajen kot element, kateremu se spreminja kapacitivnost v serijskem nihajnem krogu in je priključen na transistorsko emitorski sledilnik. Signalna informacija je dobljena prek opazovanja faznega premika, ki se odraža v kolektorskem toku transistorja, nastane pa zaradi spreminjanja kapacitivnosti. Millerjeva in kapacitivna mostična metoda predstavljata mejni metodi za merjenje malih kapacitivnosti. Slabost Millerjeve metode je v "RF sweep" signalu v območju do 40 MHz (zaradi resonančne frekvence) ter večji občutljivosti na fazni šum, kot pri mostični metodi (zaradi višjih frekvenc) in serijskim resonančnim vezjem, ki ga moramo sestaviti iz elementov L in C. Prednost Millerjeve metode je v tem, da je ena plošča kondenzatorja ozemljena. Pri obeh metodah je vprašljiva temperaturna kompenzacija in tudi vpliv motenj na celoten senzorski sistem (pri malih kapacitivnih spremembah). Metodi tudi ne zajemata korelacijske analize celotnega senzorja. Upoštevano ni

zmanjšanje vplivov A/D in D/A pretvorbe, šum in nekalibracija instrumentov.

Quartz oscilator je poznan po svoji temperaturni odvisnosti. Njegova frekvenca je odvisna v manjšem območju tudi od napajalne napetosti. Kadar je uporabljen quartz kristal v senzorski oscilatorski strukturi, je običajen pristop vpliva na quartz kristal s: temperaturo, silo, tlakom, torzijo, itd., da dobimo spremembo oscilatorjeve frekvence. V tem primeru pa je quartz kristal uporabljen kot stabilni resonirajoči element, kateremu spreminjamo električni model z dodatno vezano serijsko kapacitivnostjo Cx (Slika 1). V primeru, ko kristalu spremenimo električni model, se njegove lastnosti stabilnega nihanja s tem ne spremenijo.

2. Senzorska struktura

Diferencialna senzorska struktura je uporabljena zaradi kompenzacije motilnih vplivov. Prirejena je za delovanje z ali brez računalniške signalne analize. Analiza temelji na stohastičnem vzbujanju senzorja, pri čemer je izhodni signal frekvenca ali analogni signal /2/. Senzorska struktura, je prikazana na sliki 1. Za vzbujanje oscilatorjev 1 in 2 (prek varicap diod) sta uporabljena dva pseudonaključna trinarna signala x1(t) in x2(t) /3/. Frekvenci obeh oscilatorjev sta med 0.5 in 20 MHz. Napetostno frekvenčna odvisnost obeh oscilatorjev je v območju 6 ± 1 V in je približno enaka. Pulzno širinski modul (PWM), daje na izhodu temperaturno in napetostno kompenziran signal /4/. Tokovni pulzi polnijo in praznijo kondenzator v LPF (nizko propustni filter). Izhodna napetost filtra linearno narašča ali pada odvisno od tokovne narave pulzov na njegovem vhodu. LPF filtrira tudi motnje. Če je na izhodu senzorja frekvenčni signal (f), je primeren za prenos na večje razdalje. Tako ni potreben dodatni f/u pretvornik. Z uporabo f/u pretvornika lahko zajemamo izhodni signal prek A/D predtvorbe.

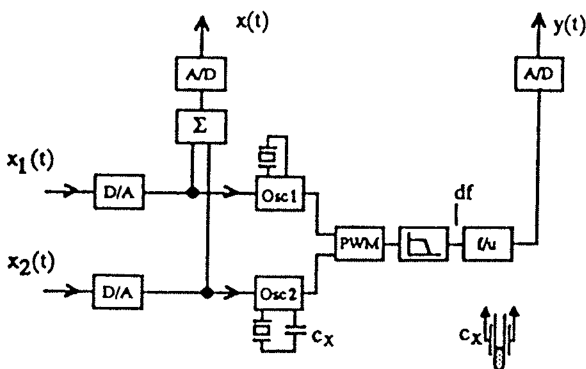

Slika 1: Senzorska struktura.

Signal x(t) je vsota dveh programsko določenih pseudo stohastičnih signalov $x_1(t)$ in $x_2(t)$ katerih srednja vrednost je enaka nič.

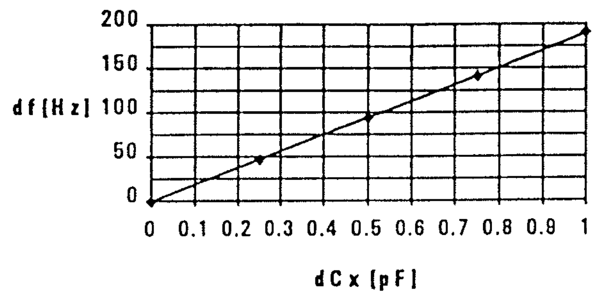

Slika 2: Odvisnost spremembe frekvence od spremembe kapacitivnosti sonde brez vzbujevalnih signalov.

Senzorska sonda Cx je kapacitivna. Pritrjena je na aktivnem mehanskem delu in zaznava kapacitivne spremembe v področju pod 1pF. Elektronsko vezje senzorja je nameščeno na razdalji 1cm od senzibilne sonde z 1cm dolgima žicama brez oklopa proti masi. S tema dvema žicama je dosežena boljša občutljivost, ker je manjša parazitna kapacitivnost proti masi. Rezultati na sliki 2 prikazujejo, da je sprememba frekvence proporcionalna spremembi kapacitivnosti v področju pod 1pF.

3. Kapacitivno odvisni quartz kristali

Električni nadomestni model quartz kristala je prikazan na sliki 3. Vrednosti elementov pa so podane v tabeli 1.

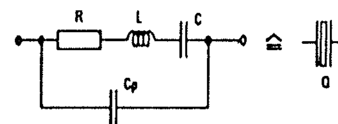

Slika 3: Električni nadomestni model quartz kristala.

Pri frekvencah 0.5-20 MHz je serijska kapacitivnost C ≅ 0.01pF (Slika 3, Tabela 1). S serijsko kapacitivnostjo Cx spreminjamo serijsko resonančno frekvenco oscilatorju 2 (Slika 1). V primeru merjenja nekaterih neelektričnih veličin (na primer malih volumnov) sta bila uporabljena dva 4MHz quartz kristala s stabilnostjo ± 3ppm v območju -5 do 55°C.

TABELA 1. Podatki za quartz model pri različnih frekvencah.

f_0	R	C	L
1-5 kHz	5-50 kΩ	0.01 pF	10^4 - 10^5 H
50-200 kHz	2-5 kΩ	0.1 pF	10-100 H
150-800 kHz	0.5-10 kΩ	0.02 pF	1-10 H
0.5-20 MHz	2-2000 Ω	0.01 pF	10-100 mH

4. Direktna digitalna metoda (DDM)

Negotovost merilnih rezultatov je izboljšana s pomočjo Direktne Digitalne Metode (DDM), ki zmanjša vpliv motenj. Konvolucijski integral (En. 1), predstavlja osnovo metode za izboljšanje preciznosti merilnih rezultatov.

$$y(t) = \int_{-\infty}^{\infty} g(u) \cdot x(t-u) \cdot du \qquad (1)$$

g(u) utežnostna funkcija

x(t) vhodni napetostni signal

y(t) izhodni napetostni signal

Enačbo 1 vstavimo v križnokorelacijsko enačbo 2 in dobimo enačbo 3.

$$\varphi_{xy}(\tau) = \lim_{T\to\infty} \frac{1}{T} \int_0^T y(t) \cdot x(t-\tau) \cdot dt \qquad (2)$$

$$\varphi_{xy}(\tau) = \lim_{T\to\infty} \frac{1}{T} \int_0^T x(t-\tau) \int_{-\infty}^{\infty} g(u) \cdot x(t-u) \cdot du \cdot dt \qquad (3)$$

S spremembo vrstnega reda integriranja dobimo enačbo 4.

$$\varphi_{xy}(\tau) = \int_{-\infty}^{\infty} g(u) \cdot \left[\lim_{T\to\infty} \frac{1}{T} \int_0^T x(t-\tau) \cdot x(t-u) \cdot dt \right] du \qquad (4)$$

Drugi integral v enačbi 4 predstavlja avtokorelacijsko funkcijo signala x(t), kot je pokazano z enačbo 5.

$$\varphi_{xx}(\tau - u) = \lim_{T\to\infty} \frac{1}{T} \int_0^T x(t-\tau) \cdot x(t-u) \cdot dt \qquad (5)$$

Sledi enačba 6:

$$\varphi_{xy}(\tau) = \int_{-\infty}^{\infty} g(u) \cdot \varphi_{xx}(\tau - u) \cdot du. \qquad (6)$$

Po izpeljavi lahko izpostavimo utežnostno funkcijo g(u) pri čemer upoštevamo še končni čas merjenja T (En. 7).

$$g(u) = \frac{\varphi_{xy}(\tau)}{\int_0^T \varphi_{xx}(\tau - u) \cdot du} \qquad (7)$$

Vzbujevalna signala (Slika 1) sta pseudostohastična trinarna signala s povprečno srednjo vrednostjo enako nič in taktno frekvenco 1kHz. Oblika funkcije $\varphi_{xy}(\tau)$ je poznana (Slika 4), če je poznan testni vzbujevalni signal x(t). S formiranjem križnokorelacijske funkcije med vhodnim in izhodnim signalom zmanjšamo vpliv vseh motilnih signalov, ki niso korelirani s testnim signalom x(t). Tako je zmanjšan vpliv stohastičnih motilnih signalov, ki se pojavljajo na vhodu in izhodu senzorja in vpliv netočnega vzbujanja senzorja ter netočnega merjenja frekvence na izhodu senzorja. V primerjavi z mostično metodo in Millerjevo metodo je pri DDM metodi izhodni signal konstantne amplitude. S testnim signalom se zmanjša tudi vpliv histereze. V primeru, ko imamo na izhodu f/u pretvornik je zmanjšan vpliv A/D kvantizacije. Tako je dobljena boljša povprečna merilna vrednost, ker je upoštevan celoten senzor. V tem primeru je DDM metoda uporabljena za statično določanje inicializacijske in nove merilne vrednosti.

5. Merjenje neelektričnih veličin

Pri meritvah neelekričnih veličin senzor opravlja naslednje tri osnovne funkcije:

- Določitev ničelne kalibracijske vrednosti in določitev končne vrednosti. Razlika med obema vrednostima (df) je proporcionalna merjeni neelektrični vrednosti v območju 0-1pF (Slika 2).
- Opazovanje dinamičnih sprememb. Dinamika senzorja (brez vzbujevalnega signala) je določena z LPF konstanto. Ker je frekvenca obeh oscilatorjev velika (4MHz) je časovna konstanta mala (1μs). Zato je senzor primeren za opazovanje hitrih dinamičnih pojavov.
- Določitev ničelne korelacijske vrednosti in določitev končne korelacijske vrednosti. Razlika korelacijskih vrednosti je proporcionalna merilni vrednosti neelektrične veličine (En. 8) v območju od 0-1pF.

Merjenje neelektrične veličine je določeno z enačbo 8, kjer je razlika integralov križnokorelacijskih funkcij proporcionalna vrednosti neelektrične veličine (pri enakem testnem signalu) in ustreznem umerjanju. Integral križnokorelacijskih funkcij (En. 8) je uporabljen zaradi upoštevanja testnega signala prek celotne periode in povprečenja vrednosti ter zmanjšanja vplivov motenj.

$$V_{el} = \left(\frac{\int_0^T \varphi_{xy_2}(\tau) d\tau}{\int_0^T \varphi_{xx}(\tau - u) \cdot du} - \frac{\int_0^T \varphi_{xy_1}(\tau) d\tau}{\int_0^T \varphi_{xx}(\tau - u) \cdot du} \right) K_3 \qquad (8)$$

Avtokorelcijski integral (En. 5) je odvisen od testnih signalov $x_1(t)$ in $x_2(t)$ s katerima vzbujamo senzor. Pri uporabi specialno programiranih testnih signalov $x_1(t)$ in $x_2(t)$ se križnokorelacijska funkcija φ_{xy1} začne in konča na X koordinatni osi, ko je $\tau = T$ (Slika 4). X os in križnokorelacijska funkcija določata kalibracijsko ploščino, ki je odvisna od testnega signala.

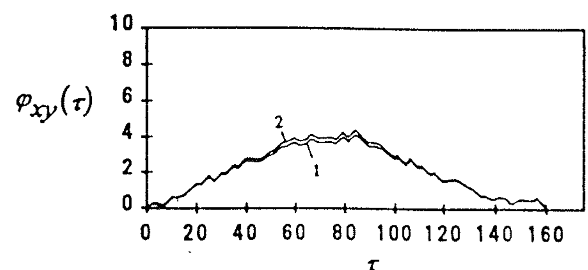

Slika 4: Funkciji φ_{xy1} in φ_{xy2}.

Neelektrična veličina je definirana kot sprememba med križnokorelacijskima funkcijama in določena s spremembo kapacitivnosti Cx ter pomnožena s kalibracijsko konstanto K_3. V tem primeru je testni signal upoštevan prek celotne periode merjenja, kakor tudi kompenzacija različnih predznakov med križnokorelacijsko in avtokorelacijsko funkcijo. K_3 je kalibracijska konstanta, ki je odvisna od mehanske realizacije senzorja.

6. Experimentalni rezultati

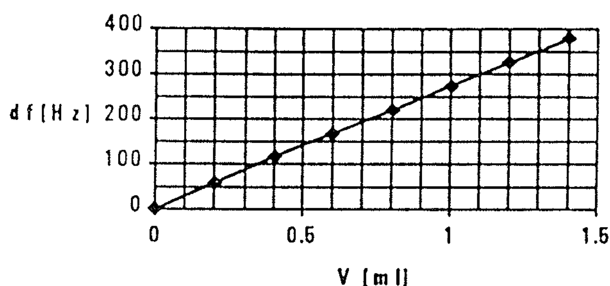

Slika 5: Občutljivost sonde pri stabilnosti izhodne frekvence senzorja ∓ 0.01Hz.

Občutljivost sonde v primeru merjenja malih volumnov je prikazana na sliki 5. Karakteristika je linearna v področju pod 1ml. Volumen V je izmerjen z negotovostjo ∓ 0.0005ml z uporabo Batne birete /5/.

Občutljivost v primeru merjenja pomikov je 10 µm/Hz.

Podobno ugodne rezultate smo dobili tudi pri meritvah nekaterih drugih neelektričnih veličin.

7. Zaključek

V delu je experimentalno opisan in prikazan primer uporabe kapacitivno odvisnih kristalov. Rezultati potrjujejo linearnost metode v določenem območju. Predstavljena je uporaba kapacitivno odvisnih kristalov in odvisnost df od dCx kapacitivne sonde, ki je splošno uporabna tudi za druge vrste meritev. Prav tako je experimentalno prikazana uporaba križnokorelacijske metode in ugotovljena dinamika. Prikazan je princip uporabe dveh testnih signalov za formiranje signala vzbujanja x(t) ter ploščinski princip merjenja, ki vsebuje vpliv testnega signala prek celotne periode in s tem vpliv A/D in D/A kvantizacije na negotovost utežnostne funkcije, občutljivost kapacitivne sonde in kalibracijski postopek.

Ker ima razmerje signal/šum zelo majhen vpliv na točnost merjenja ima korelacijska metoda prednost pred mostičnimi (Andersonovo, De Sautyjevo, Maxwellovo, Ownovo, Resonančno, Sheringovo, Wienovo in Hayevo) in Millerjevo metodo. Prednost je tudi v večji občutljivosti v femtofaradnem območju in zmanjšanju vpliva motenj. Vse tri metode predstavljajo mejne primere merjenja malih kapacitivnih sprememb.

Poleg določanja volumnov v območju 0-1ml so bili opravljeni experimentalni rezultati merjenja:

- kotov in pomikov,
- edometrične preiskave v zaprtem cilindru,
- absorpcije poroznih delcev in določanje volumna zraka v porah,
- temperature,
- nivoja,
- izhlapevanja,
- parazitnih kapacitivnosti,
- evolucije bakterij,
- evolucije rastlin,
- sušenja papirja.

Poleg navedenih experimentov lahko senzor uporabimo z drugačno sondo in ustrezno kalibracijo za merjenje:

- vlažnosti,
- tlaka,
- malih volumnov v epruvetah z milimeterskim premerom,
- sile,
- določanje "stress/strain" pogojev v mehanskih strukturah,
- dielektričnosti,
- pretokov,
- torzije,
- vibracij,
- v zaščitni tehniki.

Senzor ima naslednje prednosti: frekvenčno stabilna quartz elementa, izhodni signal ima konstantno amplitudo, razmerje signal/šum je veliko in ima konstantno vrednost v celotnem merilnem območju, filter seje motnje, ki nimajo tokovne narave pulzov, izhodni signal je temperaturno in napetostno kompenziran, občutljivost 5 fF/Hz, linearna kapacitivno frekvenčna odvisnost v področju pod 1pF, dekonvolucijski merilni postopek, ki zmanjša vpliv netočnega setiranja vhodnih napetostnih signalov in merjenja izhodne frekvence, dobra dinamika, izhod prirejen za daljinski prenos, možnost uporabe v širokem področju tehnike, enostaven kalibracijski postopek, primernost za industrijsko okolje, relativno in absolutno merjenje, takojšnja analiza podatkov in nizka cena.

Slabosti so predvsem v iskanju parov kristalov in zahteva po malih tolerancah posameznih elementov.

8. Literatura

/1/ G.L.Miller, E.R.Wagner, Resonant phase shift technique for the measurement of small changes in grounded capacitors, Rev. Sci. Instrum. 61(4) 1990, p. 1267.

/2/ K.W. Bonfig, Das Direkte Digitale Messverfahren (DDM) als Grundlage einfacher und dennoch genauer und störsicherer Sensoren, Sensor nov. 1988.

/3/ J.Tichy, G.Gautschi, Piezoelektrische Messtechnik, Springer-Verlag Berlin-Heidelberg-New York, 1980, ISBN 3-540-09448-2.

/4/ V.Matko, D.Đonlagić, J.Koprivnikar, Analysis of the Doppler Signal by Frequency Modulation in Ultrasonic Flow Measurement of Fluids, Rev. Systems Analysis Modelling Simulation Vol. 11, 4 (1993), pp. 313-323.

/5/ F.Spieweck, H.Bettin, Solid and liquid density determination, Technisches Messen 59, 6 und 7/8, 1992.

Prof. Dr. Dali Đonlagić
Doc. Dr. Jože Koprivnikar
Mag. Vojko Matko
Laboratorij za avtomatiko
Tehniška fakulteta Maribor
Smetanova 17, 62000 Maribor

Prispelo: 26.07.93 ***Sprejeto: 03.09.93***

AUTOMATIC IMAGE ANALYSIS SYSTEM TRACOS

Jure Skvarč

KEYWORDS: nuclear tracks, track detectors, crystal grains, microscopes, scanners, image analysis, automatic analysis, track evaluation, measurements, applications, software

ABSTRACT: An automatic image analysis system called TRACOS is introduced and its applications to evaluation of tracks in track etch detectors and crystal grains measurement are described.

Avtomatski sistem za analizo slike TRACOS

KLJUČNE BESEDE: sledi jedrske, detektorji sledi, zrna kristalna, mikroskopi, skanerji, analiza slik, analiza avtomatska, vrednotenje sledi, meritve, aplikacije, oprema programska

POVZETEK: Opisan je sistem za avtomatsko analizo slike, imenovan TRACOS, in njegova uporaba pri izvrednotenju sledi v trdnih detektorjih jedrskih sledi in pri meritvah kristalnih zrn.

Introduction

Nuclear tracks group of the Reactor physics division of the J. Stefan Institute started with development and application of track etch detectors twenty years ago. These detectors are able to detect heavy ions with energy range from 100 keV up to relativistic energies. They are made mostly of polymer materials and are known under different commercial names, such as LR-115, CN-85, CR-39 and so forth. Other heavy ion detecting materials are minerals, like mica and glasses. Detectors are usually shaped in foils with thickness from few microns up to 1 mm. Tracks, made by the incoming ions, are enlarged by chemical etching, so they are visible under an optical microscope. The transformation of a latent track to a visible track is possible because the etching velocity along the path of the ion is greater than the etching velocity of the bulk material. For the constant etching velocity along the path of an ion, the track has a shape of cone, which gives an elliptical intersection with the surface of the detector. Tracks are visible under an optical microscope due to steep track walls which refract light because the refractive index of the detector is higher than refractive index of the air. As a consequence tracks appear as dark spots. Typical track size, used for observation and measurement, is from 1 μm to 30 μm. From the size and optical density of the tracks the energy and the charge of the incoming ion can be derived while from the track shape the impact angle can be calculated. A micrograph of tracks is shown in Fig. 1.

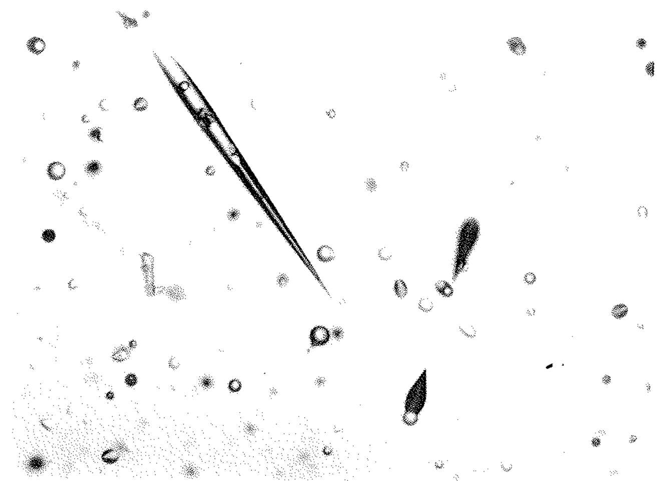

Fig. 1: The micrograph of nuclear tracks in CR-39 detector which was 5 month in Mir space station. Tracks, marked by arrows, are induced by cosmic rays. Smaller tracks are mostly due to α particles emitted by decay of radon and its decay products.

Measurements of large areas of the detector foils induced the need for automatic track evaluation. Manual measurement is usually limited to counting the number of tracks in a given area, while there is often need for finding the size or some other distribution of tracks. For this purpose an automatic track analysis system, called TRACOS (Track Counting System), was developed. It consists of an optical microscope, a computer controlled microscope stage, an autofocusing system, a video camera, a video digitizer and a personal computer. Additionally, an optical scanner output can be also processed. Technical characteristics of the individual components are summarized in the Table 1. Software for the measurement control and image analysis was completely developed in our laboratory. In the following capabilities of the system will be presented and some selected examples of measurements will be described.

Table: technical characteristics

Microscope:	Olympus Vanox magnification: 8-times to 250-times illumination: Hg or ordinary light bulb
Camera:	EEV with CCD sensor
Digitizer:	Data Translation 2853 SQ resolution:: 512*512 pixels, 256 grey levels memory: 512 kB (two images)
Moving stage:	Märzhäuser Wetzlar MAC 4000/2 scanning area: 100 mm * 100 mm step: 0.025 μm
Autofocus:	Elbek
Computer:	PC compatible processor: 80486/50MHz memory: 8 MB ram, 256 cache hard disk: 450 MB

Measurement

Before the measurement some of the settings are made by an operator. It is necessary to adjust the light intensity of the microscope, to set the minimum size of the objects which will be analyzed and to determine the grey level threshold which separates object from the background. An important tool for the light and the threshold setting is the grey level histogram which usually shows two peaks; one corresponding to dark objects and the second corresponding to bright background (Fig. 2).

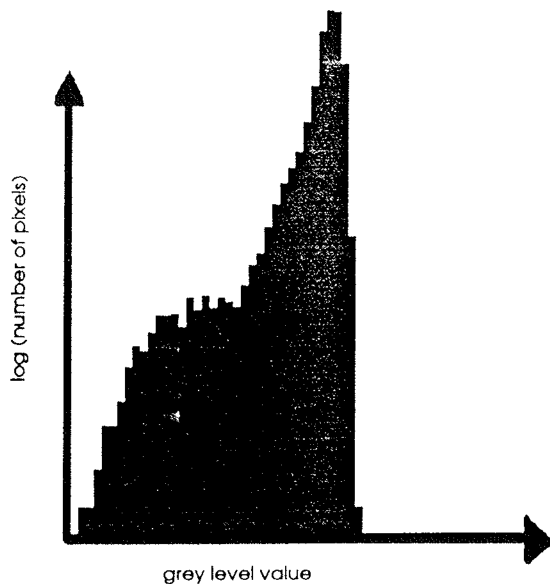

Fig. 2: Grey level distribution histogram. To achieve better visibility of the peak belonging to dark objects with relatively small total area, a logarithm scaling is used.

The concept of the analyzing program is to write measured parameters of all objects (except those smaller than the selected minimum size) in a file, which is later processed by other programs, depending on the type of application. By this approach the universality of the program is preserved what makes it more flexible and easier for adaptation to other purposes. Every record corresponding to a single object contains measured quantities, such as the object coordinates, the size of the minor and the major axis, the size of the perimeter, the area and the average grey level within a object. For the nuclear track analysis, the outer edge of the objects is fitted by an ellipse. The program is capable to fit the ellipse even when the objects overlap (Fig. 3).

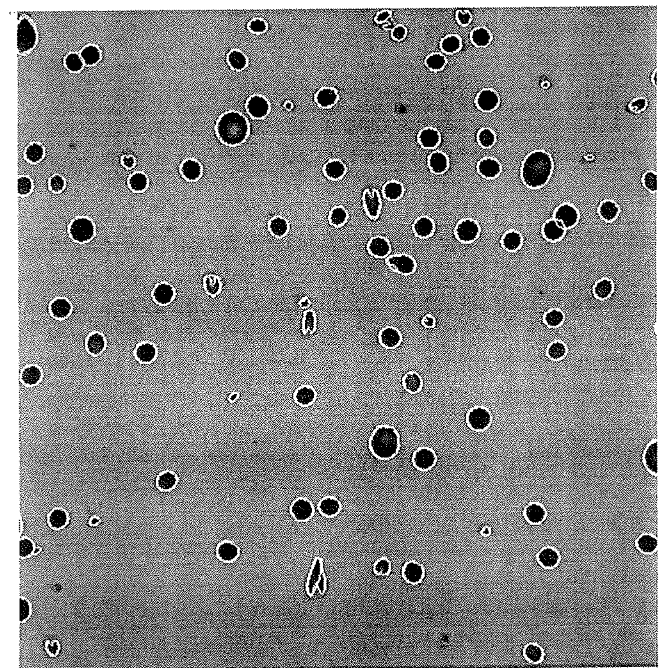

Fig. 3: Ellipse fitting to the tracks. Program is capable to fit correctly even the overlapping tracks.

Discrimination among tracks and background and/or different tracks is performed after the measurement with a help of utility programs developed for this purpose. The program for the track selection represents tracks as pixels on a computer screen for every plane that can be defined with an arbitrary pair of parameters measured by the TRACOS. Fig. 4 shows an example where track distribution is presented in a plane with the x coordinate corresponding to the major axis and the y coordinate corresponding to the minor axis of the track. The circular tracks therefore lie on the x=y curve. By the selection of the region of interest only tracks, relevant for further examination, are transferred to the next stage of processing. For the example given in Fig. 4 we could decide to select only tracks with minor/major axis ratio in the wanted range.

Representation in a two-dimensional sub-space of the parameter space is especially useful in cases when the properties of the objects are not known in advance. By

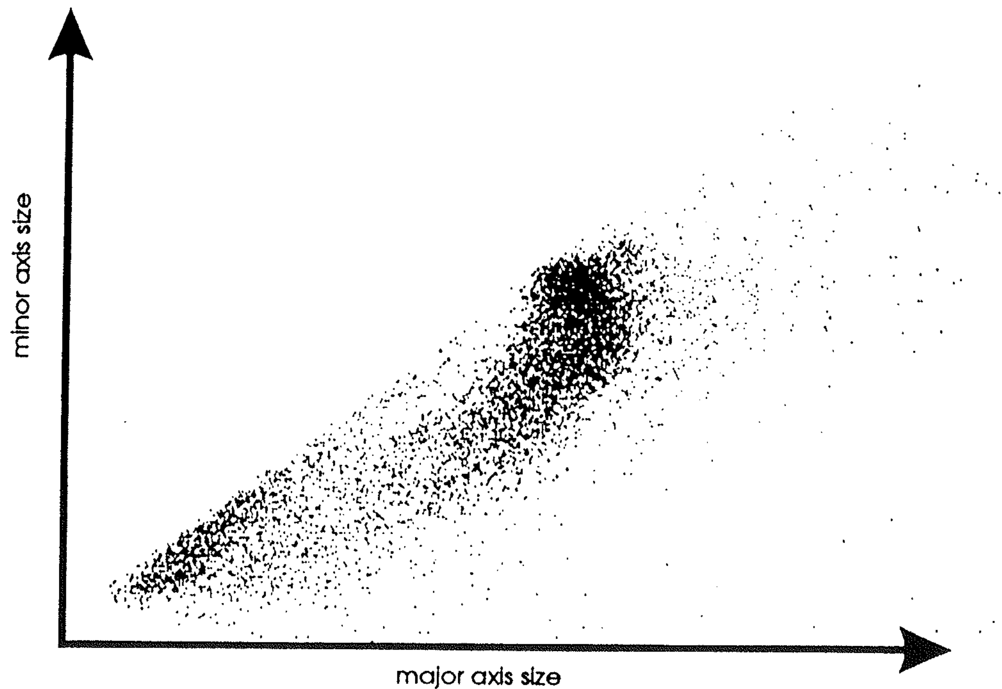

Fig. 4: Every pixel on a diagram represents an individual track. The x coordinate corresponds to the major axis of an ellipse and the y coordinate corresponds to the minor axis.

observing planes for different pairs of parameters it is easy to determine if the objects group together and to select them for the further processing. In more complicated cases of recognition it might be necessary to use more-dimensional cross sections in the parameter space. Here problems appear because it is difficult to present structures of more than two dimensions on the computer screen. Fortunately, in the most cases the two-dimensional selection is enough for the most of applications with track etch detectors.

After the selection of the region of interest, it is possible to process further the output of the measurement. Typically, distribution over some of the measured parameters is displayed as a final result. Advantages of the automatic track evaluation over the manual counting are mainly:

a) discrimination criteria are less prone to subjective judgment, b) exhaustion of the operator is less likely to influence the quality of measurement, c) the speed of the evaluation is much greater; at the optimal track density the system is capable to evaluate from $5*10^4$ up to 10^5 tracks/hour.

Examples of applications

The system was used for several types of tasks, some of which are presented here.

Discrimination of the ^{6}Li(n, α) reaction product tracks

Products of the ^{6}Li(n, α) reaction are ^{3}H and ^{4}He with an energy of 2.7 MeV and 2.1 MeV, respectively. Both nuclei are detectable with CR-39 track etch detectors.

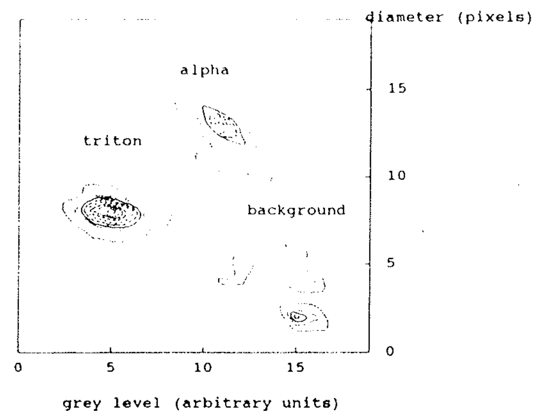

Fig. 5: Bright areas on the diagram correspond to large number of tracks with given size (y coordinate) and average grey level (x coordinate).

Due to different energy and charge of the reaction products their tracks are different. Smaller and darker tracks correspond to ^{3}H, while larger and brighter belong to ^{4}He. Fig. 5 shows a diagram where horizontal axis represents the average grey level within individual tracks, while the vertical axis represents the track diameter. Two groups of tracks are clearly visible and discerned from the background. More detailed description of this experiment can be found in (1).

Measurement of the track density as a function of the coordinate and application in radiography.

One of the application areas of track etch detectors are radiographic and autoradiographic methods. By this methods it is possible to measure spatial distribution of charged particle emitters as well as position dependence of transmissivity of the material for heavy ion or neutron beams. Due to the high spatial resolution and the possibility of individual track identification it is possible to make radiographic images at very low emitter concentrations or low beam fluxes. Using an autoradiographic technique we measured the adsorption of radon decay products on metal surfaces. In the radon decay chain there are two short-lived α-emitters: ^{218}Po and ^{214}Po. Contrary to radon, Po atoms stick to metal surfaces. Adsorption on Cu and Al when they were held in contact and separated was measured and compared. With the use of the automatic system it was found that density of Po atoms adsorbed on Cu is higher in comparison that of adsorbed on Al when the metals were held in contact while the densities did not differ when the metals were separated (Fig. 6).

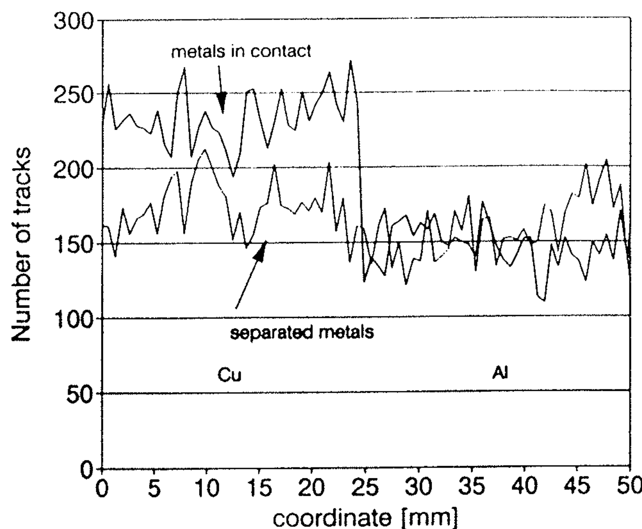

Fig. 6: Number of tracks, produced by the decay of Po, adsorbed on Cu (left) and Al (right) as function of coordinate. Curve with a step in the middle belongs to the measurement with metals in contact.

Application in metallography - Measurement of the number of sides and the number of neighbouring crystal grains

For this task the program was slightly modified. Instead of the digitized picture it accepted a scanned image. Additionally, a module for grain neighbour determination was added to the program. Before the counting, defects in picture were corrected using a drawing program. The crystal grain image, shown in its digitized form in Fig. 7 a), was taken from (2). In Fig 7 b) a number of neighbouring grains of every crystal grain is written. More of this and some other applications of the program in material science is described in (3).

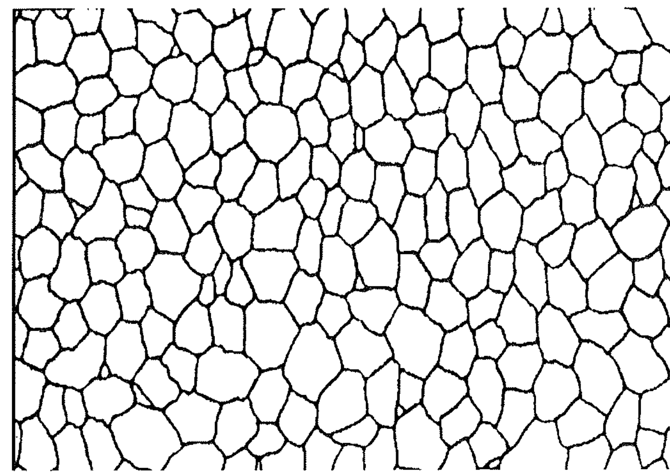

Fig. 7 a): Digitized optical micrograph of crystal grains.

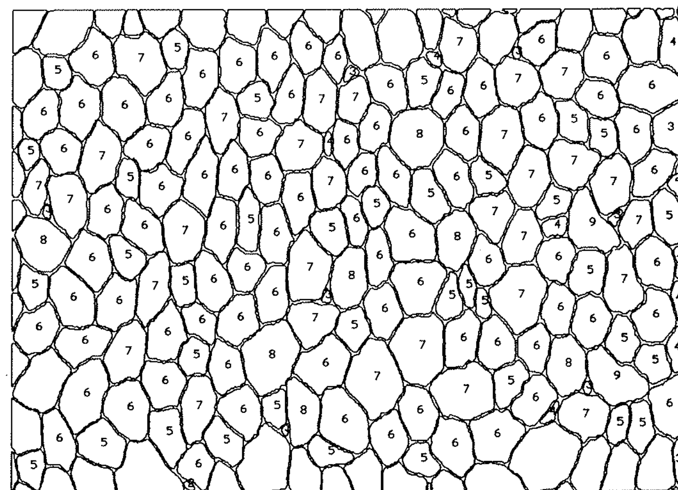

Fig. 7 b): Number of neighbours of the individual crystal grains as determined by a computer.

Conclusion

An automatic system for nuclear track measurement in track etch detectors was built and image analysis software was developed for the research and applications. The system was successfully tested in several types of

experiments and in routine use. The achieved speed and the accuracy of the measurement is better in comparison to the manual evaluation. Due to a flexible design of the image analysis program it is possible to quickly adapt it to various other tasks in materials and biological applications.

References

1. J. Skvarč, R. Ilić and A. Kodre, "Digital evaluation of 6Li(n, a) reaction product tracks in CR-39 detector", Nucl. Inst. Meth. B71, (1992) 60-64.

2. H. Schumman, Metallographie, Leipzig, (1980).

3. D. Colja, B.Sc. Thesis, Ljubljana, 1992.

mag. Jure Skvarč, dipl.ing.
Institut Jožef Stefan, Oddelek za reaktorsko fiziko, Jamova 39, 61111 Ljubljana, Slovenia

Prispelo: 01.06.93 ***Sprejeto: 20.07.93***

LASERSKI MERILNIK DEBELINE S STATISTIČNO OBDELAVO MERILNIH REZULTATOV

Darjan Gradišnik, Dali Đonlagić

KLJUČNE BESEDE: merilnik debeline, valjanje, vlečenje, stiskanje, kovanje, merilniki laserski, laserji polprevodniški, merjenje stično, merjenje brezstično, podatki dinamični, napake meritev, profili vzdolžni, avtokorelacija, histogrami, senzorji triangularni

POVZETEK: Meritev debeline je postopek, ki ga srečujemo v vseh panogah industrije. Kvaliteten merilnik je nujen pri kontroli in regulaciji valjanja, vlečenja, stiskanja, kovanja itd. raznih materialov.

V avtomatski regulaciji debeline (AGC) nas zanimajo zvezne meritve, ki pa so lahko stične ali brezstične. Zaradi doseganja večjih pretokov materiala se vse bolj uveljavljajo brezstične meritve, pri katerih tudi ne prihaja do poškodb na merilnem mestu. V ta razred sodi tudi laserski merilnik debeline, ki ima pred ostalimi tudi to prednost, da je merjenje debeline njegova primarna funkcija, medtem ko ostali podobni merilniki merijo debelino posredno prek drugih fizikalnih veličin.

Laser Thickness Measurer with Statistical Processing of Measurement

KEY WORDS: thickness measurers, rolling, extrusion, pressing, forging, laser measurers, solid-state lasers, contact measurement, non-contact measurement, dynamical data, measurement errors, longitudinal profiles, autocorrelation, histograms, triangular sensors

EXTENDED ABSTRACT: Thickness measurements are frequent in all branches of industry. A quality measurer is indispensable for process control of rolling, drawing, extrusion, pressing, forging, ... of different materials.
In Automatic Gauge Control continuous measurements are very practical. They are divided into two groups: contact and noncontact measurements. In order to attain a greater materials flow, non-contact measurements are more suitable, particulary because no damage is made on the measured region.
Laser thickness measurers are grouped into this class. Their advantage results come from the fact that the measurement of distances is their basic function, whereas other types measure the thickness indirectly from other physical magnitudes.
In the first chapter a short overview of other thickness measurements is made.
We can break semiconductor properties into two broad categories: electronic and optical. Band gap is the most important parameter of optical properties. In some semiconductors the recombination energy is released as heat, in other much of the recombination energy is released as light. The light output current is very inefficient below the threshold and becomes more efficient above it.
The laser diode is a part of triangular sensor which consist also of a PSD (Position Sensitive Device) and two lens systems. Two sensors can be used for two - sided thickness inspection, one above and one below the web. The output from both sensors subtracted from the fixed distance between sensors is proportional to the material's thickness. This procedure removes the variables caused by vibration, bounce or tension of running web.
We used an industrial PC with added opto isolation and relay output units instead of a PLC or a math unit.
Several dynamic data are avallable in the main display: thickness, thickness error, alarms, messages, profile, histogram and (or) auto correlation. After 30 samplings either auto correlation or a histogram is done, Analysing with auto correlation is very effective if some included frequencies from the plant are transferred to material's surface or in case when the control loop becomes unstable. The histogram offers a simple pattern recognition for the operator (if the thickness or the shape are inside limits).
Further research with several measurement places and an interpolation curve between them will be conducted for 3D surface analysis of the material.

1. Merjenje debeline

Kratko bomo pregledali različne metode merjenja razdalje. oz. debeline. Ponavadi z enim merilnikom merimo razdaljo, z dvema diametralno nameščenima pa debelino.

Potenciometrski dajalniki nam dajo podatek o razdalji kot funkcijo priključne napetosti (d = f(U)). Problem je pogrešek meritve (> 1%).

Pneumatski dajalniki delajo na principu šoba - odbojna ploščica, kjer ploščico predstavlja kar merjenec, ali pa je prek valjčnic ploščica povezana z merjencem. Za te dajalnike je značilno majhno linearno območje, ki ga nekoliko povečamo z uporabo dveh sistemov, primerjalnega in merilnega.

Kapacitivni dajalniki so ponavadi različne izpeljanke ploščatega kondenzatorja. Iz enačbe:

$$C = \frac{\varepsilon \cdot S\,(N-1)}{d} \tag{1.1}$$

C - kapacitivnost
ε - dielektrična konstanta
N - število plošč kondenzatorja
d - razdalja med ploščami

kot merilno spremenljivko uporabimo razdaljo med ploščami d. Ena od plošč je kar merjenec. Slabe strani metode so občutljivost na motnje iz okolice pa tudi nelinearna odvisnost kapacitivnosti od razdalje (C = f(1/d)).

Induktivni dajalniki kot merilniki razdalje se največ uporabljajo v izvedbi linearnega diferencialnega transformatorja (LVDT). Pri tem v enačbi za induktivnost:

$$L = \frac{\mu N^2 S}{l} \quad (1.2)$$

L - induktivnost ravne tuljave
μ - magnetna permeabilnost
S - presek tuljave
l - dolžina tuljave

ponavadi spreminjamo permeabilnost s premikanjem položaja jedra. Ker je jedro prek ročice povezano z merilnimi valjčnicami, je tak način meritve stičen.

Infra svetlobni merilniki temeljijo na resonančni absorbciji žarkov v atomih, oz. molekulah merjenca. Valovna dolžina svetlobe mora ustrezati kemijski konstituciji merjenca, jakost absorbcije dovedene energije pa je odvisna od gostote merjenca. Če je ta konstantna lahko prek relacije:

$$d = \frac{m}{S\sigma} \quad (1.3)$$

d - debelina materiala
m - masa materiala
S - površina merjenja
σ - gostota materiala

dobimo z umerjanjem debelino materiala direktno. Obstajata dve metodi: z odbojem in presvetlitvijo materiala.

Meritve debelin z Rötgenskimi, α, β in γ žarki prav tako temeljijo na absorbciji žarkov v materialu, ki je odvisna od gostote materiala. Ponavadi je sprejemnik ionizacijska komora, v kateri pri konstantni priključeni enosmerni napetosti, temperaturi in tlaku halogenega plina pride pod vplivom kratkovalovnega valovanja do ionizacije molekul plina in zato steče ionizacijski tok. Ta je odvisen od števila ionskih parov, število teh pa od števila radioaktivnih delcev, ki so prišli iz radioaktivnega izvora (Röntgenske cevi) skozi material do komore:

$$I(d) = I_0 \cdot e^{-kd} \quad (1.4)$$

I(d) - intenzivnost sevanja
I_0 - intenzivnost sevanja brez merjenca
k - koeficient absorbcije materiala (merjenca)
d - debelina materiala

Ta tok je velikosti 10^{-10} do 10^{-8} A in ga na visokoohmskem uporu pretvorimo v napetostni signal.

Kljub potrebni zagotovitvi varnosti pri upravljanju z izotopi in zavarovanju merilnega prostora ter obvezni linearizaciji merilne krivulje, se ta merilni postopek med brezstičnimi največ uporablja.

2. Polprevodniški laser, triangularni senzor

Lastnosti polprevodnikov lahko razdelimo v dve področji : elektronsko in optično. Elektronske lastnosti vključujejo koncentracijo prostih nosilcev, prevodnost in gibljivost elektronov, za optične pa je zelo pomemben zaporni pas, oz. njegova energijska širina, ki določa tudi valovno dolžino valovanja, ki ima dovolj energije za prestop med valenčnim in prevodnim pasom in obratno:

$$E_{zap.pas} = \frac{1240}{\lambda_{zap.pas}} \quad (2.1)$$

E - energijska širina zapornega pasu (eV)
λ - minimalna valovna dolžina (nm)

Na PN spoju prihaja do rekombinacij in rekombinacijska energija se lahko sprošča kot toplota (pri Si), ali pa kot svetloba (GaAs). Pri LED imamo spontano emisijo, ki seva v vse smeri v širšem pasu, pri laserski diodi pa je emisija v smeri polprevodniške plasti in določene valovne dolžine. Do t.i. laserskega praga tudi laserska

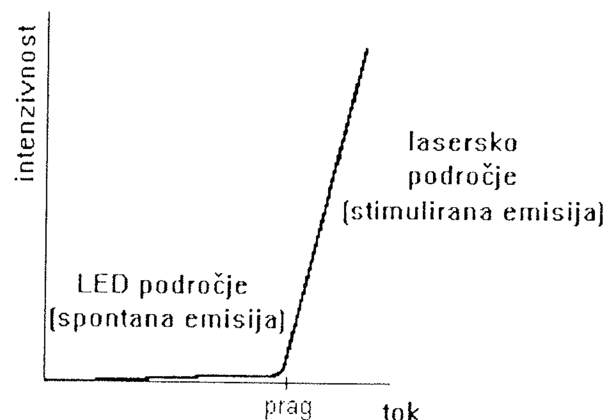

Slika 2.1: Intenzivnost svetlobnega sevanja pod in nad pragom laserskega delovanja

dioda dela v področju spontane emisije, kar vidimo na sliki 2.1:

To je seveda zelo poenostavljen opis delovanja. Laserska dioda je sestavni del laserskega senzorja razdalje, ki ga sestavljajo še PSD (Position Sensitive Device) in

sistem leč. Ker izvor svetlobe, merjenec in PSD tvorijo trikotnik, kjer se v odvisnosti od oddaljenosti merjenca

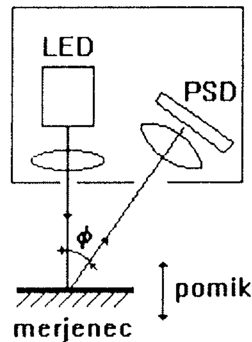

Slika 2.2: Namestitev izvora in ponora v senzorju razdalje

kot odboja spreminja, se ta razpored imenuje tudi triangularni (slika 2.2):

Funkcija odvisnosti razdalje od merjenca in kota odboja je nelinearna:

$$razdalja = \sqrt{\frac{l^2}{2 \cdot (1 - \cos(\varphi))}}$$

l - razdalja med izvorom in ponorom žarka
φ - kot odboja žarka od merjenca

Izhodni signal je nato lineariziran in ponavadi dobimo na izhodu tokovni signal. Območje 4 - 20 mA pomeni tudi merilni obseg razdalje, tako da je *razdalja = f(l_{izh})*.

3. Zasnova merilnika

Dva, na nasprotnih straneh merjenca nameščena senzorja razdalje sestavljata merilno glavo. Princip je enostaven: če poznamo razdaljo med senzorjema, potem se debelina izračuna kot:

$$debelina = D - d_1 - d_2 \qquad (3.1)$$

D - razdalja med senzorjema
d_i - oddaljenost objekta od i - tega senzorja

Ker obravnavamo dinamično merjenje, kar pomeni, da se merilni objekt giblje mimo merilne glave, pride do merilnega pogreška zaradi časovnega zamika Δt med odčitkom prve in druge razdalje (slika 3.1). Vpliv tega pogrešeka pa je majhen, če je tipalni čas ustrezno izbran glede na pričakovano dinamiko spremembe debeline merjenega objekta.

Klasična zasnova merilnika je taka, da ima vsak senzor mikro kontroler, ki daje analogni signal razdalje, oba pa sta priključena še na matematično enoto (kontroler), ki daje na izhodu vsoto, oz. razliko vhodnih signalov, ki jo potem uporabimo v regulacijski zanki. Če hočemo opravljati še statistične izračune, je potrebno signal prek

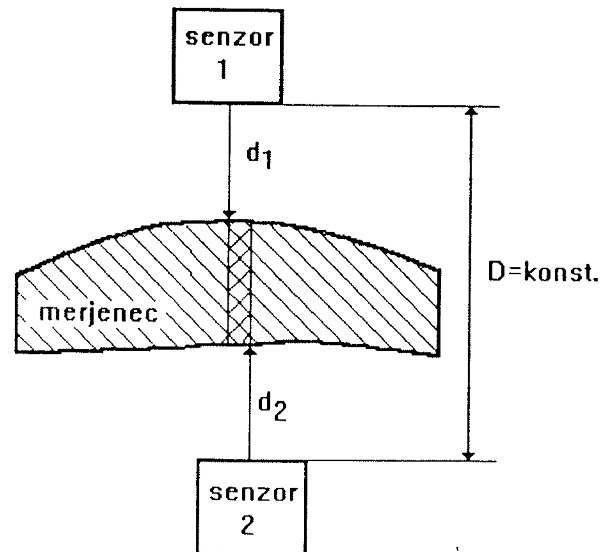

Slika 3.1: Princip merjenja debeline z dvema diametralno nameščenima senzorjema

serijskih kanalov ali pa prek A/D pretvorbe peljati na nadzorni računalnik.

Odločili smo se, da namesto mikrokontrolerjev uporabimo kar PC računalnik industrijske izvedbe, saj novejši procesorji (Intel 80386, ...486) omogočajo dovolj hitre obdelave merilnih rezultatov. Za povezavo s senzorji in digitalnimi vhodi, oz. izhodi pa smo izbrali kar multifunkcijsko karto, ki ima 16 A/D, 1 D/A, 8 DI in 8 DO. Sam sistem se je že od začetka snoval za industrijsko okolje, tako da smo dodali še karto z relejskimi izhodi in opto ločitev za digitalne vhode.

Merilnik je nameščen na okviru C oblike in ga na merilno pozicijo pomakne pneumatski ventil. Zaradi odstranitve prahu, oljnih emulzij in drugih nečistoč, so ohišja senzorjev oblikovana tako, da skozi reže piha zrak pod tlakom in tako tvori zračno zaveso. Ker lahko umazanija kljub temu prekrije površino senzorja, ima sam senzor digitalni izhod, ki javlja, če je odbiti žarek premajhne intenzivnosti.

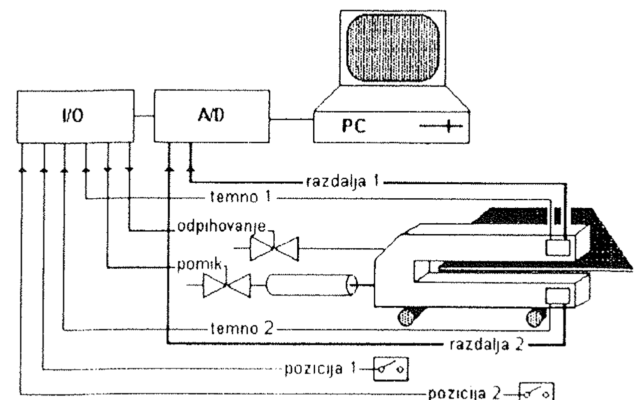

Slika 3.2: Shematski prikaz merilnika debeline

Ko senzor pomaknemo v merilni položaj ali pa je v mirovnem položaju, opravimo kontrolo pozicije s končnimi stikali. Sistem skupaj z opisanimi elementi je predstavljen na sliki 3.2:

4. Izvedba merilnika

Senzor razdalje, ki smo ga uporabili, ima referenčno merilno točko na razdalji 50mm ± 1mm in merilno območje ± 5mm z odstopanjem ± 0.01mm. Valovna dolžina svetlobe je 790nm (nevidna) z močjo 5mW. Merilno območje (MO) merilnika je potem:

$$MO = 2.10\ \text{mm} - \Delta \qquad (4.1)$$

Δ - maksimani možni pomik (vibracija) merjenca v smeri merilnega snopa

Senzor lahko meri oddaljenost predmetov, ki imajo primerno odbojno površino. Preizkusili smo meritve aluminija, iverice, nekaterih plastičnih materialov, papirja, pertinaksa,... tako da ocenjujemo, da je uporaben za vse veje industrije.

Za izvajanje merjenja in algoritma je izbran tipalni čas 10 ms zaradi naslednjih razlogov:

- časovna konstanta laserskega senzorja je 5 ms
- frekvence, ki se pojavljajo na strojih, so < 50Hz
- take tipalne čase srečujemo tudi pri merilnikih z drugimi vhodnimi senzorji.

4.1 Izvedba izhoda

Ker smo hoteli na ekranu opazovati kar največ dinamičnih podatkov, smo se odločili za uporabo semigrafike, ki omogoča dovolj natančen prikaz, hkrati pa zaradi ohranitve delovanja v tekstualnem načinu pridobimo na hitrosti. Na ekranu lahko tako opazujemo naslednje dinamične podatke (slika 4.1) :

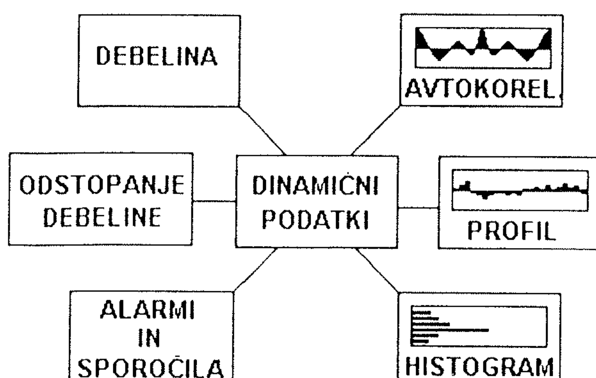

Slika 4.1: Dinamični podatki na zaslonu

Debelino dobimo po nekoliko modificiranem postopku, saj se za izračunavanje uporablja le celoštevilčna aritmetika. Da dobimo kvazi 16- bitno število, najprej pomaknemo 12- bitno vrednost iz A/D pretvornika za 4 bite v levo, . Tako zmanjšamo pogrešek pri celoštevilčnem deljenju. Ker nas pri tem merilniku zanima podatek o debelini do razreda 10^{-2} mm, opravimo tudi množenje s faktorjem 100. Tako dobimo naslednjo odvisnost:

$$\text{razdalja} = \left(\frac{\text{vhod} << 4 + \text{ofset}}{\text{naklon}}\right) .\ 100 \qquad (4.2)$$

vhod - 12-bitna vrednost iz A/D pretvornika
ofset, naklon - faktorja, ki ju dobimo po preslikavi iz toka v razdaljo.

Ker je referenčna točka 50mm podana ± 1mm, je potrebno senzor pred vgraditvijo umeriti in določiti ofset (slika 4.2) po enačbi:

$$\text{ofset} = -3276.25\ .\ I_{vh} + 262067 \qquad (4.3)$$

I_{vh} - tokovni signal iz senzorja (mA)

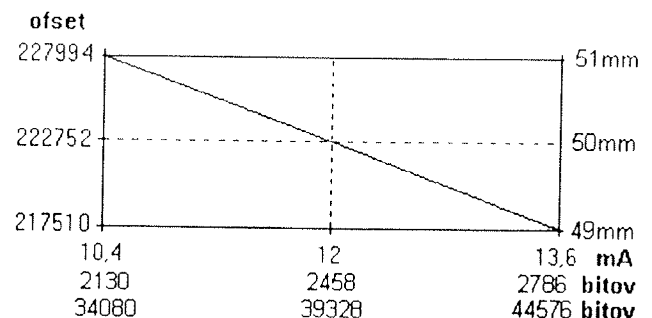

Slika 4.2: Ofset - korekcijska krivulja

Merilno odstopanje uporabimo v regulacijski zanki avtomatske kontrole debeline (AGC). V konfiguracijsko datoteko lahko vpišemo faktor občutljivosti v V/mm.

Vzdolžni profil merjenca se prikazuje v pomičnem časovnem diagramu in sicer vidimo 30 preteklih merjenj. Tak diagram uspešno nadomešča panelni instrument z ničlo na sredini.

V posebnem oknu se prikazujejo **alarmi in sporočila**, ki nas obveščajo o stanju merilnika. Ta sporočila se shranjujejo tudi v pomični pomnilnik, tako da lahko na samostojnem zaslonu pregledamo 23 zadnjih sporočil.

Histogram se izrisuje za 30 merilnih vrednosti. Področje izrisa je razdeljeno na dovoljeno (zelena) in na prekoračeno (rdeča barva) območje. Velikost dovoljenega območja se določi na osnovi vpisa tolerančnih mej pred pričetkom merjenja. Zaradi neproblematičnosti spominskega prostora in dovolj velike širine zapisa celoštevilčnih vrednosti razdalje, se kumulativno shranjujejo vse vrednosti debeline in se na koncu meritve izračuna

povprečni histogram za celotno meritev enostavno po enačbi za povprečno vrednost:

$$\bar{x} = \frac{1}{n}\sum_{i=1}^{n} x_i \qquad (4.4)$$

x_i - posamezna meritev
n - število vseh meritev

Med samo meritvijo je možen takojšen preklop med histogramom in avtokorelacijo. Zakaj avtokorelacija? Idealno bi bilo, da je površina merjenca čim bliže zahtevani in da z merjenjem dobimo mimimalno odstopanje, oz. nek šumni signal minimalne amplitude. To pa pomeni, da bi naj šla vrednost avtokorelacijske funkcije proti 0. Zaradi različnih vzrokov (nelinearna regulacijska proga, zračnosti na obdelovalnem stroju) pa se nam lahko na površini pojavi vzorec, ki vsebuje tudi določene periodične signale. Prav te pa z avtokorelacijsko funkcijo dobro vidimo in jih potem po analizi vzroka odpravljamo. Avtokorelacijska funkcija je soda, tako da izračunamo le člene do n/2, zaradi dovolj spominskega prostora pa vhodni vektor kar podvojimo:

$$vh_i = vh_{i+n}, \forall i \leq n \qquad (4.5)$$

n - dolžina vhodnega vektorja

saj s tem enačbo za izračun avtokorelacije močno poenostavimo:

$$iz_i = \sum_{i=1, j=1}^{\frac{n}{2}, n-1} vh_{i+j+1} \cdot vh_j \qquad (4.6)$$

zaradi simetrije pa velja tudi:

$$iz_i = iz_{n-i-1} \qquad (4.7)$$

4.2 Izvedba časovne baze

Na A/D karti je programabilni timer, kjer lahko nastavimo različne načine proženja, oz. štetja. Izbran je način, ko se po vpisu števne konstante prične odštevanje in ko pride števec na nič, se na izhodu sproži signal za čas trajanja ene periode urinih pulzov. Princip postopka uporabljenega za dosego želenega tipalnega časa je predstavljen na sliki 4.3:

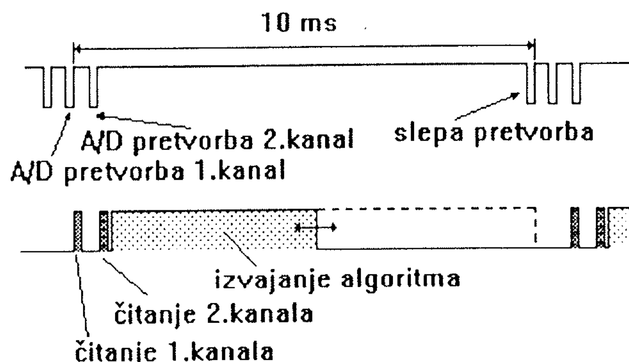

Slika 4.3: Časovni prikaz zaporedja A/D pretvorb in izvajanja algoritma

Pretvorbi merilnih rezultatov opravimo z minimalnim časom pretvorbe, nato pa opravimo "slepo" pretvorbo, tako da je vsota vseh časov enaka tipalnemu času. Pri takem načinu je nujno da se algoritem opravi v krajšem času kot "slepa" pretvorba.

Na koncu meritve se izriše v grafičnem načinu še celoten vzdolžni profil merjenca, v datoteko pa vpišejo odstopanja in kumulativni histogram, kar je pri sodobnem sledenju proizvodnje nujno (standard ISO 9000).

5. Zaključek

S prototipom merilnika smo preskusili meritve debeline mnogih materialov. Posebej je potrebno biti pozoren pri umerjanju vsakega laserskega senzorja, da ne vnesemo v merilno verigo dodatnih pogreškov.

Sistem, ki je zgrajen z opisanim senzorjem razdalje, ima uporabno območje merjenja 20 mm z odstopanjem $\pm 3.10^{-2}$ mm. Pri tem je potrebno omejiti maksimalni odmik merjene površine z dodatnimi valjčnicami pred merilno glavo, ker maksimalni odmik od srednje pozicije pomeni zmanjšanje merilnega območja in povečuje dinamični pogrešek. Sistem je časovno stabilen in ne potrebuje zagonskega časa (delovna temperatura, drift parametrov), tako da je takoj po vklopu pripravljen za merjenje. Merilne rezulatate smo potrjevali na Al pločevini različnih debelin in na ivernih ploščah različnih debelin z brušeno in nebrušeno površino.

Ker je možno priključiti več merilnih glav, ki so razporejene prečno, se ukvarjamo z določitvijo ustrezne interpolacijske funkcije in 3D izrisom celotne površine.

Prečni profil je možno dobiti tudi z ustreznim pogonom (koračni elektromotor, proporcionalni ventil), ko merilno glavo prečno pomikamo

Laserski merilnik lahko v večini primerov uspešno zamenja izotopske merilnike, ki s sevanjem v okolico povzročajo dodatne probleme (shranjevanje izotopov, periodični pregledi osebja, zavarovanje merilnega mesta, dodatna signalizacija...).

Z ustrezno analizo merilnega signala je možno dograditi diagnosticiranje napak na stroju (odprava zračnosti na ležajih, vodilih ...). Ker je možen vnos tehnologije direktno v merilnik (z disketo, serijska komunikacija), se merilnik enostavno vključuje v CIM ali pa povezuje z računalnikom na stroju.

Zaradi načina zajemanja podatkov se merilno območje spremeni enostavno z zamenjavo senzorjev, ki merijo v drugem merilnem območju.

Merilnik je nastal v sodelovanju med TF Maribor, Inštitutom za avtomatiko in Impol TEHNIKA d.o.o. Prva vgradnja naj bi bila na valjarni v DO IMPOL, Slovenska Bistrica

6. Zahvala

Za pomoč pri praktični izdelavi merilnika se zahvaljujem sodelavcu mag. Bojanu Marčiču in podjetju Impol TEHNIKA, d.o.o.

7. Literatura:

/1/ Thomas G.Beckwith, Roy D.Marangoni, MECHANICAL MEASUREMENTS, str.365 - 401, 1990 University of Pittsburgh

/2/ Several authors, PROCESS INSTRUMENTS AND CONTROLS HANDBOOK, str. 9-5 do 9-18, 1974 Los Angeles

/3/ Ray Butow, DIMENSIONAL INSPECTION, Februar 1993, Measurements & Control, str. 124 - 127

/4/ A. Bauer, OPTISCHE DICKENMESSUNG, MAREC 1992, SENSOR REPORT, str. 20 - 22

/5/ FAG Radiometrie, INFORMATIONEN ZUM ANGEBOT, 1987

/6/ J. Hecht, UNDERSTANDING LASERS, IEEE 1991 New York,

Darjan Gradišnik, dipl.ing.
Impol TEHNIKA d.o.o.
Partizanska 38
Slovenska Bistrica

prof. Dali Đonlagić, dr.dipl.ing.
Laboratorij za aplikacije v avtomatiki
TF Maribor

Prispelo: 29.07.93 ***Sprejeto: 03.09.993***

UPORABA POLPREVODNIŠKIH IN MIKROELEKTRONSKIH KOMPONENT

ASICs - selecting the optimum solution

Conrad F. Heberling

ASICs can provide many advantages over SSI and MSI PCB designs. But there are different types of ASICs and finding the most favourable solution for your specific application is important in creating a new system on a chip.

Gate arrays, standard cell and custom ICs comprise the three major types of application specific ICs. And all can improve system performance, increase reliability, reduce component count, reduce power consumption, lower manufacturing costs and provide protection against unauthorized copying. However, there are trade-offs in design flexibility, development span, development cost and production prices of each ASIC product.

Gate Arrays

Gate arrays have a fixed architecture which typically consists of predesigned rows of uncommitted logic gates separated by interconnect routing channels. For a given array size, these base layers are identical for all applications. The only difference from one application to the next is the metal interconnections between gates.

Gate level interconnections are normally specified by gate array macro overlays (metal interconnect patterns) and these are conceptually similar to standard cells. Macros are superimposed on the gate arrays' base transistors to perform the logic function and afterwards the macros are connected using the arrays' fixed routing channels.

Biggest advantage of gate arrays is short development time compared to standard cell circuits and cell-based custom circuits. Through using common base layers, gate array wafers can be partially fabricated prior to customization for a given use. When the logic is defined, metallization is all that need be carried out.

To achieve fast development, trade-offs to take seriously are that the fixed architecture limits design flexibility and causes production costs to be higher than a functionally identical standard cell or custom IC. And, the design is restricted to digital elements only.

Standard Cells

Standard cells are really circuit building blocks which have been previously designed, characterized and subsequently stored in a computer data-base.

Cells can range from simple digital circuit elements such as logic gates to more complex digital sub-systems such as ALU, UART, CPU, PLA, RAM and ROM memory cells. The cells can also include basic analogue circuit elements such as operation amplifiers and comparators, as well as the even more complicated analogue subsystems, such as ADCs and switched capacitor filters.

Such cells come in a standard cell library and by selecting the appropriate cells and interconnecting them, a unique IC can be created. Because each standard cell IC requires a unique fabrication mask set, the development cost and time spans are higher than gate arrays. However, standard cell circuits offer significant advantages in unit pricing, design flexibility, circuit performance and analogue and digital functional capabilities.

Compared with optimized full custom circuits, standard cell circuits offer lower development costs, reduced development time and a greater probability of first-time IC success.

In exchange for these benefits, the production unit prices of a standard cell circuit are slightly higher than the prices of a comparable optimized custom circuit.

Cell Based Custom Design

Within custom design, cell based custom design has largely replaced full custom design, which requires that each transistor is individually designed and manually connected to the rest of the circuit. In a cell-based approach, only critical parts of the circuit are designed in a full custom mode for particular applications while a major part of the design consists of previously available standard cells.

Advantage of cell-based custom is that optimum performance and minimum die sizes can realistically be achieved, while minimizing design risks, development

costs and development time compared to a full custom circuit.

By deciding on a cell-based ASIC, a system design engineer needs to pay for a state-of-the-art performance only where it is required. In other portions of the circuit, pre-designed standard cells are used to obtain the desired reductions in cost and development times.

Silicon Compiler Circuits

Silicon compiler circuits can be considered a separate type of ASIC but they actually represent a variation of cell-based custom circuits. A silicon compiler is an extremely sophisticated computer programme which can be used to create customized IC designs.

By supplying a high-level circuit description and the necessary design specifications, a cell or even an entire chip can be created by a compiler programme. Thus, instead of drawing from a library of predesigned cells and creating the desired full custom cells, a silicon compiler can be used to create a type of cell-based IC.

In evaluating specific ASIC choices, the trade-offs of each design alternative must be considered. Companies such as AMS offer experienced technical guidance to help the customer make that decision.

And by establishing close working relationships with such experienced companies, there is also valuable advice to be had on system design, optimal ASIC implementation and CAE interface options. With this assistance, any experienced logic designer can subsequently create his own ASIC for the next generation of electronic system products.

Dr. Conrad Heberling
AMS
Schloss Premstätten
A-8141 Unterpremstätten
Austria
tel. (03136) 500-0
fax (03136) 52501

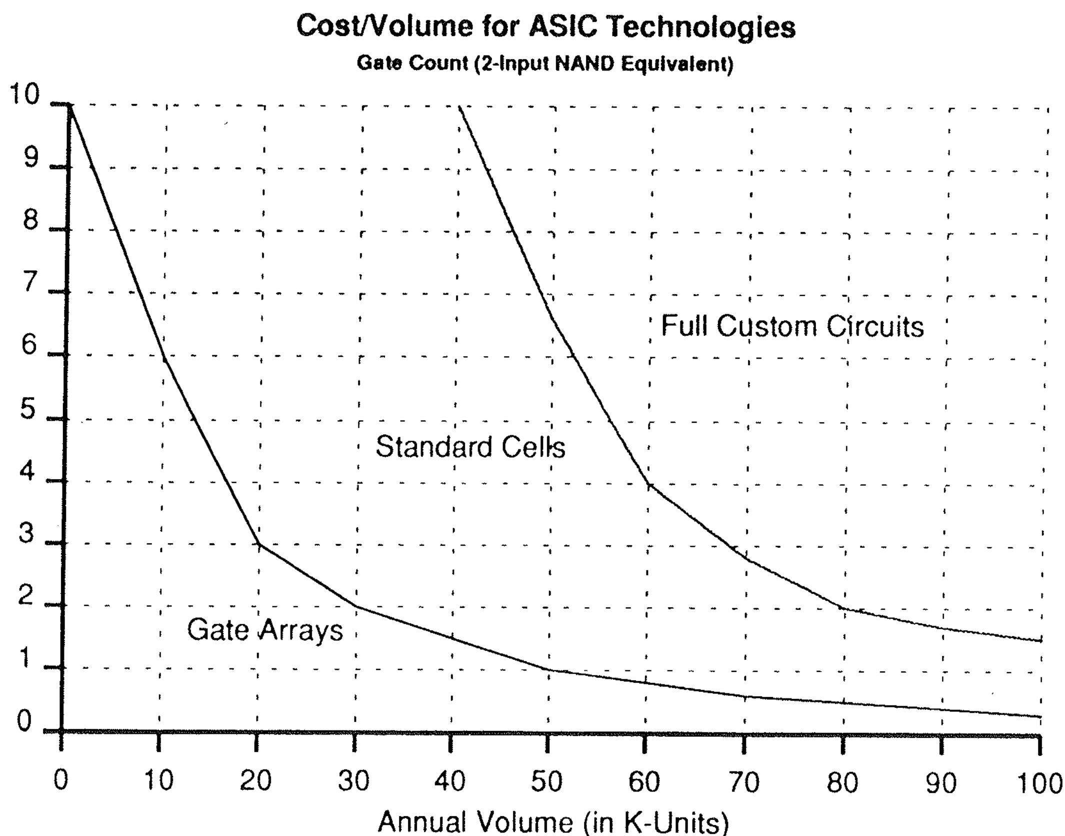

ELEKTRONSKO VEZJE ZA MINI ČASOVNI ŠTEVEC

J.Varl, J.Žmavc

UVOD

Mini časovni števci so nova smer v razvoju in izdelavi časovnih števcev s težnjo miniaturizacije in poseganja na nova področja štetja obratovalnih ur na zahtevnejših sistemih in napravah. Števci se priključijo vzporedno s tokokrogom in obratujejo samo, kadar je naprava vklopljena. Časovni števec je v bistvu kvarčna elektronska ura z elektromehanskim pretvornikom in decimalnim prikazom časa. Prikaz časa je izdelan v mehanski izvedbi števnih kolutov, podobno, kot pri števcih električne energije. Elektromehanski pretvornik je v osnovi števec električnih impulzov. Poganja ga elektronsko vezje, ki skrbi za napajanje, točnost in pravilno delovanje pretvornika. Osnova elektronskega vezja je čip s kvarčnim oscilatorjem.Skupaj generirata časovno zaporedje impulzov, s katerimi se napaja in krmili pretvornik.

ELEKTRONSKO VEZJE

V mini časovnem števcu je vgrajeno elektronsko vezje izdelano v SMD tehnologiji. Na vezje je bondiran čip EMZ 1447. Čip je naročniško vezje. Pri njegovem razvoju smo upoštevali zahtevane karakteristike delovanja časovnih števcev. Vezje v čipu je razdeljeno na oscilatorski del, delilno verigo, oblikovanje izhodnih impulzov in ojačevalno stopnjo. Oscilatorski del skupaj s kvarcem tvori samostojni oscilator frekvence 32768 Hz. Delilnik osnovne frekvence je dvajset stopenjski in na izhodu tvori zaporedje impulzov na 36 sek. širine 200 ms ali 1 sekunde, odvisno od izbire kontakta pri bondiranju. Na elektronskem vezju je poleg čipa še vgrajen napetostni regulator, končna stopnja ojačevalnika impulzov, kvarc s kondenzatorji za oscilator ter izbira dodatne funkcije vklop/izklop. Napetostni regulator ima nalogo vzdrževanje konstantne napetosti na vezju ne glede na predpisane različne vhodne napetosti ter posredovanje zadostne energije ojačevalniku za premik tuljavice v stalnem magnetnem polju. Dodatna izbira vklop/izklop se uporablja samo v posebnih primerih. V normalni vezavi se ta funkcija izvaja ob vklopu/izklopu naprave v katero je mini števec vgrajen.

Tehnični podatki:

Napetost	5, 12, 24 VDC +/- 10 %
Poraba	71, 158, 311 mW
Frekvenca osc.	32768 Hz
Velikost pl. vezja	20.2 x 24.8 mm

Tehnični podatki za čip:

Napetost	3 - 6 VDC
Tipična poraba	50 µA (pri Vdd = 5 V)
Max. tok na izhodu	5 mA (pri Vdd = 5 V)
Max. padec Vdd na tranzistorju	0,5 V (pri Ic = 5 mA)
Frekvenca osc.	32768 Hz
Frekvenca impulzov	36 s
Širina impulzov	0.2 / 1 s
CMOS tehnologija	
Nivo kakovosti	C2
Velikost tabletke	2.95 x 2.17 mm

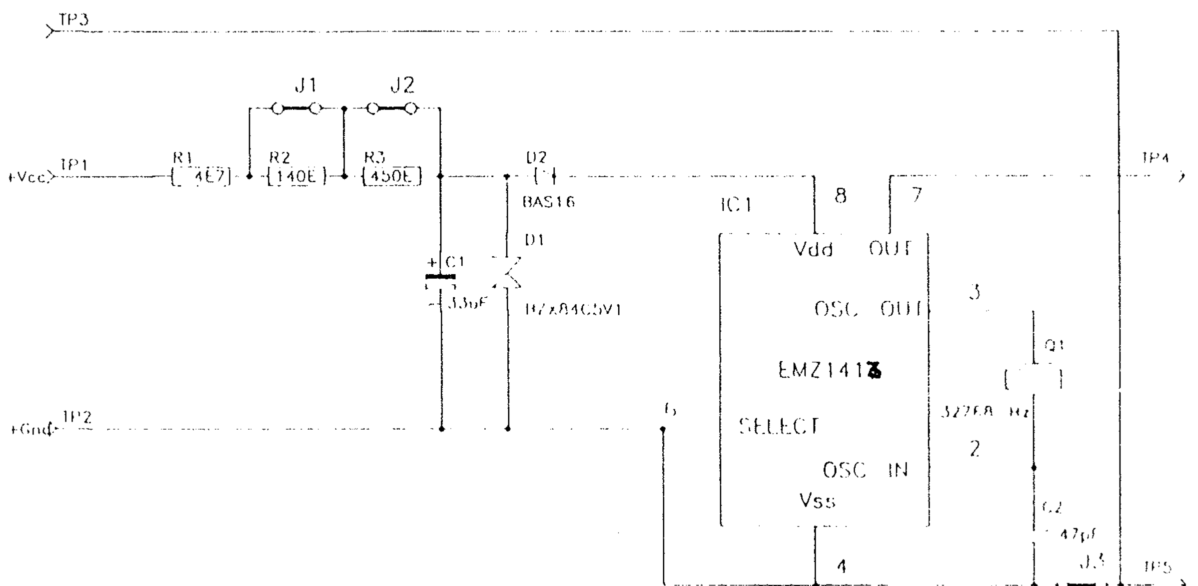

MINI ČASOVNI ŠTEVEC

Miniaturni časovni števci so izdelani za montažo na tiskano vezje ali za vgradnjo v ohišje. Števci za montažo na tiskano vezje so prilagojeni za avtomatično spajkanje in so vodotesni. So tudi neobčutljivi za zunanja magnetna polja. Mini časovni števci se uporabljajo za ugotavljanje obratovalnega časa najrazličnejših strojev ali naprav. Števci se priključijo vzporedno s tokokrogom naprave in obratujejo samo kadar je ta vklopljena.

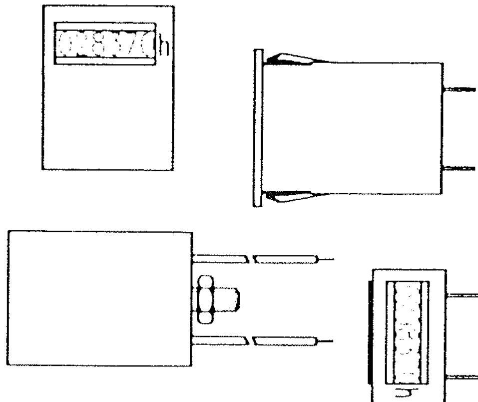

Števce odlikujejo naslednje tehnične lastnosti:

- točnost delovanja
- visoka odpornost na vibracije in udarce
- neobčutljivost na motnje zunanjega magnetnega polja
- majhne dimenzije
- majhna poraba energije
- konstrukcija omogoča spajkanje na TIV ali samostojno vgradnjo
- vodotesna izvedba ohišja

Tehnični podatki:

Število mest	6 mestni - 4 cele, 2 decimalni 7 mestni - 5 celih, 2 decimalni
Velikost številk	1.7 x 4mm (6 mestni) 1.2 x 4mm (7 mestni)
Temp. območje delovanja	- 10 st.C / + 50 st.C
Življenska doba	5 let
Pogrešek	+/- 20 sek/dan
IP zaščita	IP 65
Odpornost na zunanje magnetno polje	100 KA/m
Ohišje	prozorna plastika
Velikost	25,2 x 31 x 13,9
Lega vgradnje	poljubna

Janez Varl, dipl.ing.str
Jože Žmavc, dipl.ing.el.
Iskra Mehanizmi Lipnica
Lipnica 8, 64245 Kropa

SUPPRESSOR AND LIMITER DIODES FROM ISKRA SEMICON

For several years now manufacturers of electronic equipment have been investigating the couses and effects of transients produced by atmospheric disturbances and other sources such as inductive charges from relays, motors, cables, etc.

With introduction of electro mechanical switchboards and the use of protection gas valves, the damage caused by transient voltage decreased dramatically but the response delay (so important in these cases) was not very good.

The effect is short as the energy source stored in the inductance is limited and is generally dissipated by an instant increase in power (energy = power x time). It can be repeated several times due to a simple effect of switching and this effect, if accumulated, can be significant. Because of this, a demand for quicker response, using solid state physics, was required for complete protection of circuits.

The advantages of semiconductors has led to the use of varistors and more recently to suppressor diodes as elements for discharging over voltages.

It is therefore obvious, that suppressor diodes will play an important part in modern comunication systems, as a suppressor of transient over voltage produced by current pulses.

There are basically two kinds of protection: clamping and crowbar. Clamping protectors: the most common are varistors and suppressor diodes.

Varistors are clamping devices used in alternating current supplies. It has non-linear symetric features and a response time in the region of 25 nsec. Although it has a lower current capacity than gas valves, the breakdown is more reliable. Gas valves are to be found among crowbar protectors. These devices use the gap between two electrodes. This gap goes from tens of volts to kilovolts.

It's most important features are:

- High current capacity
- High noise
- Slow response time
- It shortcircuits when breakdown voltage is reached

– Requires high dropout voltages which may be damaging for the rest of the circuit.

Supressor diodes made from silicon, formed through a diffusion process and specificaly conceived short response time (1 pico sec.). They are manufactured in two versions:

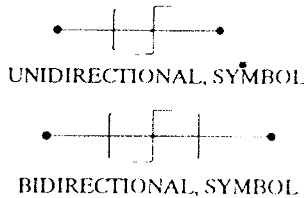

UNIDIRECTIONAL SYMBOL

BIDIRECTIONAL SYMBOL

CONCEPT OF PROTECTION	GAS VALVES	VARISTORS	SUPPRESOR DIODES
Range of breakdown voltage	65 V - 10 KV	20-2000 V	1.33 - 10.7 6.8 - 440 V
Current capability	Very high	Medium	Medium
Resistance in area of conduction	Very Low	Medium	Low
Resistance in area of no conduction	High	High	High
Capacitance	Very Low	Medium	Low
Response time	Medium (250 ns)	Fast (25 ns)	Very fast (1 pico sec.
U/I Feature	Symetric	Symetric	Symetric Asymetric
Failure Mechanism	Open Circuit	Short Circuit	Short CIrcuit
Kind of protection	Crowbar	Clamping	Clamping
Noise	Very high	Low	Very Low

To protect continuous current, unidirectional ones are used with the cathode in the positive part of the voltage. Bidirectional ones are used with either positive or negative voltage as they are basically two diodes in opposition. These are commonly used in AC circuits due to its simetrical characteristic U-I. These components fail when presented with power peak higher then the maximum Ppp of the diode which causes the silicon to fuse thereby short circuiting the diode.

It's advisable to have a circuit breaker fitted, which cuts off the supply of current for an excessively long time. When a circuit has to be protected from over voltages of higher voltage, these diodes may be grouped in serie with the aim of creating a higher voltage.

The most important properties of these diodes are:

– very short responce time: typical 1 psec - very small dynamic impedances in the conduction zone
– good clamping capability
– good stability in long term storage and operation
– high power dissipation absorbtion combined with over voltages of a short duration.

The test pulse for the peak current and the clamping voltage is a shock wave pulse characterized by a rise time and a fall time.

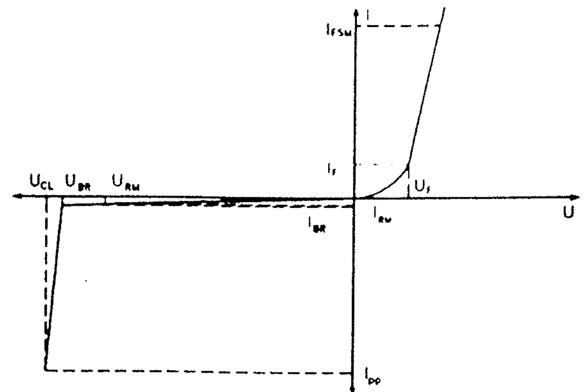

FORWARD CHARACTERISTIC

UF - FORWARD VOLTAGE
IF - FORWARD CURRENT
IFSM - RATED FORWARD PULSE CURRENT

REVERSE CHARACTERISTICS

URM - REVERSE VOLTAGE IN WHICH POINT THE DIODE DOES NOT CONDUCT
IRM - MAXIMUM REVERSE LEAKAGE CURRENT AT URM
UBR - VOLTAGE VALUE WHERE THE CURRENT INCREASSES VERY FAST (AVALANCHE POINT)
IBR - TEST CURRENT FOR UBR
UCL - MAXIMUM PROTECTION VOLTAGE FOR A PULSE WITH A IPP VALUE
IPP - PEAK PULSE CURRENT DETERMINATED BY A TIME AND WAVE AMPLITUDE (EXPO. PULSE 10/1000 μ sec.)

The rise time lasts between 8 and 10 μsec and is defined between 10 and 80% of the maximum current value. The fall time is, when current decreases to 50 % of the peak value, (between 20 and 1.00 msec).

	t_1 (μs)	t_2 (μs)
Wave 8/20 μs	8	20
Wave 10/1000 μs	10	1000

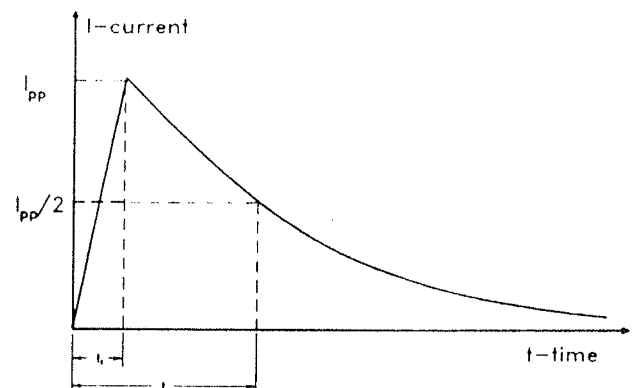

PEAK CURRENT PULSE WAVE FORM

PEAK PULSE POWER [1] P_{pp} (w)				BZW04 400	BZW06 600	BZW1.5 1500
type [2]	Breakdown voltage at I_R U_{BR} (V) 5%	(mA)	Clamping voltage at I_{pp} U_{CL} (V)	Peak pulse current Ipp[1] (A)	Peak pulse current Ipp[1] (A)	Peak pulse current Ipp[1] (A)
5V8	6.8	10	10.5	38	57	143
5V4	7.5	1	11.3	35.4	53	132
7V0	8.2	1	12.1	33	50	124
7V8	9.1	1	13.4	30	45	112
8V5	10	1	14.5	27.6	41	103
9V4	11	1	15.6	25.7	38	96
10	12	1	16.7	24	36	90
11	13	1	18.2	22	33	82
13	15	1	21.2	19	28	71
14	16	1	22.5	17.8	27	67
15	18	1	25.2	16	24	59.5
17	20	1	27.7	14.4	22	54
19	22	1	30.6	13	20	49
20	24	1	33.2	12	18	45
23	27	1	37.5	10.7	16	40
26	30	1	41.5	9.6	14.5	36
28	33	1	45.7	8.8	13.1	33
31	36	1	49.9	8	12	30
33	39	1	53.9	7.4	11.1	28
37	43	1	59.3	6.7	10.1	25.3
40	47	1	64.8	6.2	9.3	23.2
44	51	1	70.1	5.7	8.6	21.4
48	56	1	77	5.2	7.8	19.5
53	62	1	85	4.7	7.1	17.7
58	68	1	92	4.3	6.5	16.3
64	75	1	103	3.9	5.8	14.6
70	82	1	113	3.5	5.3	13.3
78	91	1	125	3.2	4.8	12
85	100	1	137	2.9	4.4	11
94	110	1	152	2.6	3.9	9.9
102	120	1	165	2.4	3.6	9.1
111	130	1	179	2.2	3.4	8.4
128	150	1	207	2	2.9	7.2
136	160	1	219	1.8	2.7	6.8
145	170	1	234	1.7	2.6	6.4
154	180	1	246	1.6	2.4	6.1
171	200	1	274	1.5	2.2	5.5
188	220	1	301	1.4	2	4.6
213	250	1	344	1.3	2	5
239	280	1	384	1.3	2	5
256	300	1	414	1.2	1.6	5
273	320	1	438	1.2	1.6	4.5
299	350	1	482	0.9	1.6	4
342	400	1	548	0.9	1.3	4
376	440	1	603	0.8	1.3	3.5
case				DO - 41		DO - 27

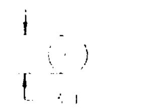

DO -41

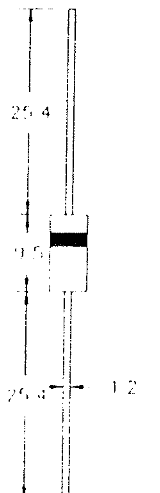

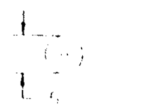

DO - 27

1) EXPONENTIAL PULSE 10 / 1000 μS
2) UNIDIRECTIONAL, FOR BIDIRECTIONAL ADD "B" TO BASIC PART NUMBER, E.G. BZW04 - 5V8B

BIDIRECTIONAL LOW VOLTAGE, LOW CAPACITANCE, TRANSIENT SUPPREESSOR DIODES

Type	Stand-off voltage U (A)	Breakedown voltage at I_R = 10mA 10% U_{BR} (V)	Peak pulse current [1] Ipp (A)	Capacitance U = 0V C (pF)	Temerature coeficient αC (mV / oC)	Case
SV 0.8	0.8	1.33	30	1040	-3.6	DO - 41
SV1.2	1.2	2	25	346	-5.4	
SV 1.6	1.6	2.7	15	260	-7.2	
SV 2	2	3.3	15	208	-9	
SV 2.4	2.4	4	15	173	-10.8	
SV 2.8	2.8	4.7	15	148	-12.6	case similar DO-41
SV 3.2	3.2	5.4	15	130	-14.4	
SV 3.6	3.6	6	15	115	-16.2	
SV 4	4	6.7	15	104	-18	
SV 4.4	4.4	7.3	15	94	-19.8	
SV 4.8	4.8	8	15	86	-21.6	
SV 5.2	5.2	8.7	15	80	-23.4	
SV 5.6	5.6	9.4	15	74	-25.2	
SV 6	6	10	15	69	-27	
SV 6.4	6.4	10.7	15	65	-28.8	
SVP 0.8	0.8	1.33	100	1550	-3.6	DO - 27
SVP 1.2	1.2	2	75	1050	-5.4	
SVP 1.6	1.6	2.7	50	840	-7.2	
SVP 2	2	3.3	50	660	-9	
SVP 2.4	2.4	4	50	550	-10.8	
SVP 2.8	2.8	4.7	50	470	-12.6	case similar DO-27
SVP 3.2	3.2	5.4	50	412	-14.4	
SVP 3.6	3.6	6	50	366	-16.2	
SVP 4	4	6.7	50	330	-18	
SVP 4.4	4.4	7.3	50	300	-19.8	
SVP 4.8	4.8	8	50	275	-21.6	
SVP 5.2	5.2	8.7	50	253	-23.4	
SVP 5.6	5.6	9.4	50	235	-25.2	
SVP 6	6	10	50	220	-27	
SVP 6.4	6.4	10.7	50	206	-28.8	

TYPICAL APPLICATIONS OF SUPPRESSOR DIODES

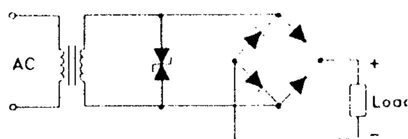

AC SUPPLY PROTECTION

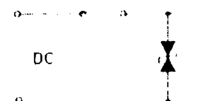

RELE AND CONTACTOR TRANSIENT LIMITING

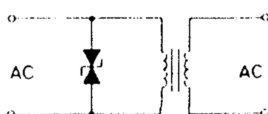

OVER VOLTAGE POWER SUPLLY PROTECTION

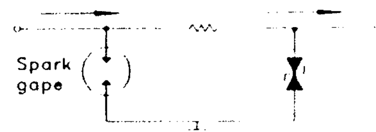

DATA LINE PROTECTION

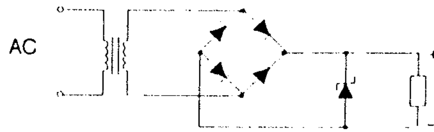

DC SUPPLY PROTECTION

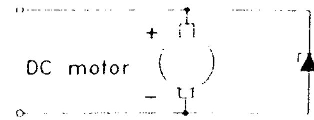

EMI SUPPRESING

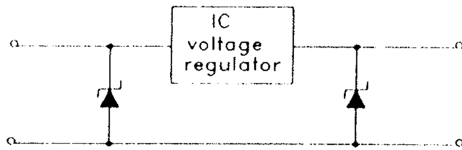

INPUT-OUTPUT PROTECTION

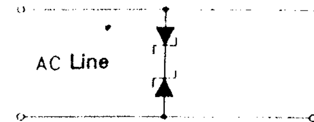

PROTECTION BY TWO UNIDIRECTIONAL DIODES

BIDIRECTIONAL LIMITER DIODES

Type	Steady state current I_F (mA)	Power dissipation Ptot (mw)	Peak pulse current[1] Ipp (A)	Temeperature αC (mV/°C)	Voltage U_F (V) at I_F = 10 A	1 mA		10 mA	70 mA		100mA	1A	10 A*	case
					min	min	max	min	min	max	max	max	max	
SV02	500	1000	30	-3.8	0.2						0.9			DO-41
SV022	250		25	-5.7	0.4						1.8			
SV03	166		15	-7.6	0.6						2.7			
SV04	125		15	-9.5		2.05	2.56			3.35				
SV05	100		15	-11.4		2.55	3 18			4.18				
SV12	750	1500	100	-3.8	0.21			0.61				0.88	1.05	DO-27
SV122	375		75	-5.7	0.42			1.22						
SV13	250		50	-7.6	0.63			1.83						
SV14	188		50	-9.5	0.84			2.44						
SV15	150		50	-11.4	1.50			3.50						

* Pulse test. Pulse widh 1msec

UNDIRECTIONAL LIMITING (STABISTOR) DIODES

Type	Steady state current I_F mA	Power dissipation Ptot (mW)	Minimum reverse voltage U_R (V)	Voltage U_F (V) at I_F = 5 mA		10 mA		100 mA		200 mA		case
				min	max	min	max	min	max	min	max	
2360	1.000	1000	55			0.63	0.71					DO-41
BY02A	500			1.1	1.35					1.4	1.7	
BY03A	300			1.7	2			2	2.15			
BY04A	200			2.25	2.75			2.7	3.25			

TYPICAL APPLICATIONS OF LIMITER DIODES

- temperature compensation of transistor and "voltage regulator diode" circuits
- amplitude stabilization of touch-tone telephone oscillation
- voltage limiters and dividers
- wave squarers for threshold limiters, level shifters, etc.
- secondary arrestors in repeater amplifiers
- click absorbtion in telephone handsets

ISKRA SEMICON d.d.
SLO 61420 Trbovlje
Gabrsko 12
tel. (0601) 24155
fax (0601) 22376

KONFERENCE, POSVETOVANJA, SEMINARJI, POROČILA

Tečaj osnove vakumske tehnike

V dneh 15., 16., in 17. junija je bil v organizaciji DVT Slovenije izveden prvi letošnji tečaj "Osnove vakumske tehnike". Potekal je na Inštitutu za elektroniko in vakumsko tehniko, prva dva dni dopoldne in popoldne, zadnji dan pa le dopoldne. Udeležencev je bilo sedem in sicer iz naslednjih delovnih organizacij: Labod Trebnje - Novo mesto, Iskra avtoelektronika Nova Gorica, Inštitut Zoran Rant Škofja Loka, IEVT Ljubljana in 2 zasebni podjetji (iz M. Sobote in iz Benedikta). Program je kot običajno obsegal 20 h predavanj in vaj z naslednjo tematiko:

- pomen in razvoj vakuumske tehnike
- fizikalne osnove
- vakumske črpalke
- meritve vakuuma
- materiali v vakumski tehniki
- hermetičnost in odkrivanje netesnosti
- tehnike čiščenja in spajanje
- analize površin
- tankoplastne in druge vakuumske tehnologije
- čiščenje in preiskave plinov

Tečajniki so si ogledali tudi nekatere laboratorije in specialno tehnologijo na Inštitutu za elektroniko in vakuumsko tehniko ter na koncu prejeli potrdilo o udeležbi.

Andrej Pregelj

1. Srečanje vakuumistov Slovenije in Hrvaške

Po razpadu Zveze Jugoslovanskih društev za vakuumsko tehniko TUVAK, zaradi Srbske agresije v bivši Jugoslaviji, sta hrvaško in slovensko društvo sklenili ohraniti in celo izboljšati že obstoječe strokovne stike. Že lani v Haagu, ob sprejetju v mednarodno zvezo IUVSTA smo se vakuumisti obeh novih držav dogovorili za pripravo 1.skupne konference letos spomladi v Zagrebu. 21. aprila se nas je na enodnevnem srečanju zbralo na Institutu za fiziko pri Mirogoju (Zagreb) cca 50 strokovnjakov iz institutov in industrije, od tega 31 aktivno z referati. Predavanja omejena na 15 - 20 minut so potekala od 8.30 do 18.50; za izmenjavo mnenj in navezavo stikov je bilo le malo časa: dve kratki coffee pavzi in kosilo. Tematika, splošno vakuumska je posegala na vsa strokovna področja mednarodne zveze. Vzporedno je potekala mala razstava vakuumskih elementov, kjer so domači proizvajalci in zastopniki tuijih firm seznanili strokovnjake s svojo ponudbo. Lokalni organizator - Hrvaško društvo je srečanje izvedlo v prisrčnem in gostoljubnem vzdušju ter pripravilo za vsakega udeleženca zbornik abstraktov. Referati bodo objavljeni v strokovni reviji Vakuumist slovenskega vakuumskega društva.

Andrej Pregelj

PREDSTAVLJAMO PODJETJE Z NASLOVNICE

"Austria Mikro Systeme International AG", AMS for short

Founded only 10 years ago, AMS has grown to be one of the leading European manufacturers in the semiconductor market. At its headquarers in Unterpremstätten near Graz, AMS designs and produces "custom circuits", so- called ASICs for "Application Specific Integrated Circuits". Expressed very simply: AMS designs and produces tailor-made chips for the most individual customer requirements.

No mass market

"We are thus not only incredibly flexible, but also not exposed to the enormous risk of the mass products, such as memory chips", says President and CEO Horst Gebert, who has led the company successfully since 1986.

Everything under one roof - optimum flexibility

AMS combines every technological step "under one roof":

- research and development,
- product idea,
- chip design,
- production,
- test and
- sales and marketing.

Thus AMS is quite extraordinarily flexible. "In recent years we have been able to reduce the product life of our ASICs by 50% from its original four down to its present-day two years", says Gebert proudly. "And this year 60% of our sales will be with products only developed in 1992".

The AMS "three column concept"

AMS concentrates on market segments which it services with innovative system solutions. These three columns are:

- telecomunications,
- automotive industry and
- industrial electronics.

Today tailor-made AMS chips are just as common as the control elements in handy phones as they are in intensive care stations, industrial robots or in the safety system of our cars. There is hardly any other ASIC manufacturer as capable as AMS at adapting to the specific needs of each individual customer and designing and producing precisely those tailor-made ICs which the client needs.

1992 - European champion

This flexibility on the one hand, but also the quality level on the other, and AMS' innovative strength and the environmental protection measures, were the reasons for the American trade magazine "Semiconductor International, USA" to elect AMS as the "best semiconductor factory in Europe in 1992" (TOP FAB OF 1992).

Internationally active

From its headquarters in Unterpremstätten (the AMS research centre Premstätten Castle already bears the synonym of Austria's "Sillicon Castle") - AMS controls sales offices and design centres in Paris, Milan, London, Stockholm, Münich, Hamburg, Dresden and Cupertino/USA.

AMS operates in rapid growth markets

The three "market columns" of AMS, telecomunications, automotive and industrial electronics are heavy growth markets. Thus the number of telephone lines in Europe is predicted to increase to 330 million by 1995, the number of comfort telephones in Europe is expected to rise from 4.5 million in 1992 to 8 million by 1995. In the same period standard telephones will increase from 30 million to 40 million units, and with special telephones a doubling is forecast in the next three years (to 4 million units). And by 1995 the worldwide market for mobile communications might even achieve US$ 35 billion.

Despite the recession in the automotive industry - electronics will continue to grow

Despite the almost worldwide recession in automobile production the use of advanced electronics will grow. Thus it is estimated that by 1995 the electronics share in a car will increase from its present 8% (of the overall production costs) to 20%(!).

AMS sales 1992: ATS 725 million, a plus of 17%

In the year 1992 AMS was able to increase sales by 17% to ATS 725 million (1991: ATS 617). The workforce average 584 (1991 : 554).

ATS 65 million profit according to ÖVFA

With a profit increase of 8% according to ÖVFA - ATS 56 million - a cash flow of approx. 20% of the sales was achieved.

Export quota 97%

Last year 97% of AMS sales went abroad. The most important export markets for the Styrian high-tech company were:

- Nordic countries 33%
- Germany 19%
- Italy/Spain 12%
- USA 8%
- France/Benelux 6%
- England/Ireland 6%
- Rest of the world 7%

Contact: Dr. Conrad Heberling, ext. 277
Schloss Premstätten
A-8141 Unterpremstätten, Austria
Telex 312547 ams a
fax (03136) 52 501, 53 650
*tel.: (03136) 500-0**

VESTI

Aprilska številka Novic - MZT prinaša predstavitev 53 raziskovalno-razvojnih projektov, ki jih je Ministrstvo za zanost in tehnologijo financiralo v letih 1991 in 1992. Za bralce Informacij MIDEM smo pripravili predstavitev nekaterih projektov iz dveh raziskovalnih polj.

Raziskovalno polje: ELEKTRONSKE KOMPONENTE IN TEHNOLOGIJE

Naslov: Senzor za merjenje pritiska do 500 bar s pripadajočo električno mersko enoto
Naročnik projekta: Kladivar, Žiri
Vodja projekta: mag Marjan Hudomalj, Senzolab, Ljubljana
Izvajalec projekta: Senzolab, Ljubljana
Trajanje projekta: januar 1992 - december 1992
Delež sredstev MZT: 1.000.000,00 SIT

Rezultati projekta:

Dosedanji rezultati so zaključili uvodni del v obsežnejšem razvojnem delu pri tem projektu. Rezultati slonijo na intenzivnosti, saj je bilo treba združiti postopke in metode, ki med seboj niso kompatibilni.

V tem delu so bile določene lastnosti in na njihovi podlagi izbrana kovina za izdelavo membrane, razviti pa so bili tudi površinske obdelave in zaščite membranske folije ter postopka mehanskega puščanja.

Področje implementacije rezultatov:

Namen raziskave in razvoja tankoplastnih senzorjev za pritisk je bil izdelati prototip in vzpostaviti redno proizvodnjo.

Tržni (ekonomski) učinki:

Analiza tržnosti napoveduje ugodne tržne učinke.

Sodelovanje raziskovalcev iz znanstveno-raziskovalne in proizvodne sfere:

V dosedanjem delu je sodelovala skupina strokovnjakov z Univerze v Ljubljani, iz Kladivarja in Senzolaba, pred temi raziskavami pa so večletne temeljne raziskave potekale na Institutu "Jožef Stefan" v Ljubljani.

Naslov: Visokovakumski naparevalnik ogljika C_{60}
Naročnik projekta: Institut "Jožef Stefan", Ljubljana Inštitut za avtomatizacijo procesov p.o., Ljubljana
Vodja projekta: izr.prof.dr. Jože Gasperič, Institut "Jožef Stefan", Ljubljana
Izvajalec projekta: Institut "Jožef Stefan", Ljubljana
Trajanje projekta: januar 1992 - december 1992
Delež sredstev MZT: 6.821.100,00 SIT

Rezultati projekta:

Končni rezultat projekta je laboratorijski prototip vakuumskega naparevalnika ogljika C_{60}, ki že rabi kot rutinska naprava za pridobivanje fluerena C_{60}.

Področje implementacije rezultatov:

Fuleren C_{60} je osnova za izdelavo novih snovi z odličnimi tribološkimi ter superprevodnimi lastnostmi.

Tržni (ekonomski) učinki:

Ekonomski učinki še niso znani, pričakovanja v svetu pa so velika.

Sodelovanje raziskovalcev iz znanstveno-raziskovalne in proizvodne sfere:

Rezultat projekta je posledica sodelovanja med Institutom "Jožef Stefan" in Inštitutom za avtomatizacijo procesov ter tujimi univerzami.

Naslov: Ultra hitra dioda
Naročnik projekta: Iskra Semicon d.d., Trbovlje
Vodja projekta: Zmago Zupančič, dipl. ing., Iskra Semicon d.d., Trbovlje
Izvajalca projekta: Iskra Semicon d.d., Trbovlje; Mikroiks d.o.o., Ljubljana
Trajanje projekta: januar 1991 - december 1992
Delež sredstev MZT: 3.000.000,00 SIT

Rezultat projekta:

Vzporedno so razvili slojno in planarno tehnologijo za izdelavo ultra hitrih silicijevih diod. Obe tehnologiji se dopolnjujeta, saj se v prvi laže izdela visoko napetostne diode z daljšimi preklopnimi časi, medtem ko se s planarno tehnologijo laže izdela diode z nižjo prebojno napetostjo in krajšimi preklopnimi časi.

Izdelane diode so dale pričakovane rezultate in ustrezajo zahtevam kupcev.

Pri obeh tehnologijah je difuzija dopantov najpomembnejši korak. S spreminjanjem pogojev difuzije se vpliva na distribucijo dopantov, ki ima skupaj s površinsko koncentracijo dopanta pomembno funkcijo pri zagotavljanju ustreznih preklopnih karakteristik diode. Pri tem imajo glavno vlogo vgrajena električna polja in z difuzijo tvorjeni defekti. Z izdelavo ultra hitrih diod so razvili in optimirali difuzije tako, da dajo zahtevane lastnosti. Zelo pomembno je bilo zagotoviti čim večjo uniformnost in ponovljivost postopka.

Preklopni čas diod se uravnava z vsebnostjo zlata v siliciju. Z difuzijo zlata se lahko zagotovi koncentracija zlata velikostnega reda 10^{15} at/cm^3 Si, kar pomeni 0,1 ppm zlata v siliciju. Izredno zahtevnost postopka kaže tudi zahtevana natančnost doseganja koncentracije zlata. Tolerančna meja je 10% (0,01 ppm).

Zaradi doseganja visokih zapornih napetosti so potrebne ustrezne zaključitve polprevodniške strukture in pasivacije. Površinski tokovi ob zaključni strukturi so funkcija nečistoč. Poleg tega je silicij zaradi kompenzacije z zlatom skoraj intrinsičen in zelo občutljiv na električna polja in naboje v okolici. Strukturo diode so uspeli primerno oblikovati in pasivirati in tako dosegli skoraj teoretično vrednost reverznega toka diode.

Celoten proces jim je uspelo optimirati do te mere, da so dosegli za tovrstne tehnlogije izjemno visok izplen - 95%. Zaradi vedno večjih zahtev kupcev bo treba nadaljevati delo pri optimiranju procesa.

Področje implementacije rezultatov:

Hitre in ultra hitre diode se uporabljajo povsod, kjer je prisotna visoka frekvenca.

V svetu so vedno bolj popularni stikalni napajalniki (switch - mode power supplies), ki delajo na višji frekvenci, zato se povečuje proizvodnja in prodaja hitrih in ultra hitrih diod.

Tovrsten napajalnik razseka izmenično napetost na frekvenčno področje od 20 do 200 kHz. Vhodna dioda je standardna usmerniška dioda, ena od izhodnih dveh diod je zaradi visoke frekvence ultra hitra, druga pa zaradi nizke usmerniške napetosti schottky dioda.

Vsi osebni računalniki, monitorji, TV sprejemniki, naprave za izkoriščanje sončne energije, regulatorji, brezprekinitvene napajalne naprave in ostale moderne naprave vsebujejo stikalne napajalnike. Razmerje med uporabnimi diodami je: 25% standardna usmerniška dioda, 75% hitra in ultra hitra dioda.

Tržni (ekonomski) učinki:

Ultra hitre diode že uspešno prodajajo, poteka pa tudi marketinška obdelava tržišča.

Sodelovanje raziskovalcev iz znanstveno-raziskovalne in proizvodne sfere:

Uporabili so raziskovalne možnosti Instituta "Jožef Stefan" in Inštituta za elektroniko in vakuumsko tehhniko.

Naslov: Vakuumske tehnologije in karakterizacije površin za elektroniko in optoelektroniko
Naročniki projekta: Iskra Elektrooptika, Ljubljana; Iskra Zaščite, Ljubljana; Inštitut za elektroniko in vakuumsko tehniko, Ljubljana
Vodja projekta: France Brecelj, dipl. ing., Inštitut za elektroniko in vakuumsko tehniko, Ljubljana
Izvajalec projekta: Inštitut za elektroniko in vakuumsko tehniko, Raziskovalno-razvojni oddelek, Ljubljana
Trajanje projekta: januar 1992 - december 1992
Delež sredstev MZT: 15.831.650,00 SIT

Rezultat projekta:

Projekt je bil sestavljen iz treh delno med seboj povezanih raziskovalno-razvojnih podprojektov.

Razvoj 25 mm elektronskega slikovnega ojačevalnika 2. generacije z izboljšanimi karakteristikami je bil zaključen s funkcionalnem modelom slikovnega ojačevalnika z izboljšanimi karakteristikami: med drugimi z občutljivostjo fotokatode 450 uA/lm, ojačanjem 30000, ločljivostjo 30 lp/mm in distorzijo < 4%, Z računalniško simulacijo se je določilo primerno geometrijo, ki pa bi jo še morali optimizirati z izdelavo serije ojačevalnikov. Razviti so bili postopki visokotemperaturne metalizacije obročkov iz visokoglinične keramike in izdelana keramično-kovinska ohišja za ta tip elektronke. Razvit je bil postopek sinteze visokoobčutljive multialkalijske fotokatode. Izdelani sta bili konstrukcijska in tehnološka dokumentacija.

Razvoj kratke miniaturne enocolske katodne elektronike z elektrostatskim odklonom - MKES2 je bil zaključen z izdelavo laboratorijskih prototipov, ki so izpolnjevali tehnične zahteve naročnika za vgradnjo v novo termovizijsko kamero. Vzorci elektronk so bili na testiranju v tujini odlično ocenjeni. Elektronka je bila predstavljena na Sejmu elektronike v Ljubljani.

Razvoj linearnega polimernega senzorja in industrijskih merilnikov vlage je bil zaključen z izdelavo serij tankoplastnih polimernih senzorjev v čip obliki in v TO5 ohišju. Senzorji ustrezajo zahtevam splošne uporabe. Stabilno delovanje naj bi se doseglo tudi pri višjih temperaturah in vlagah, kar bi razširilo njihovo uporabnost v industriji. Razvitih je bilo nekaj tipov dajalnikov relativne vlage z napetostnim ali tokovnim izhodom oz. z optičnim prenosom merilnih podatkov. Razvili so dajalnik relativne vlage na kapacitivnem načelu s senzorjem v TO5 ohišju, namenjenem krmiljenju gospodinjskih sušilnih strojev, ki pa zaradi fizikalnih zakonitosti ni primeren za meritve vlage v izpuhu sušilnika. Osvojili so izdelavo kalibrov relativne vlage z nasičenimi raztopinami soli po DIN

50008 za meritve senzorjev vlage in umerjanje merilnikov vlage. Delo nadaljujejo z izdelavo računalniško nadzorovane klimatizacijske komore za umerjanje merilnikov relativne vlage. Vzorčni merilniki vlage so bili predstavljeni na Sejmu elektronike v Ljubljani.

Področje implementacije rezultatov:

Pri prvem podprojektu osvojeno znanje je omogočilo sodelovanje z inozemskim partnerjem na področju slikovnih elektronk, vključno z izdelavo serije ohišij zanje ter predvidenim sodelovanjem pri uporabi snemalnih elektronk pri varovanju objektov v izredno slabih svetlobnih razmerah.

Nov tip elektronke MKES2 je primeren za vgradnjo v sodobne termovizijske kamere, kar pa ni njegova izključna uporaba.

Razvoj linearnega polimernega senzorja in industrijskih merilnikov vlage omogoča vključevanje na področju, ki je v svetu še v razvoju in doseženi rezultati ne zaostajajo veliko. Laboratorij za meritve relativne vlage in pripravo kalibrov vlage se bo vključil v slovenski sistem laboratorijev.

Tržni (ekonomski) učinki:

Delo pri prvem podprojektu je spodbudilo naročilo prve serije kovinskih ohišij elektronk znanega tujega naročnika in sodelovanje pri njegovem razvoju, sicer v manjšem obsegu, vendar z možnostjo večjega vključevanja. Možna pa bi bila tudi pomoč pri vpeljavi proizvodnje.

Proizvodnja elektronk MKES2 je povsod v svetu maloserijska in zato so brez večjih kapitalskih vložkov lahko konkurenčni, ker prodajajo znanje in potrebujejo le nekaj več kot 10% materiala. Prodaja nekaj 100 katodnih cevi pomeni realizacijo blizu 0.5 mio DEM.

Prodaja kakovostnih senzorjev vlage ima veliko možnosti. V Sloveniji obstaja tudi potreba po umerjanju merilnikov vlage, ki so v uporabi v industriji in laboratorijih, saj tudi najugodnejše svetovne firme predpisujejo preverjanje vsakih nekaj mesecev, najpozneje pa po enem letu.

Raziskovalno polje: MATERIALI

Naslov: Razvoj tehnologije injekcijskega brizganja za izdelavo nove generacije keramike na osnovi aluminijevega oksida
Naročnik projekta: Iskra AET, Tolmin
Vodja projekta: mag. Saša Novak, Institut "Jožef Stefan", Ljubljana
Izvajalca projekta: Institut "Jožef Stefan", Ljubljana; Iskra AET, Tolmin
Trajanje projekta: januar 1992 - december 1992
Delež sredtev MZT: 3.789.500,00 SIT

Rezultati projekta:

Injekcijsko brizgana keramika je tržno zanimiv proizvod, s katerim Iskra AET, Tolmin, že leta uspešno prodira na tuja tržišča. Zanimanje za tovrstne izdelke (predvsem tesnilne ploščice za armature) je v zadnjem času še večje, ker Iskra AET uporablja tehnologijo nizkotlačnega brizganja. Ta je postala aktualna zlasti zaradi večje ekonomičnosti v primerjavi z visokotlačnim brizganjem (manjša poraba energije zaradi nižjih tlakov in znatno manjša obraba orodja za brizganje). Da bi ohranili konkurenčnost svojih izdelkov, je bilo nujno poglobiti nekatera znanja, ki omogočajo večje obvladovanje procesa in zmanjševanje odpadkov zaradi napak v keramiki.

Analiza napak v izbranih izdelkih iz proizvodnje je pokazala vir napak že v zelo zgodnji fazi proizvodnje, t.j. v pripravi mase za brizganje. Na temelju poglobljene analize lastnosti izhodnih surovin in analize reoloških lastnosti vodnih in parafinskih suspenzij keramičnega prahu ter študija kritičnih faz proizvodnje so definirali sestavo parafinske suspenzije in nekatere tehnološke parametre. Za zagotovitev stabilnosti kakovosti je nujno treba zagotoviti minimalno prisotnost vlage v izhodnih surovinah in med samim tehnološkim postopkom. Optimalna koncentracija ustrezne kombinacije površinsko aktivnih snovi zagotavlja pa rafinski suspenziji primerne reološke lastnosti, zlasti večjo stabilnost in nizko viskoznost pri visoki vsebnosti keramičnega prahu. Posodobitev nekaterih kritičnih faz bo v prihodnje omogočila optimalno izkoriščanje pridobljenih znanj in s tem doseganje visoke kakovosti injekcijsko brizgane keramike.

Področje implementacije rezultatov:

Rezultati razvojnega dela bodo omogočili izboljšanje kakovosti injekcijsko brizgane tehnične keramike za tribološke aplikacije.

Tržni (ekonomski) učinki:

S prenosom rezultatov razvojnega dela v proizvodnjo se je za 2 do 3% zmanjšal odpadek in povečal izvoz za približno 16%.

Naslov: Magnetni materiali na osnovi NdFeB spojin
Naročnik projekta: Iskra Magneti p.o., Ljubljana
Vodja projekta: dr. Spomenka Kobe-Beseničar, Institut "Jožef Stefan, Ljubljana
Izvajalec projekta: Institut "Jožef Stefan", Ljubljana
Trajanje projekta: januar 1992 - december 1992
Delež sredstev MZT: 3.392.497,00 SIT

Rezultati projekta:

Rezultat projekta so izdelani trajni magnetni materiali na osnovi spojine NdFeB z izboljšanimi magnetnimi lastnostmi. Z majhnim dodatkom ZrO_2 so dosegli izboljšanje koercitivne sile sintranih magnetov za 20 %, ne da bi se pri tem poslabšala remanentna magnetizacija. Z znatnim izboljšanjem temperaturnih koeficientov obeh karakterističnih magnetnih lastnosti pa so povečali tudi temperaturno območje uporabe teh magnetov.

Dodatek Zr oksida izboljša magnetne lastnosti NdFeB magnetov, obenem poveča tudi njihovo korozijsko obstojnost, ki je za uporabo teh materialov prav tako pomembna kot njihova magnetna stabilnost.

Izboljšanje magnetnih lastnosti in povečano korozijsko stabilnost so razložili z nastankom nove faze, ki so jo s pomočjo elektronske mikroskopije in EDS analize identificirali kot ZrB_2 fazo. Novo nastala faza v obliki heksagonalnih ploščic vpliva na razvoj mikrostrukture med sintranjem, zavira rast zrn trdomagnetne faze in tako posredno vpliva na magnetne lastnosti. Vsebnost prostega Nd na mejah med zrni se zaradi reakcije z ZrO_2 zmanjša, s tem se zmanjša občutljivost mej med zrni. Korozija poteka le na površini vzorcev, medtem ko je pri nedopiranih vzorcih globinska. Korozijska obstojnost se poveča za faktor 10.

Področje implementacije rezultatov:

Razvojno-raziskovalno delo se vklaplja v dolgoročno usmeritev tovarne Iskra Magneti. Z novimi programi želijo razširiti in posodobiti svoj proizvodni program, to pomeni, v nekaj letih nekatere proizvode iz Alnico programa zamenjati z modernejšimi materiali, ki omogočajo miniaturizacijo na vseh področjih njihove uporabe in med katere sodijo tudi sintrani magneti na osnovi NdFeB spojine.

Naslov: Razvoj keramičnih granulatov in konstrukcijskih delov

Naročnik projekta: COMET, umetni brusi in nekovine, Zreče
Sopredlagatelj: Iskra AET, Tolmin
Vodja projekta: dr. Miloš Komac, Institut "Jožef Stefan", Ljubljana; COMET, Zreče; Iskra AET, Tolmin
Trajanje projekta: 1990 - 1991
Delež sredstev MZT: 878.657,00 SIT

Rezultati projekta:

Cilj projekta je bil povečati izbiro izdelkov iz tehnične keramike, hkrati pa povečati izkoriščenost proizvodne opreme. To bi bila tudi osnova za razvoj tržno zanimivih izdelkov v obeh podjetjih, t.j. v Cometu in Iskri AET. Končni izdelek iz granulata pa je bil bat za visokotlačno črpalko. V okviru projekta so bili razviti novi tipi granulatov za izostatsko stiskanje z dobro obdelovalno sposobnostjo z odvzemanjem materiala. Razvita sta bila dva granulata (interna oznaka A11 in A12, pogojno uporabljen je tudi granulat pod oznako A13), ki pomenita nov možni artikel v Cometu, Zreče. Vzporedno z razvojem granulata so se razvijali tudi bati za visokotlačno črpalko v Iskri AET, Tolmin, za znanega kupca.

Področje implementacije rezultatov:

Razvoj nove vrste granulata za izostatsko stiskanje v Cometu pomeni poleg tržnega učinka tudi obogatitev strokovnega znanja pri pripravi keramičnih granulatov in s tem tudi nujno prilagodljivost proizvodnji. V Iskri AET je bil razvit prvi izdelek iz potencialno zelo široke družine izdelkov podobnih karakteristik.

Tržni (ekonomski) učinki:

Trženje izdelka (bat za visokotlačno črpalko) je še v začetni fazi, prav tako pa tudi granulat, razvit za ta izdelek. Osnovni problem pri hitrejšem trženju so ekonomske težave in dokaj dolgi razvojni ciklus (predvsem končno testiranje pri kupcu), ki se zaključijo s prvimi dobavami in podpisom pogodb.

Naslov: Razvoj visokoenergijskih magnetov na osnovi $Sm(Co,Fe,Cu,Zr)_{7.5}$

Naročnik projekta: Iskra Magneti p.o., Ljubljana
Vodja projekta: dr. Spomenka Kobe-Beseničar, Institut "Jožef Stefan", Ljubljana
Izvajalec projekta: Institut "Jožef Stefan", Ljubljana; Iskra Magneti, Ljubljana
Trajanje projekta: januar 1991 - december 1992
Delež sredstev MZT: 3.256.797,00 SIT

Rezultati projekta:

Konkreten rezultat projekta je v laboratoriju razvita tehnologija izdelave magnetov na osnovi zlitine $Sm(Co,Fe,Cu,Zr)_{7.5}$, ki je bila uspešno prenešena v proizvodnjo. Vzorci, izdelani v proizvodnji, so si že pridobili potrdilo o kakovosti. To potrdilo je osnova za večja naročila. Vzorci za tovarno motorjev Faulhaber (Švica), ki po kakovosti tudi dosegajo zahtevane lastnosti pa so še v fazi pridobivanja certifikata o kakovosti.

Na osnovi rezultatov projekta je bila vpeljana nova moderna tehnologija izdelave trajno magnetnih materialov novejše generacije, kar pomeni modernizacijo proizvodnega programa tovarne kovinskih magnetov Iskra Magneti in s tem tudi ohranitev zahodnoevropskega trga. Vpeljava te tehnologije pomeni dopolnitev dosedanjega proizvodnega programa na področju intermetalnih zlitin samarija in kobalta, kjer so že razvili in uspešno prenesli v proizvodnjo tehnologijo izdelave $SmCo_5$ magnetov.

Področje implementacije rezultatov:

Magnetni materiali novejše generacije so trajni magnetni materiali, ki se uporabljajo v proizvodnji elektromotor-

jev, akcelerometrov, klistronov itd., torej predvsem tam, kjer je potrebna velika temperaturna stabilnost magnetnih lastnosti. Zaradi nižje cene surovin zlitine $Sm(Co,Fe,Cu,Zr)_{7.5}$ od $SmCo_5$ zlitine, pa se ti magneti uporabljajo tudi tam, kjer zahteve po temperaturni stabilnosti niso tako visoke.

Tržni (ekonomski) učinki:

Tržni učinki še niso znani, jih je pa mogoče predvideti v okviru dosedanjih učinkov pri prodaji $SmCo_5$ magnetov na tujem in delno domačem trgu.

Naslov: Oplemenitenje površin s PVD trdimi prevlekami
Naročniki projekta: Iskra Avtoelektrika, Šempeter pri Gorici; Iskra Elektromotorji, Železniki; Saturnus, Ljubljana
Vodja projekta: prof. dr. Boris Navinšek, Institut "Jožef Stefan", Ljubljana
Izvajalci projekta: Institut "Jožef Stefan"; Fakulteta za strojništvo; I.E.V.T., Ljubljana
Trajanje projetka: januar 1991 - december 1993
Delež sredstev MZT: 3.163.167,00 SIT

Rezultati projekta:

a) Z razvojem nove tehnologije - trde prevleke kromovega nitrida (CrN) so rešili problem oplemenitenja vseh vrst orodij in strojnih delov, ki prenesejo temperaturo nanašanja do 220°C. Te nekaj μm debele zaščitne prevleke z visoko mikrotrdoto so izredno odporne proti obrabi, koroziji v vseh medijih ter oksidaciji do temperature okolice do 800°C. Prevleke CrN so posebno primerne za oplemenitenje orodij za rezanje in preoblikovanje bakra, aluminija, niklja in titana ter superzlitin (pri katerih TiN prevleka odpove). Zaradi visoke temperaturne obstojnosti so CrN prevleke namenjene predvsem izboljšanju kokil za tlačno litje aluminija in Al-zlitin (npr. v proizvodnji elektromotorjev in tehnoloških komponent). Prvi uspešen poskus uporabe nove CrN prevleke je bil narejen v tovarni svetil Sijaj v Hrastniku (orodje za hladno vlečenje Fe pločevine, izdelano iz orodnega jekla OCR 12). Drugi testi se še analizirajo.

b) V okviru raziskav novih področij uporabe TiN tehnologije trdih prevlek (JOSTiN^R) je bila izdelana ekonomska analiza 5- letne uporabe. Pokazala je njene prednosti za serijsko proizvodnjo v slovenski strojno-predelovalni, elektro in lesni industriji. V letu 1992 so sistematično testirali uporabo JOSTiN^R tehnologije za številna specialna orodja in strojne dele, ki so v serijski proizvodnji podvrženi močni obrabi (npr. v živilski industriji). Njihovo tehnologijo stalno uporablja 28 slovenskih tovarn in tovarna FLUID-TEC iz Milana, kar pomeni začetek prodora teh tehnologij in visokokvalitetnih orodij, oplemenitenih z JOSTiN^R prevleko, v prostor Alpe-Adrija. TiN prevleka ima zlato barvo, mikrotrdoto 2000 HV ter visoko korozijsko in obrabno odpornost. Zato so JOSTiN^R prevleko inovacijsko uporabili tudi kot dekorativno prevleko, ki bo v proizvodnji nadomestila trdo zlatenje (npr. pri posodi EMOTON v Celju) ali večslojno zaščito pri ohišjih halogenskih svetil (npr., V Sijaju, Hrastnik). Vsi testi so bili nadvse uspešni, za serijsko uporabo pa je potrebna še ekonomska analiza, ocena tržišča v tujini (kot izjemno kakovosten nov proizvod) in seveda odločitev v tovarnah.

c) Za potrebe industrije so v letu 1992 razvili novo vrsto 2-5 μm debelih ultratrdih prevlek iz zirkonijevega nitrida (ZrN) z mikrotrdoto prek 3200 HV. Poleg izjemno visoke mikrotrdote pa ima ZrN prevleka tudi visoko obrabno, oksidacijsko in korozijsko odpornost. Prav te lastnosti pa so potrebne za oplemenitenje delov, ki so podvrženi visoki eroziji na delovnih površinah pri proizvodnji ali uporabi tekstilnih vlaken.

Področje implementacije rezultatov in tržni učinki

Uspeh tega tehnološko-razvojnega projekta je možen le ob najtesnejšem sodelovanju med izvajalskimi institucijami in industrijo, saj vse teste izvajajo neposredno na strojih v serijski proizvodnji. 8-letne izkušnje kažejo, da je ekonomski učinek izmerljiv. Za JOSTiN^R tehnologijo velja, da strošek npr. 100.000 SIT za depozicijo prevleke prinese uporabniku vsaj 650.000 SIT prihranka pri stroških proizvodnje. Pri tem pa te vrste tehnologij lahko uporabljajo vsi, od obrtnika do velikoserijske proizvodnje.

Only Austrian Independent Semiconductor Manufacturer Leads Top Position for First Half 1993

Austria Mikro System International AG (AMS), the only Austrian IC manufacturer and listed on the Vienna Stock Exchange and the SEAQ in London since July 12, 1993, has further strengthened its top position with its innovative products and services in the semiconductor market within the last half year. AMS is leading in the European market: No. 1 in the field of cell based mixed analoge/digital ASICs (application specific integrated circuits).

AMS has again increased its **order entry** in the first half of 1993 from 393 million ATS (first half of 1992) to approximately **514 million ATS (31% increase!)**. A **sales increase** from 346 million ATS (first half of 1992)

to **359 million ATS** and a raise in **earnings** of far more than 10% relative to the same period of the last year could be achieved. Noteworthy is the fact that the accomplishment of this strong increase in business was realized with basically an unchanged employee count of 586. The high **investments** of **69 million ATS** (19% of sales in the first half of 1993, an increase of 46% relative to 1992, will largely contribute towards the effectivity of the company in regards to the high order entry. Due to the extremely good course of the business an increase in the order entry for the year 1993 of 20% (more than forecast at the beginning of 1993) is now expected; thus, AMS will go into the year 1994 with a distinctly higher backlog.

Mr. Horst Gebert, President and CEO of AMS: "The ceaseless miniaturization of complex systems requires an increasing integration of high complexity which can only be achieved through microelectronics. The ASIC has its key function in this development. And, for the ASIC's development and production AMS has systematically generated the necessary intellectual capital and investments in the past years to further maintain its leading role in this prime function. Therefore, the demand for high quality ASICs from AMS will continue for the second half of 1993."

New 20 Number One Touch Dialler with Serial Bus for Display Driver

AMS announces the immediate availability of a completely new ASIC for the telecommunications market - the AS2574B, a 20 number one touch dialler with a serial bus for a display driver circuit. The AS2574B is an integrated circuit in CMOS technology for feature telephones.

The device which operates from 2.5V to 5.5V is a versatile LD/MF dialler with a serial interface to a display driver. The device is designed to be used in a wide variety of applications in handsets together with the AMS display driver AS2590.

The on-chip RAM can contain up to 20 memories, each with a maximum of 18 digits, a 36 digit Last Number Redial (LNR) and an 18 digit notepad. Access to the 20 memories is either with direct keys, abbreviated dial code or a combination of both.

The AS2574B provides a unique feature, referred to as Automatic Call Progress (ACP) on all memory keys, i.e.

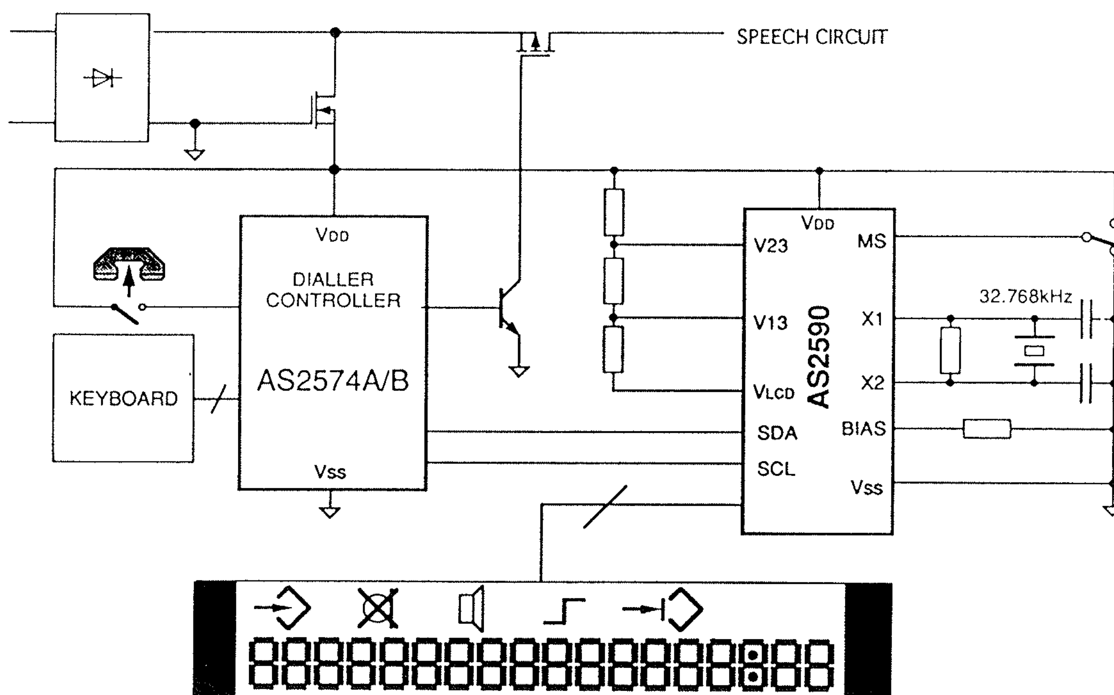

the circuit automatically seizes the line and waits for the dial tone and dials the number just by pressing any of the memory keys (including LNR).

The circuit features two different access code procedures to allow easy use under a PABX. A dial tone input enables the use of a dial tone recognizer. Additional features include: Diode options for different PTT requirements, automatic pause generation after access code and direct wake-up from the keyboard.

The device is now available in 28 pin DIP or PLCC packages. For a free data sheet and further information please contact your local AMS Sales Office or AMS Corporate Communications, Schloss Premstätten, A-8141 Unterpremstätten, Austria.

Note to the Editor: Direct wake-up is an AMS patented solution providing line seizing with a telephone that is entirely powered by the telephone line. This is achieved by pressing a key in a key matrix linked to a dialler/controller that is constantly connected to the line by means of a line voltage limiter which maintains a high DC isolation resistance in idle state (on-hook).

The wake-up feature allows the user to go off-hook by pressing a direct memory key or a loudspeaker key - so called on-hook dialling or call progress monitoring - and thereby to seize the line.

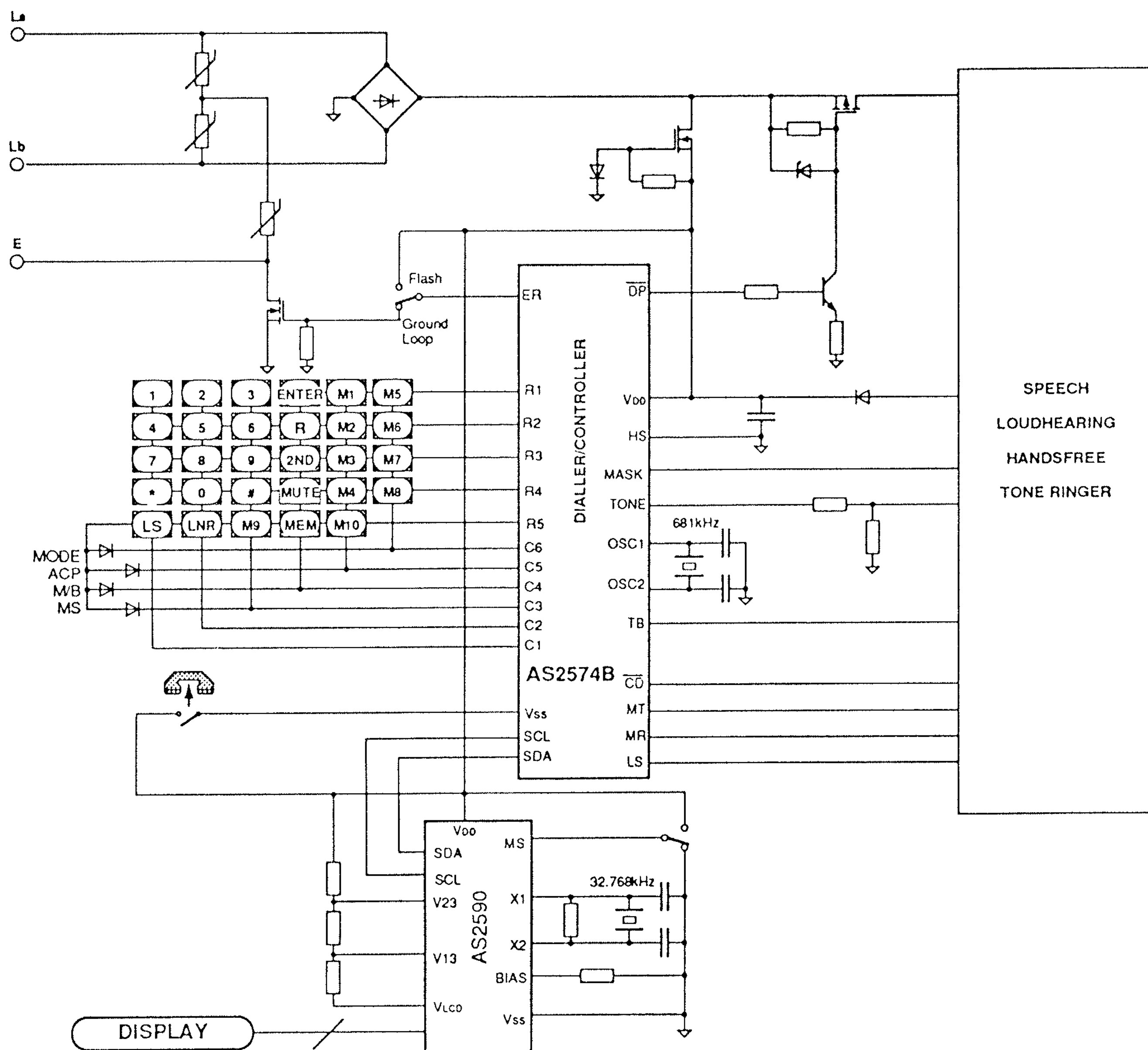

NAVODILA AVTORJEM

Informacije MIDEM je znanstveno-strokovno-društvena publikacija Strokovnega društva za mikroelektroniko, elektronske sestavne dele in materiale-MIDEM. Časopis objavlja prispevke domačih in tujih avtorjev, še posebej članov MIDEM, s področja mikroelektronike, elektronskih sestavnih delov in materialov, ki so lahko:

izvirni znanstveni članki, predhodna sporočila, pregledni članki, razprave z znanstvenih in strokovnih posvetovanj in strokovni članki.

Članki bodo recenzirani.

Časopis objavlja tudi novice iz stroke, vesti iz delovnih organizacij, inštitutov in fakultet, obvestila o akcijah društva MIDEM in njegovih članov ter druge relevantne prispevke.

Strokovni prispevki morajo biti pripravljeni na naslednji način

- 1. Naslov dela, imena in priimki avtorjev brez titul.
- 2. Ključne besede in povzetek (največ 250 besed).
- 3. Naslov dela v angleščini.
- 4. Ključne besede v angleščini (Key words) in podaljšani povzetek (Extended Abstract) v angleščini.
- 5. Uvod, glavni del, zaključek, zahvale, dodatki in literatura.
- 6. Imena in priimki avtorjev, titule in naslovi delovnih organizacij, v katerih so zaposleni.

Ostala splošna navodila

1. V članku je potrebno uporabljati SI sistem enot oz. v oklepaju navesti alternativne enote.

2. Risbe je potrebno izdelati s tušem na pavs ali belem papirju. Širina risb naj bo do 7.5 oz. 15 cm. Vsaka risba, tabela ali fotografija naj ima številko in podnapis, ki označuje njeno vsebino. Risb, tabel in fotografij ni potrebno lepiti med tekst, ampak jih je potrebno ločeno priložiti članku. V tekstu je potrebno označiti mesto, kjer jih je potrebno vstaviti.

3. Delo je lahko napisano in bo objavljeno v kateremkoli jugoslovanskem jeziku v latinici in v angleščini.

Uredniški odbor ne bo sprejel strokovnih člankov, ki ne bodo poslani v dveh izvodih.

Avtorji, ki pripravljajo besedilo v urejevalnikih besedil, lahko pošljejo zapis datoteke na disketi (360 ali 1,2) v formatih ASCII, wordstar (3.4, 4.0), wordperfect, word, ker bo besedilo oblikovano v programu Ventura 2.0. Grafične datoteke so lahko v formatu HPL, SLD (AutoCAD), PCX ali IMG/GEM.

Avtorji so v celoti odgovorni za vsebino objavljenega sestavka. Rokopisov ne vračamo.

Rokopise pošljite na naslov

Uredništvo Informacije MIDEM
Elektrotehniška zveza Slovenije
Dunajska 10, 61000 Ljubljana

UPUTE AUTORIMA

Informacije MIDEM je znanstveno-stručno-društvena publikacija Stručnog društva za mikroelektroniku, elektronske sestavne dijelove i materijale - MIDEM. Časopis objavljuje priloge domaćih i stranih autora, naročito članova MIDEM, s područja mikroelektronike, elektronskih sastavnih dijelova in materijala koji mogu biti:

izvorni znanstveni članci, predhodna priopćenja, pregledni članci, izlaganja sa znanstvenih i stručnih skupova i stručni članci.

Članci će biti recenzirani.

Časopis takoder objavljuje novosti iz struke, obavijesti iz radnih organizacija, instituta i fakulteta, obavijesti o akcijama društva MIDEM i njegovih članova i druge relevantne obavijesti.

Stručni članci moraju biti pripremljeni kako slijedi

- 1. Naslov članka, imena i prezimena autora bez titula.
- 2. Ključne riječi i sažetak (najviše 250 riječi).
- 3. Naslov članka na engleskom jeziku.
- 4. Ključne riječi na engleskom jeziku (3Key Words) i produženi sažetak (Extended Abstract) na engleskom jeziku.
- 5. Uvod, glavni dio, zaključni dio, zahvale, dodaci i literatura.
- 6. Imena i prezimena autora, titule i naslovi institucija u kojima su zaposleni.

Ostale opšte upute

1. U prilogu treba upotrebljavati SI sistem jedinica od. u zagradi navesti alternativne jedinice.

2. Crteže treba izraditi tušem na pausu ili bijelom papiru. Širina crteža neka bude do 7.5 odnosno 15 cm. Svaki crtež, tablica ili fotografija treba imati broj i naziv koji označuje njen sadržaj. Crteže, tabele i fotografije nije potrebno lijepiti u tekst, već ih priložiti odvojeno, a u tekstu samo naznačiti mjesto gdje dolaze.

3. Rad može biti pisan i biti će objavljen na bilo kojem od jugoslavenskih jezika u latinici i na engleskom jeziku.

Autori mogu poslati radove na disketama (360 ili 1,2) u formatima tekst procesora ASCII, wordstar (3.4. i 4.0), word, wordperfect pošto će biti tekst dalje obraden u Venturi 2.0. Grafičke datoteke mogu biti u formatu HPL, SLD (AutoCAD), PCX ili IMG/GEM.

Urednički odbor će odbiti sve radove koji neće biti poslani u dva primjerka.

Za sadržaj članaka autori odgovaraju u potpunosti. Rukopisi se na vraćaju.

Rukopise šaljite na adresu:

Uredništvo Informacije MIDEM
Elektrotehnična zveza Slovenije
Dunajska 10, 61000 Ljubljana
Slovenija

INFORMATION FOR CONTRIBUTORS

Informacije MIDEM is professional-scientific-social publication of Professional Society for Microelectronics, Electronic Components and Materials. In the Journal contributions of domestic and foreign authors, especially members of MIDEM, are published covering field of microelectronics, electronic components and materials. These contributions may be:

original scientific papers, preliminary communications, reviews, conference papers and professional papers.

All manuscripts are subject to reviews.

Scientific news, news from the companies, institutes and universities, reports on actions of MIDEM Society and its members as well as other relevant contributions are also welcome.

Each contribution should include the following specific components:

- 1. Title of the paper and authors' names.
- 2. Key Words and Abstract (not more than 250 words).
- 3. Introduction, main text, conclusion, acknowledgements, appendix and references.
- 4. Authors' names, titles and complete company or institution adress.

General information

1. Authors should use SI units and provide alternative units in parentheses wherever necessary.

2. Illustrations should be in black on white or tracing paper. Their width should be up to 7.5 or 15 cm. Each illustration, table or photograph should be numbered and with legend added. Illustrations, tables and photografphs are not to be placed into the text but added separatelly. Hower, their position in the text should be clearly marked.

3. Contributions may be written and will be published in any Yugoslav language and in english.

Authors may send their files on formatted diskettes (360 or 1,2) in ASCII, wordstar (3.4 or 4.0), word, wordperfect as text will be formated in Ventura 2.0. Graphics may be in HPL, SLD (AutoCAD), PVX or IMG/GEM formats.

Papers will not be accepted unless two copies are received.

Authors are fully responsible for the content of the paper. Manuscripts are not returned.

Contributions are to be sent to the address:

Uredništvo Informacije MIDEM
Elektrotehniška zveza Slovenije
Dunajska 10, 61000 Ljubljana,
Slovenia

4 Seznama v tujih jezikih

4.1 Abecedni seznam izrazov v angleškem jeziku

A

Alloyed junction 2.1.8
Avalanche breakdown (of semiconductor PN junction) 2.1.16
Avalanche rectifier diode 2.2.11
Avalanche rectifier diode, controlled 2.2.12
Avalanche voltage 2.1.17

B

Backward diode 2.2.10
Bipolar transistor 2.2.14
Breakdown (of a reversebiased PN junction) 2.1.15
Breakdown (of a semiconductor PN junction), avalanche 2.1.16
Breakdown (of a semiconductor PN junction), thermal 2.1.18
Breakdown (of a semiconductor PN junction), Zener 2.1.19
Breakdown voltage 2.4.3

C

Capacitance, equivalent thermal network 2.4.7
Capacitance, (of a semiconductor device), thermal 2.4.5
Carrier 2.1.11
Carrier (in a semiconductor region), majority 2.1.12
Carrier (in a semiconductor region), minority 2.1.13
Case temperature 2.5.1
Cell, photoconductive 2.2.19
Cell, photovoltaic 2.2.20
Charge carrier (carrier) 2.1.11
Constant, Hall 2.1.24
Controlled avalanche rectifier diode 2.2.12
Cut-off frequency 2.6.1

D

Depletion layer 2.1.14
Device, semiconductor 2.2.1
Diffused junction 2.1.9
Diode, avalanche rectifier 2.2.11
Diode, backward 2.2.10
Diode, controlled avalanche rectifier 2.2.12
Diode, photo 2.2.8
Diode, semiconductor 2.2.2
Diode, semiconductor rectifier 2.2.5
Diode, signal 2.2.9
Diode, tunnel 2.2.7
Diode, unitunnel 2.2.10
Diode, voltage reference 2.2.3
Diode, voltage regulator 2.2.4
Direction (of a PN junction), forward 2.3.3
Direction (of a PN junction) reverse 2.3.4

E

Effect, Hall 2.1.23
Effect, photo-electric 2.1.25
Effect, photovoltaic 2.1.26
Effect, tunnel 2.1.21
Electrode (of a semiconductor device) 2.3.2
Equivalent thermal network 2.4.6
Equivalent thermal network capacitance 2.4.7
Equivalent thermal network resistance 2.4.8
Extrincic semiconductor 2.1.2

F

Field-effect transistor 2.2.16
Floating voltage 2.4.2
Forward direction (of a PN junction) 2.3.3

G

Grown junction 2.1.10

H

Hall coefficient (of a semiconductor) 2.1.24
Hall constant 2.1.24
Hall effect 2.1.23

I

Impedance, transient thermal 2.4.9
Impedance under pulse conditions, thermal 2.4.10

K

Karakteristike 2.6
Krmiljena plazovna usmerjalna dioda 2.2.12

L

Legirani spoj 2.1.8

M

Manjšinski nosilec (v polprevodniškem področju) 2.1.13
Mejna frekvenca 2.6.1

N

Napetost plazovnega preboja 2.1.17
Nečistotni polprevodnik 2.1.2
Nosilec elektrine 2.1.11

O

Osiromašeni sloj 2.1.14

P

Plazovna usmerjalna dioda 2.2.11
Plazovni preboj 2.1.16
PN-spoj 2.1.7
Poljski transistor 2.2.16
Polprevodnik 2.1.1
Polprevodnik tipa I 2.1.5
Polprevodnik tipa N 2.1.3
Polprevodnik tipa P 2.1.4
Polprevodniška dioda 2.2.2
Polprevodniška komponenta 2.2.1
Polprevodniška usmerjalna dioda 2.2.5
Polprevodniški element 2.2.1
Polprevodniški usmerjalni stavek 2.2.6
Preboj (inverzno polariziranega PN-spoja) 2.1.15
Prebojna napetost 2.4.3
Prehodna toplotna impedanca 2.4.9
Prepustna smer (PN-spoja) 2.3.3
Priključek (polprevodniškega elementa) 2.3.1

R

Referenčna dioda 2.2.3

S

Selenski omejevalnik prenapetosti 2.2.21
Signalna dioda 2.2.9
Splošni izrazi 2.3
Splošni izrazi in definicije 2
Spoj 2.1.6
Stabilizacijska dioda 2.2.4

T

Temperature 2.5
Temperatura okrova 2.5.1
Temperatura skladiščenja 2.5.2
Temperaturni razbremenitveni faktor 2.5.3
Termični preboj (polprevodniškega PN-spoja) 2.1.18
Tiristor 2.2.18
Toplotna impedanca pri impulznem obratovanju 2.4.10
Toplotna kapaciteta (polprevodniškega elementa) 2.4.5
Toplotna upornost (polprevodniškega elementa) 2.4.4
Transistor 2.2.13
Transistor na poljski pojav 2.2.16
Tunelska dioda 2.2.7
Tunelski pojav 2.1.21
Tunelski proces (v PN-spoju) 2.1.22

U

Unipolarni transistor 2.2.15
Unitunelska dioda 2.2.10

V

Večinski nosilec (v polprevodniškem področju) 2.1.12
Virtualna temperatura 2.5.4
Vlečeni spoj 2.1.10
Vrste elementov 2.2

Z

Zaporna napetost 2.4.1
Zaporna smer (PN-spoja) 2.3.4
Zenerska napetost 2.1.20
Zenerski preboj (polprevodniškega PN-spoja) 2.1.19

Тиристор 2.2.18
Топлинска импеданса за импулсна струја 2.4.10
Топлинска импеданса, преодна 2.4.9
Топлинска капацитивност, еквивалентна 2.4.7
Топлинска капацитивност (на полупроводнички елемент) 2.4.5
Топлинска отпорност, еквивалентна 2.4.8
Топлинска отпорност (на полупроводнички елемент) 2.4.4
Топлинска шема, еквивалентна 2.4.6
Топлински фактор на намалување на граничната моќност на дисипација 2.5.3
Транзистор 2.2.13
Транзистор, биполарен 2.2.14
Транзистор, полев 2.2.16
Транзистор, униполарен 2.2.15
Транзистор, фото 2.2.17
Тунел–диода 2.2.7
Тунелирање, ефект 2.1.21
Тунелирање (низ PN–спој) 2.1.22

Ќ

Ќелија, фотонапонска 2.2.20
Ќелија, фотопроводна 2.2.19

У

Униполарен транзистор 2.2.15

Ф

Фактор на намалување на граничната моќност на дисипација, топлински 2.5.3
Фото–диода 2.2.8
Фотоелектричен ефект 2.1.25
Фотонапонска ќелија 2.2.20
Фотонапонски ефект 2.1.26
Фотопроводна ќелија 2.2.19
Фото–транзистор 2.2.17
Фреквенција, гранична 2.6.1

Х

Холов ефект 2.1.23
Холов коефициент 2.1.24

Ш

Шема, еквивалентна топлинска 2.4.6

3.4 Abecedni seznam izrazov u slovenskem jeziku

B

Bipolarni transistor 2.2.14

D

Difuzijski spoj 2.1.9
Drsna napetost 2.4.2

E

Ekvivalentna toplotna kapaciteta 2.4.7
Ekvivalentna toplotna upornost 2.4.8
Ekvivalentno toplotno vezje 2.4.6
Elektroda (polprevodniškega elementa) 2.3.2

F

Fizikalni izrazi 2.1
Fotodioda 2.2.8
Fotoelektrični pojav 2.1.25
Fotonapetostna celica 2.2.20
Fotonapetostni pojav 2.1.26
Fotoprevodna celica 2.2.19
Fototransistor 2.2.17

H

Hallov koeficient (polprevodnika) 2.1.24
Hallov pojav 2.1.23

I

Inverzna napetost 2.4.1
Inverzna smer (PN-spoja) 2.3.4
Izrazi za mejne vrednosti in karakteristike 2.4

TERMINOLOŠKI STANDARDI

К

Капацитивност, еквивалентна топлинска 2.4.7
Капацитивност (на полупроводнички елемент), топлинска 2.4.5
Коефициент (на полупроводник) Холов 2.1.24
Куќиште, температура 2.5.1

Л

Лавински напон 2.1.17
Лавински пробив (на полупроводнички PN-спој) 2.1.16
Лебдечки напон 2.4.2
Легиран спој 2.1.8

Н

Напон, Зенеров 2.1.20
Напон, инверзен 2.4.1
Напон, лавински 2.1.17
Напон, лебдечки 2.4.2
Напон, пробивен 2.4.3
Насока (на PN–спој), директна 2.3.3
Насока (на PN–спој), инверзна 2.3.4
Насочувачка диода, полупроводничка 2.2.5
Насочувачка диода со контролиран лавински пробив 2.2.12
Насочувачка диода со лавински пробив 2.2.11
Насочувачки блок, полупроводнички 2.2.6
Носител 2.2.11
Носители (во некоја област на полупроводникот), основни 2.1.12
Носители (во некоја област на полупроводникот), споредни 2.1.13
Носител (на електрицитет) 2.1.11

О

Одводник на пренапони, селенски 2.2.21
Осиромашен слој 2.1.14
Основни носители (во некоја област на полупроводникот) 2.1.12
Отпорност, еквивалентна топлинска 2.4.8
Отпорност (на полупроводнички елемент), топлинска 2.4.4

П

Полев транзистор 2.2.16
Полупроводник 2.1.1
Полупроводник од I–тип 2.1.5
Полупроводник од N–тип 2.1.3
Полупроводник од P–тип 2.1.4
Полупроводник, примесен 2.1.2
Полупроводничка диода 2.2.2
Полупроводничка насочувачка диода 2.2.5
Полупроводнички елемент 2.2.1
Полупроводнички насочувачки блок 2.2.6
Премин (спој) 2.1.6
Преодна топлинска импеданса 2.4.9
Приклучок (на полупроводнички елемент) 2.3.1
Примесен полупроводник 2.1.2
Пробивен напон 2.4.3
Пробив (на инверзно поларизиран PN–спој) 2.1.15
Пробив (на полупроводнички PN–спој), Зенеров 2.1.19
Пробив (на полупроводнички PN–спој), лавински 2.1.16
Пробив (на полупроводнички PN–спој), топлински 2.1.18

С

Селенски одводник на пренапони 2.2.2
Сигнална диода 2.2.9
Складирање, температура 2.5.2
Слој, осиромашен 2.1.14
Спој, дифундиран 2.1.9
Спој, извлекуван 2.1.10
Спој, легиран 2.1.8
Спој, PN 2.1.7
Спој (премин) 2.1.6
Споредни носители (во некоја област на полупроводникот) 2.1.13

Т

Температура, виртуелна 2.5.4
Температура, внатрешна еквивалентна 2.5.4
Температура на куќиштето 2.5.1
Температура на складирање 2.5.2

TERMINOLOŠKI STANDARDI

Tranzistor, foto 2.2.17
Tranzistor s efektom polja 2.2.16
Tranzistor, unipolarni 2.2.15
Tuneliranje (kroz PN–spoj) 2.1.22
Tunelska dioda 2.2.7
Tunelski efekt 2.1.21

U

Unipolarni tranzistor 2.2.15
Unutrašnja nadomjesna temperatura (virtualna temperatura) 2.5.4

Uskladištenje, temperatura 2.5.2

V

Većinski nosioci (u nekom području poluvodiča) 2.1.12
Virtualna temperatura (unutrašnja, nadomjesna temperatura) 2.5.4

Z

Zaporni (inverzni) smjer PN–spoja 2.3.4
Zenerov napon 2.1.20
Zenerov proboj (poluvodičkog PN–spoja) 2.1.19

3.3 Azbučni seznam izrazov v makedonskem jeziku

Б

Беспримесен полупроводник 2.1.5
Биполарен транзистор 2.2.14

В

Виртуелна температура 2.5.4
Внатрешна еквивалентна температура 2.5.4

Г

Гранична моќност на дисипација, топлински фактор , на намалување 2.5.3
Гранична фреквенција 2.6.1

Д

Диода, еднотунелна 2.2.10
Диода за референтен напон 2.2.3
Диода за стабилизација на напон 2.2.4
Диода, полупроводничка 2.2.2
Диода, сигнална 2.2.9
Диода со контролиран лавински пробив, насочувачка 2.2.12
Диода со лавински пробив, насочувачка 2.2.11
Диода, тунел 2.2.7
Диода, фото 2.2.8
Директна насока (на PN–спој) 2.3.3
Дифундиран спој 2.1.9

Е

Еднотунелна диода 2.2.10
Еквивалентна температура, внатрешна 2.5.4
Еквивалентна топлинска капацитивност 2.4.7
Еквивалентна топлинска опорност 2.4.8
Еквивалентна топлинска шема 2.4.6
Електрода (на полупроводнички елемент) 2.3.2
Елемент, полупроводнички 2.2.1
Ефект на тунелирање 2.1.21
Ефект, фотоелектричен 2.1.25
Ефект, фотонапонски 2.1.26
Ефект, Холов 2.1.23

З

Зенеров напон 2.1.20
Зенеров пробив (на полупроводнички PN–спој) 2.1.19

И

Извлекуван спој 2.1.10
Импеданса за импулсна струја, топлинска 2.4.10
Импеданса, преодна топлинска 2.4.9
Инверзен напон 2.4.1
Инверзна насока (на PN–спој) 2.3.4

TERMINOLOŠKI STANDARDI